

**UNCLASSIFIED**

---

**AD 298 260**

---

*Reproduction  
by NSA*

ARMED SERVICES TECHNICAL INFORMATION AGENCY  
ARLINGTON HALL STATION  
ARLINGTON 12, VIRGINIA



---

**UNCLASSIFIED**

NOTICE: When government or other drawings, specifications or other data are used for any purpose other than in connection with a definitely related government procurement operation, the U. S. Government thereby incurs no responsibility, nor any obligation whatsoever; and the fact that the Government may have formulated, furnished, or in any way supplied the said drawings, specifications, or other data is not to be regarded by implication or otherwise as in any manner licensing the holder or any other person or corporation, or conveying any rights or permission to manufacture, use or sell any patented invention that may in any way be related thereto.

298260

CATALOG BY: STD  
AS AD 110.



meteorology research, inc. • 2420 n. lake ave. • altadena, calif.

ASTIA  
RECEIVED  
MAR 18 1963  
TISIA

VERTICAL DIFFUSION FROM A  
LOW ALTITUDE LINE SOURCE

- DALLAS TOWER STUDIES -  
Volume I

Final Report  
to

U. S. Army Chemical Corps  
Dugway Proving Ground

Contract DA-42-007-CML-504

by

P. B. MacCready, Jr.  
T. B. Smith  
M. A. Wolf

December 1961

Meteorology Research, Inc.  
2420 North Lake Avenue  
Altadena, California

## SUMMARY

A series of diffusion tests using an aerial line source release were made in the vicinity of the Dallas TV tower at Cedar Hill, Texas. A total of thirty-seven tests were carried out in three two-week intervals in April, June, and August, 1961. Extensive use has been made of Air Force-sponsored wind and temperature measurements made at various levels on the 1420 foot TV tower. Bivane wind sensors were added to the tower instrumentation to provide direct measurements of turbulence. Vertical sampling of the FP material was accomplished by sequential filter samplers at various levels on the tower and by rotorod samplers located on the ground one mile apart to a distance of about 30 miles downwind from the release line. During a portion of the tests a crosswind rotorod line was added near the downwind end of the main ground sampler line.

The primary objective of the program was to relate measured diffusion characteristics of the cloud to observed turbulence, wind velocity, and temperature observations in a quantitative manner. This information was to be obtained under a variety of meteorological and release height conditions.

The principal analysis effort concerned itself primarily with explanations of the observed cloud widths on the tower, the distance from the release line to the first appearance of the cloud at the ground, and the location and magnitude of the maximum dosage at the ground. Time limitations did not permit analysis of numerous other features of interest obtainable from the data.

Theoretical expressions which relate the diffusional growth of a small cluster of particles to measured turbulence parameters have been developed by Smith-Hay (1961). These authors suggest that, for a considerable portion of the cloud growth history, the rate of growth of the cluster can be approximated by:

$$\frac{d\sigma}{dx} = 3i^2 \quad \text{where } \sigma \text{ is a measure of the cloud size, } x \text{ is the}$$

downwind distance, and  $i$  is the measured turbulent intensity (measured in radians as a ratio of turbulent velocity to mean velocity). This expression may be applied to the vertical growth of the line source cloud in the Dallas tests as a possible method of relating observed meteorological parameters to measured particle dosages. The vertical cloud size,  $\sigma_z$ , measured on the tower would then be given by  $3i^2x$  where  $x$  is the total distance from the release line to the tower.

At the ground level, under these conditions, dosages may be shown to be given by:

$$D = \frac{2 Q}{3 i_e^2 x u \sqrt{2\pi}} e^{-H^2/18 i_e^4 x^2} \quad \text{for a distance } x \text{ from the release}$$

line, a release height  $H$ , total source strength  $Q$ , average wind velocity  $u$ , and effective turbulence intensity  $i_e$ . The effective turbulent intensity and average wind are calculated as weighted averages of measured turbulence and wind at various levels between the release height and ground level. The dosage model given above also assumes that the cloud spreads upward from the release height at the same rate. Since nighttime turbulence decreases markedly with height, this assumption results in underestimates of ground dosages since diffusion of the cloud upward is not as marked as the model describes.

Results of the tests showed that vertical cloud sizes measured on the tower were consistently larger than calculated from the approximation  $d\sigma/dx = 3i^2$ . One reason for the discrepancy between observed and calculated cloud sizes can be attributed to the initial size of the cloud immediately after release. From Dugway calibration trial data it is apparent that the cloud cannot be considered as a line source but has an appreciable initial size due to rapid spreading in the vortex velocity wake created by the airplane. In addition, turbulent energy in the wake of the aircraft is superimposed on natural atmospheric turbulence levels and results in more rapid cloud growth than would be caused by the natural turbulence alone. With reasonable assumptions concerning the effect of the aircraft wake it is shown that the cloud sizes measured on the tower can be adequately explained in terms of the combined effect of natural turbulence (expressed by the  $3i^2$  relationship) and aircraft-created turbulence.

Observed ground dosage characteristics are in good agreement with the implications of the above model when the release is made within a well-developed turbulent layer near the ground. Observed maximum dosages averaged 23 per cent higher than forecast by the model for 14 cases which satisfied this condition. For releases above this turbulent layer, ground dosages were much more erratic in comparison with the model.

Horizontal dilution from the ends of the release line occurs with an angular spreading rate  $d\sigma_y/dx = i_H$ , where  $i_H$  is the average horizontal turbulence in the layer between the ground and release height. This is in contrast to the vertical diffusion spreading rate of  $d\sigma/dx = 3i^2$ . This horizontal spreading rate is in accordance with the rate of dilution experienced by a continuous source, and the long aircraft line release may be thus considered to follow the laws of an instantaneous source in the vertical and a continuous source in the horizontal along the line of release.

A method is shown for estimating the effective turbulent intensity,  $i_e$ , from standard meteorological data without direct turbulence measurements. This method applies in quantitative detail only in the Texas area but should apply in principle in any location. The extent to which the method must be modified for other terrain areas will be the subject of further field studies.

Through use of the graphical technique for estimating the effective turbulent intensity,  $i_e$ , it is possible to estimate the effectiveness of potential releases at various altitudes in the Dallas tests regardless of actual test release height. If a simple criterion is assumed which specifies that the cloud reach the ground within 15 miles of the release, releases at 450 feet on virtually all test nights would have been classed as successful. At 750 feet, releases on most of the test nights would not be classed as successful by this criterion and at 1050 feet, a successful release would have been possible in only one case out of 35.

Volume I of this report covers an analysis of the Dallas diffusion tests. The accumulated data for each test have been gathered together into Volume II for the benefit of other workers who may wish to use the data for other studies.

# TABLE OF CONTENTS

	Page
SUMMARY	i
I. INTRODUCTION	1
A. Background	1
B. Objective	1
C. Site Description	1
D. Scope	2
II. FIELD OPERATION	4
A. Tracer System	4
1. Tracer	4
2. Disseminator	5
3. Sampling Devices	5
a. Filter Type Samplers	5
b. Rotorod Samplers	6
B. Meteorological Observations	7
1. Bivane System	7
2. Wind Velocity and Temperature System	7
3. Synoptic	8
C. Communications	8
D. Operational Procedure	8
III. DATA REDUCTION	11
A. Particle Assessment	11
B. Wind and Temperature Data	11
C. Bivane Data	11
IV. DIFFUSION CONSIDERATIONS	12
A. Meteorological Factors	12
B. The Diffusion of Clusters	14
C. The Diffusion Model	16
1. Tower Dosage	16
2. Ground Dosage	16
D. Limitations of the Diffusion Model	19
1. Turbulence Scale	19
2. Homogeneous Turbulence	19
3. Average Wind	20
4. Time Homogeneity of Turbulence	20
V. TEST RESULTS	22
A. Introduction	22
B. The Turbulence Environment	22
1. Effects of Stability and Geostrophic Wind on Vertical Velocity Variance	22
2. Vertical Velocity Variance and Richardson Number	22
3. Depth of Turbulent Layer	23

C.	Vertical Diffusion	25
1.	Particle Budget Calculations	25
2.	Computation of Vertical Cloud Size	27
3.	Mean Height of the Cloud Center	29
4.	Comparison of Observed and Computed Vertical Cloud Sizes	30
5.	Effect of Aircraft Wake on Vertical Cloud Size	30
6.	Summary	33
D.	Downwind Ground Sampling	33
1.	Maximum Dosage	33
2.	Cloud Touchdown Distance	35
3.	Downwind Dosage Distribution	36
E.	Crosswind Ground Sampling	38
F.	Estimation of Effective Turbulence ( $i_e$ )	41
VI.	CONCLUSIONS	43
VII.	RECOMMENDATIONS	45
	ACKNOWLEDGMENTS	47
VIII.	REFERENCES	48
	APPENDIX A - COMPARISON OF ROTOROD AND FILTER SAMPLERS	49
	APPENDIX B - TURBULENCE MEASUREMENTS AND ANALYSIS	50
A.	Turbulence Information and Summary	50
B.	Bivane Characteristics	52
C.	Sigma Meter Characteristics	53
D.	Energies and Spectra from the Sigma Meters	53
E.	Complete Spectrum Measurements	55
	APPENDIX C - DISSIPATION FACTORS AND AIRCRAFT WAKE EFFECTS	57
A.	General	57
B.	Review of the Concepts	57
C.	Decay of a Turbulence Field	58
D.	Effect of the Aircraft Wake	60
E.	Estimates of $\epsilon$ and Spectra	63

## I. INTRODUCTION

### A. Background

During the period between August 1959 and February 1960, thirteen diffusion tests were carried out in central Texas by Dugway Proving Ground under the designation of Project Windsoc. The tests involved low-level aircraft releases along a crosswind line at various altitudes and under various meteorological conditions. Analyses of the test data are given in report DPG 60-2811.

After completion of the Windsoc analysis, a number of questions remained concerning the specific conditions under which reasonable amounts of material would be transported to the ground from an elevated aircraft release. In particular, a quantitative connection between measured meteorological parameters and observed ground dosage patterns was not achieved during Project Windsoc.

Shortly after the close of the Windsoc field operations an Air Force-sponsored program of meteorological observations was commenced on a television tower near Dallas and in the grid area previously used during the Windsoc studies. Wind and temperature data, measured at various levels on the 1420-foot tower, provided the meteorological data required for detailed studies of the lower layers of the atmosphere which had previously not been feasible.

The availability of the instrumented television tower at Dallas thus provided a unique opportunity for detailed diffusion studies related to a low-level aircraft release and made it possible to investigate the physical mechanisms responsible for the transport of material to the ground. By obtaining an understanding of these mechanisms it should become possible to relate the diffusion results obtained in the Dallas tests to those expected in other areas where terrain, turbulence, and meteorological conditions are somewhat different.

### B. Objective

The primary objective of the Dallas tests has been to obtain a quantitative understanding of the meteorological factors influencing nighttime vertical diffusion from an aerial line source release. Included in this objective is a quantitative relation between observed ground dosages and measured meteorological parameters.

### C. Site Description

The site of the vertical diffusion tests shown in Fig. 1 is an area of 30-mile radius centered on the 1420-foot television tower at Cedar Hill, Texas,

about fifteen miles southwest of Dallas. This tower, operated jointly by stations WFAA-TV and KRLD-TV as Hill Tower, Inc., provides an excellent platform for vertical investigations of the atmosphere. The University of Texas, under a contract to the Geophysics Research Directorate of the Air Force Cambridge Research Laboratories, operates a wind velocity and temperature network on the tower which provides a continuous, integrated record of the above parameters from twelve levels, located at 30, 70, 150, 300, 450, 600, 750, 900, 1050, 1200, 1300, and 1420 feet. At each level from which the U. T. - G. R. D. instrumentation projects on a 12-foot boom there is an access platform which provides space for additional instrumentation. Bivane sensors to measure turbulence were mounted on the booms at the 30, 150, 450, 750, and 1050-foot levels, and the platforms held the filter samplers used to measure tracer dosage.

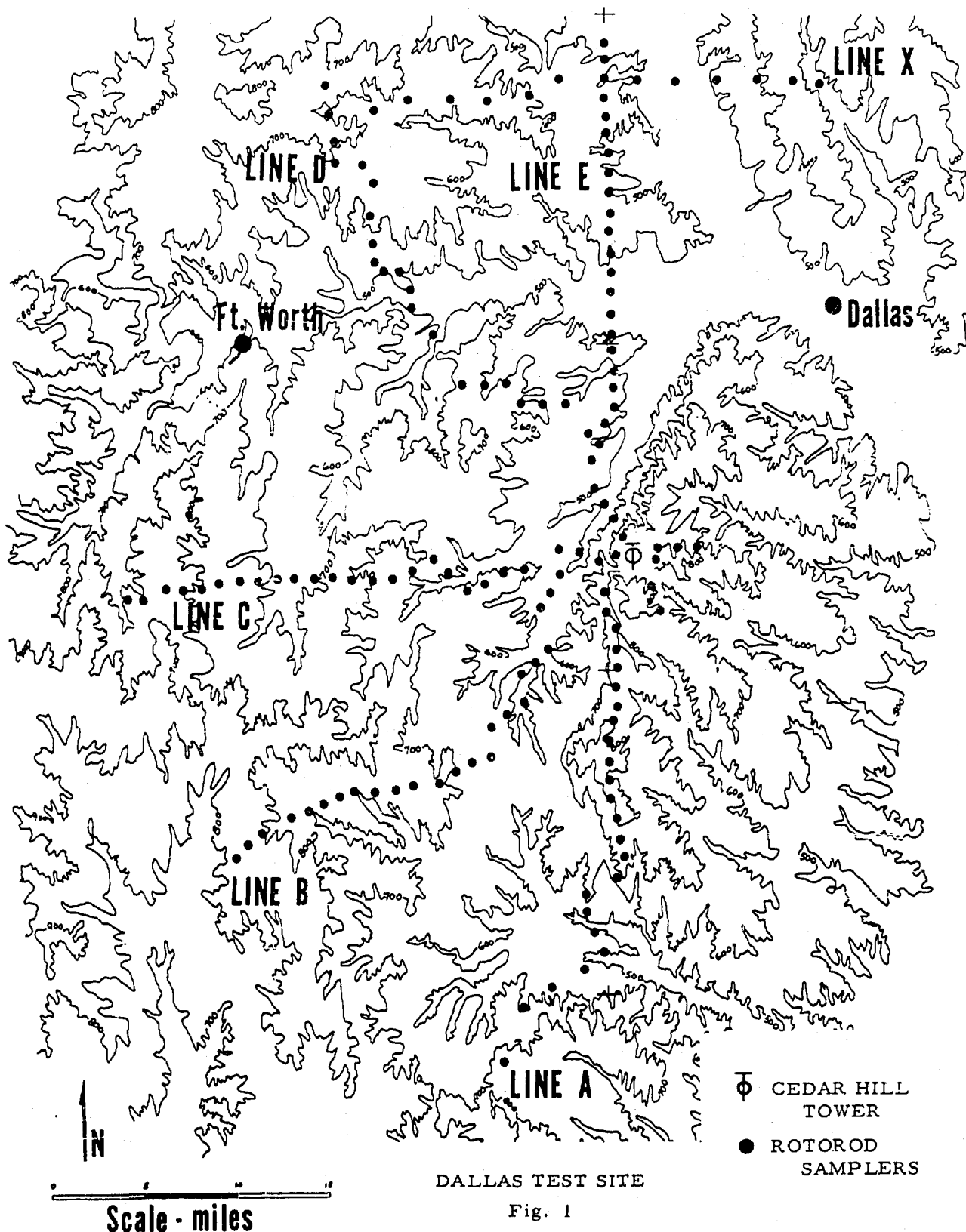
Rolling terrain immediately surrounds the tower which is located near the peak of a hill at an elevation of 820 feet above sea level. To the east and south the terrain elevation is about 750 feet while to the north and west there is an abrupt drop to 500 feet. In the immediate vicinity of the tower much of the land is heavily forested, but the greater portion of the test area is quite open.

#### D. Scope

In thirty-seven individual trials, line sources of fluorescent particle aerosol tracer (FP) were generated from a Dugway Proving Ground light aircraft in crosswind traverses upwind of the Cedar Hill tower. The trials were undertaken in three test periods in April, June, and August, 1961. All releases were made during the night to minimize the effect of thermal convection on the turbulent diffusion process. Source lines ranged from 9 to 26 miles in length, between one and seven miles upwind of the tower, and between 360 and 1050 feet above the tower base. While the release height and distance were determined by the test requirements and existing turbulence situations at release time, the length of the line was generally maximized in an attempt to produce an effectively infinite line source.

The tower data available from each trial consisted of the wind velocity-temperature record from 12 levels, the bivane turbulence record from 5 levels, and filter accumulations of FP from 13 levels in the first two test periods and 30 levels in the third test period. The wind velocity-temperature record was made available through the cooperation of the University of Texas and the Geophysics Research Directorate of the Air Force. Bivane installation and turbulence records were the responsibility of MRI. Filter installation, servicing, and filter data collection were the responsibility of DPG.

The rotorod sampler network used to obtain the horizontal dosage distribution was the primary surface instrumentation. This network,



DALLAS TEST SITE

Fig. 1

consisting of five downwind lines and one crosswind line, shown in Fig. 1, was also the responsibility of DPG. The downwind lines were oriented in a manner assuring suitable coverage in a variety of wind directions. A sixth downwind line was not used and will not be discussed further. The crosswind line which was situated near the end of the sampler line running north from the tower was used in thirteen of the trials to establish to what degree downwind dosages were affected by dilution of the edge of the cloud.

Additional instrumentation was used periodically to determine the time interval of cloud passage, the attainment of zero dosage between trials, a comparison of surface wind at the tower and at downwind locations, etc.

Planning and execution of the tests was the responsibility of MRI. Operational criteria were obtained from the tower instrumentation and from the facilities of the U.S. Weather Bureau office at Love Field in Dallas.

Filter and rotorod particle assessment was accomplished at Utah State University under a contract with DPG. DPG prepared wind velocities and Richardson Number tabulations from the U. of T. -G. R. D. tower data. Pertinent weather data from the teletype circuits were made available by the Weather Bureau. These data, together with the bivariate data, the reduction of which was the responsibility of MRI, were utilized in the analysis by MRI which is detailed in this report.

## II. FIELD OPERATIONS

### A. Tracer System

#### 1. Tracer

The aerosol tracer which was used in the vertical diffusion studies at the Cedar Hill tower was zinc cadmium sulfide containing one per cent by weight of micronized Valdron estersil for increased fluidity. The property of this material to fluoresce under ultra-violet illumination provides ready identification and facilitates visual assessment of the dosage on the collectors.

Lot 16 produced in February 1960 by U.S. Radium Corp. was used for all 37 trials. Table I shows an inspection report prepared by the Technical Evaluation Division of the U.S. Army Chemical Corps Biological Laboratories of this particular lot. It is shown that about 90 per cent of the particles are between one and five microns in size, thus assuring a negligible settling rate in an investigation of this scale.

TABLE I

#### Inspection Report - Zinc Cadmium Sulfide

Lot 16 (Blend of Batches 52, 53, 54)

<u>Particle Size Range</u>	<u>Per Cent of Particles in Each Size Range</u>
0.00 to .47 microns	1.28
.47 to .66	1.47
.66 to .93	3.80
.93 to 1.32	5.50
1.32 to 1.87	14.93
1.87 to 2.64	29.67
2.64 to 3.73	33.01
3.73 to 5.27	7.47
5.22 to 7.45	2.95

Mean particle count  $1.24 \times 10^{10}$  per gram.

#### 2. Disseminator

The dissemination of the fluorescent aerosol tracer was accomplished by a disseminator mounted in an L-23 aircraft. This disseminator was designed and fabricated by the Stanford Aerosol Laboratory under contract to DPG. Modifications subsequent to initial calibration runs were made by DPG. An average dissemination efficiency of 39 per cent with a range of efficiencies between 24 and 59

per cent was obtained in the five reliable calibration runs which followed the necessary modifications. Since the efficiency was determined with a flow rate of approximately 3.25 pounds per mile, it was considered inadvisable to disseminate at a rate much different from this. However, in the first test series the average dissemination rate was 2.80 pounds per mile and, in order to secure a longer source line in Test Series 2 and 3, the dissemination rate was reduced to an average value of 2.45 pounds per mile with no apparent change in average efficiency. An increase from fifty pounds of FP disseminated in Test Series 1 to sixty-five pounds in Test Series 2 and 3 resulted in a further increase in the length of the source line to 25 miles. The particle recovery on the samplers was considerable even at the lowest dissemination rates used. Further reduction in the dissemination rate in order to increase the length of the source line appears feasible for diffusion studies where comparable downwind distances are considered.

### 3. Sampling Devices

Two distinct aerosol sampling techniques were utilized in the Cedar Hill tests. The filter samplers which were used on the tower accumulated FP by drawing air through a Millipore filter while the rotorod samplers depended on impacting FP onto high-speed, rotating rods. **The former system with its sampling efficiency rated at 100 per cent** was limited to use on the tower by the 110-volt a. c. power requirement of the Gast pump. The rotorod sampler, powered by dry cell batteries and therefore both compact and mobile, proved quite successful in measuring the downwind dosages on the ground.

#### a. Filter Type Samplers

The filter samplers were operated in two different ways during the Cedar Hill tests. In the first two test periods a total of thirteen samplers were located on the twelve tower levels and at the base of the tower. Each sampler was equipped with ten filters and the timing mechanism was pre-set to activate within a half hour prior to the expected time of the first release and to cycle hourly for the following ten hours. Throughout the time of operation, an appropriate critical orifice maintained the flow at 12.5 liters per minute. It was expected that the operation schedule would insure that the filters contaminated by each trial would be separated by one or more zero count filters. Failure in the first test series to attain zero counts between tests in all cases resulted in the positioning of inert control filters during the second test period. These control filters indicated that particles were being accumulated on the inert filters by impaction.

In order to eliminate the impaction problem and to achieve better vertical definition of the aerosol cloud, the filter network

operation was substantially modified for the third test period. With the aid of a booster pump and reduction of the sampling rate to 6.5 liters per minute, it was possible to operate up to three filters simultaneously from each sampler. Consequently, the number of filters on the tower was increased to thirty with a spacing of 50 feet, in general. The cycling capability of the samplers was not utilized during the third test period. Instead, only one set of filters was exposed during a trial with activation of the sampler pre-set for half an hour prior to release and terminated approximately three hours after the release when the filters were replaced for the following trial. Impaction of FP from one trial on filters of following trials was thus prevented.

#### b. Rotorod Samplers

The rotorod samplers were used for surface sampling on the five downwind and one crosswind lines shown in Fig. 1. The entire sampler consists of a small electric motor whose speed of rotation is maintained at 2400 r.p.m. by a governor. The motor is powered by two 6-volt dry cell batteries in series and is used to drive a set of U-shaped rods. The impaction surfaces of the rods, measuring .015 inch by 6 cm., are covered with a light layer of silicone grease. **The entire package, scarcely larger than the dry cell batteries, is designed for emplacement atop a 2-inch by 2-inch wooden post.** By virtue of their compactness and simplicity, they can be installed and activated on a thirty-mile line at intervals of one mile in approximately two hours providing the posts are already in position. Consequently, five lines of posts extending radially from the tower were installed by DPG personnel prior to test operations to provide adequate downwind coverage regardless of wind direction. The post height permitted sampling at approximately five feet above the surface.

During the second test period a crosswind line of rotorods was installed across the northern end of rotorod line E. The purpose of this line was to indicate the existence of dilution near the ends of the source line. Such dilution, which would be absent from the infinite line source which was assumed, must be recognized in order to account for reduced dosages along the downwind line due to this effect. In addition, the crosswind line permits an attempt to correlate horizontal dilution at the cloud edge with horizontal wind fluctuations. After the establishment of the crosswind line X, it was used in the 13 succeeding trials in which the downwind E line was used. Similar crosswind lines on the other four downwind lines were not installed due to limitation of time and budget. However, only five trials were conducted in the last two test series without the benefit of crosswind lines.

The sampling rate of the rotorod sampler is less well defined than that of the filter sampler. However, if meaningful total dosage data is to be obtained the two systems must be comparable and the effective rate must be known. A nominal flow rate of 40 liters/minute was attributed to the rotorod sampler on the basis of its operating geometry by the Aerosol Laboratory at Stanford University (Aerosol Laboratory, 1960). In the same report the efficiency of the rotorod is placed at 38.9 per cent for an effective sampling rate of 15.5 liters/minute. However, comparisons of the filter and rotorod counts, where possible, from the Cedar Hill data showed the effective rate of the rotorod sampler to be about 33 liters/minute suggesting an efficiency of about 80 per cent. This comparative data has been used in the present analysis rather than the Stanford information. Details of the comparison of filter and rotorod test data are given in Appendix A.

## B. Meteorological Observations

### 1. Bivane System

Turbulence measurements were made at the 30, 150, 450, 750, and 1050-foot levels with MRI bivanes. The bivanes measure both the vertical and horizontal components of wind fluctuations. However, recording limitations prevented full utilization of the bivanes. Therefore, measurements of the vertical components were made at all five levels and of the horizontal at one level. A full description of the bivane with its response characteristics is given in Appendix B.

A seven-channel tape recorder located at the tower base recorded the six bivane component signals and time. Simultaneously, recording of these seven quantities was made on the paper tape of a modified two-channel Brush recorder in order that the turbulence measurements could be monitored to obtain criteria required for the test operation.

### 2. Wind Velocity and Temperature System

The wind velocity and temperature system on the tower was installed and operated by the University of Texas under Air Force contract. Bendix-Friez Aerovanes and aspirated copper-constantan thermocouples were mounted at the 12 levels which were previously noted. The Aerovanes presented wind velocities in their north-south and east-west components. Temperature was obtained only at the 30-foot level and temperature differences between adjacent levels were measured above that point. All of the University of Texas instrumentation was wired into a computer room at the tower base where integration and averaging of the input signals was provided automatically.

Averaging intervals of ten minutes during the first two test series and five minutes during the third test series were used. Output was recorded on punched tape and, through use of a Friden Flexowriter, was also printed. The printed output allowed ready utilization of these data for operational planning. All printed data were subsequently made available by GRD for the analysis phase. A complete description of the University of Texas instrumentation is given elsewhere (Mitcham and Gerhardt, 1960).

### 3. Synoptic

Additional meteorological information for operational planning and analysis was provided by the U.S. Weather Bureau office at Love Field in Dallas. Maps and teletype data were consulted prior to proposed test nights. Detailed interpretation in terms of the expected winds, thunderstorms, and cloud cover was provided by Weather Bureau personnel prior to and during the test nights. In addition, all teletype data were released to MRI for the analysis phase.

### C. Communications

Coordination during the test nights was provided through radio and **telephone communication. Contact with the surface crews who maintained the rotorod lines was achieved with telephone and FM radio. Preliminary** instructions to the aircraft crew were given by telephone and in-flight contact was maintained on a VHF radio channel. Frequent telephone contact with the Weather Bureau during the test nights provided current information on the synoptic situation.

### D. Operational Procedure

During a test period of two weeks, it was planned that alternate nights would be designated as test nights, weather permitting. It was further anticipated that three trials could be made on each test night. As a consequence of rain, thunderstorms, light and variable winds, and low clouds, 37 trials out of a maximum of 54 were made during the three test periods.

Several factors controlled the scheduling of trials during a test night. It was considered inadvisable to operate the rotorod samplers in excess of four hours due to the chance of obscuring FP by dust, pollen, and insects impacted on the rods. This limitation occasionally conflicted with the desire to sample throughout passage of the entire cloud. Movement of a cloud which reached the surface shortly after release would require in excess of four hours to clear the downwind end of the rotorod line under conditions of low surface wind.

A further complication in securing three trials per night was the brief extent of darkness during the summer. With about 10 hours of darkness

available, low wind conditions would require that either the first or the third trial extend into daylight. The latter course was taken since thermal convection remains high until sunset but is fairly low in the first hours following sunrise.

On the basis of the foregoing factors, a tentative test night schedule was developed for releases at 2000, 2400, and 0400 CST. In the event that winds were sufficiently high to flush the cloud from the area in less than four hours, the three trials were completed in darkness on a revised schedule. The schedule given below in Table II is typical of a night during the third test period when the operational procedures had been optimized. Absent from the schedule are the times required for maintenance and calibration of equipment which necessarily preceded all operations.

TABLE II

Typical Operations Schedule

1400-1500	Analysis of synoptic weather situation at Weather Bureau.
1500	Inform ground and air crews of intention to conduct trials.
1800	<b>Check Weather Bureau forecast and inform ground and air crews of confirmation to test. Commence installation of filters on the tower and pre-set to activate at 1945.</b>
1845	Check wind conditions at the tower. Commence installation and activation of appropriate downwind rotorod sampler line.
1915	Inform aircraft crew of probable release height, track, and upwind distance from tower.
1930	Commence operation of bivariate system. Completion of tower installation.
1945	Commence installation and activation of crosswind sampler line (if available). Contact aircraft with confirmed flight plan, wind velocity, and temperature at release height as determined from tower instrumentation.
2000	Begin release of FP.
2045	Completion of all rotorod installation.

The schedule for subsequent trials was identical to the schedule beginning at 1800 for the first trial with all operations occurring four hours later for each succeeding trial. Tower and rotorod samplers were

deactivated from the previous test and reactivated for the following test at the same time. Thus, final deactivation of the rotorods was completed at 0845. Fresh magnetic tapes were installed in the bivariate system also at four-hour intervals. Following a test night, the particle samples on rods and filters were packaged and sent to Dugway for evaluation. Turbulence records were stored and returned to MRI at the completion of each test period.

### III. DATA REDUCTION

#### A. Particle Assessment

Particle assessment was performed at Utah State University under contract from Dugway Proving Ground. The total counts were determined manually with recounting of random samples by a different person as an error assessment. Examination of the dual counts reveals that on the average they differ from their mean by less than 5 per cent. Tabulation of the count data was forwarded to MRI within a few weeks following the test series.

#### B. Wind and Temperature Data

Wind and temperature data from the tower were forwarded to MRI from GRD in two forms. In addition to the tabulation of wind components, 30-foot temperature, and temperature gradients, identical information on IBM punch cards was made available. The punch cards were forwarded to Dugway where, with computer processing, resultant wind speeds and direction and Richardson Numbers were calculated and, subsequently, returned to MRI.

#### C. Bivane Data

The wind fluctuations which were recorded during the diffusion tests are in themselves difficult to interpret since they are composed of a random mixture of wavelengths of varying intensity. Consequently, reduction of bivane data to a usable form is of considerable importance. Through use of the sigma meter, which is fully described in Appendix B, the fluctuations were examined for their standard deviation (sigma) from the mean for three ranges of frequencies. The sigma meter output consists of three continuous, integrated and averaged records of sigma, corresponding to the three frequency ranges. From this information, the intensity of turbulence can be related to eddy size and the correlation with particle distribution can be examined.

The final step in the data reduction process is the presentation of the above mentioned processed data with the geometry of the FP release to give an integrated representation of each trial.

#### IV. DIFFUSION CONSIDERATIONS

##### A. Meteorological Factors

In the recent literature on atmospheric diffusion there has been an increasing tendency to relate diffusion observations directly to the turbulent properties of the atmosphere which cause the diffusion. This approach is in contrast to earlier studies which related gradients of the mean temperature and wind fields to observed diffusion under the implicit assumption that these gradients were directly related to the turbulence parameters. The present study is confined entirely to the direct relationship between turbulence and diffusion. The large scale synoptic features of the weather and the properties of the mean wind and temperature fields are considered primarily as they may influence the turbulence itself.

The geostrophic wind is a measure of the pressure gradient associated with the large scale synoptic weather pattern. It may be considered as the ultimate reservoir from which any turbulent wind energy must be derived. In low geostrophic wind cases there is little kinetic energy of motion available at any time for the creation of turbulent energy which can, in turn, result in diffusion. In cases of stronger geostrophic winds there must exist a turbulent mixing layer close to the ground surface in which the frictional influence of the ground operates to slow down the pressure gradient - driven wind aloft. Thus the geostrophic wind is a rough but immediate indication of the turbulence existing in the layers close to the ground under nighttime, non-convective conditions.

The geostrophic winds for the Texas tower tests were computed by plotting hourly pressure maps from airways weather reports for the hour nearest to release time. These maps were plotted for the area of Oklahoma and Texas. Isobars were drawn for each millibar pressure interval on these maps and the geostrophic wind (sea level) computed from the spacing between isobars in the vicinity of Dallas. Results of the geostrophic wind calculations, which are given in Part II, Volume II, suggest weaker turbulence conditions in Trials 33 - 38 than during the remainder of the tests.

Provided sufficient ordered energy is available in the geostrophic wind, a mechanism for conversion into turbulent energy must be present. The primary mechanism at night is wind shear and the primary source of the shear is friction induced by ground roughness. It is well known that density forces operate to suppress the turbulence effects created by wind shear. Thus the effects of wind shear and temperature have been traditionally combined into the Richardson number:

$$Ri = \frac{g}{T} \frac{(\frac{\partial T}{\partial z} + \Gamma)}{2 \left( \frac{\partial u}{\partial z} \right)^2}$$

where  $T$  is the air temperature,  $\Gamma$  the adiabatic lapse rate of temperature, and  $u$  is the mean horizontal wind velocity. The Richardson number expresses the relation between a buoyancy force (temperature stability) tending to restrict turbulent motion in the numerator and a wind shear force in the denominator which tends to create turbulence. Originally a  $Ri < 1$  criterion was believed to be associated with turbulent flow but subsequent measurements and theory suggest a  $Ri$  value  $< .3$  as a more reasonable criterion for generation of turbulence.

Turbulence measurements from bivane sensors are given in terms of the angle of the vector sum of the horizontal velocity and the vertical velocity with rapid time-response. If the mean horizontal velocity is known (from Friez Aerovane sensors in the Dallas case) the vertical velocity component at any instant can be found by:

$w' = u' \tan \alpha$ , where  $u'$  is the vertical velocity,  $u$  is the horizontal velocity, and  $\alpha$  is the instantaneous angle measured by the bivane.

An angle  $\sigma$ , measured by the sigma meter, can be defined as the RMS value of  $\alpha$  over a specified interval of time and under the assumption of a normal distribution of  $\alpha$  around the mean position of the vane. As a consequence:

$$w_1' = u \tan \sigma$$

gives the RMS value of the vertical velocity over the specified interval of time. By definition,  $\rho/2 (w_1')^2$  is the average turbulent energy of vertical motion for the specified interval of time. For simplicity,  $(w_1')^2$ , the vertical velocity variance, is usually used as a measure of turbulent energy without the complicating factor of  $\rho/2$ .

The angle  $\sigma$ , in general, (and the turbulent energy) increases within the period of time over which the average wind fluctuation (RMS value) is taken. This is discussed further in Appendix B. As the time interval is increased further,  $\sigma$  increases at an increasingly slower rate and a near-asymptotic value can be established. Following the notation of Smith and Hay (1961), this asymptotic value of  $\sigma$  has been referred to as  $i$ , the intensity of turbulence.

The characteristics of the vertical velocity variance in the Dallas tests as a function of height, stability, geostrophic wind, and Richardson number are given in Section V. Details of the turbulence measurements themselves are included in Appendix B.

The following sections will discuss the connection between turbulence and diffusion with special reference to the aerial line source case.

## B. The Diffusion of Clusters

An aerial line source may be considered as a long series of instantaneous point sources. The center of each small cluster of particles drifts with the mean wind, diffusing in all directions. In a direction parallel to the release line, there is a continual interchange of particles along the line due to diffusion among the adjacent point sources and an essentially uniform particle distribution is maintained in this direction except near the ends of the release line. In a direction along the mean wind the cloud diffuses according to the characteristics of an instantaneous point source. However, the primary practical interest is in the total dosage at a fixed point resulting from passage of the entire cloud. Consequently, diffusion along the mean wind is usually not considered to any extent.

In the vertical direction diffusion also occurs according to instantaneous point source characteristics. Although the rate of spreading of the cloud is the same as the point source, concentrations in all regions of the cloud are greater than the point source values due to lateral mixing from adjacent portions of the release line. The attention of the present project is directed entirely toward the quantitative characteristics associated with the vertical diffusion of the cloud.

It has been recognized for the past few years or more that the rate of growth of a cluster of particles was, in part, dependent on the size of the cluster. Only turbulent eddies of a size comparable to the size of the cluster contribute significantly to the diffusional growth of the cluster. Eddies of much smaller size influence only a small portion of the cloud and thus do not contribute greatly to diffusion growth.

This concept immediately suggests that a knowledge of the turbulent energies existing in the atmosphere at various eddy sizes is essential for an understanding of the aircraft line source release. This requirement has formed the fundamental basis for the Dallas Tower Project.

The turbulent energy spectrum gives the amount of turbulent energy existing in the atmosphere as a function of eddy size. A typical spectrum is shown as Fig. B-4 in Appendix B. Kolmogoroff (1941) has termed a portion of the small eddy size range as the "inertial subrange" and has shown that

$$E(l) \sim l^{-5/3}$$

in this range where  $E$  is the turbulent energy at a wavelength  $l$ . The existence of the  $-5/3$  law has been demonstrated in the atmosphere for a wide range of eddy sizes (MacCready, 1962).

After a brief period of travel but when the cluster size is still comparable to the small wavelengths where the inertial subrange concepts apply, Batchelor (1950) was able to show that the particle cloud size should increase as a function of  $t$  (time) initially and subsequently increase according to  $t^{3/2}$ . The increase in growth rate is in accordance with the typical energy spectrum which shows that, in the inertial subrange, particle clouds of increasing size come under the influence of greater supplies of turbulent energy (larger wavelength) and their growth rate is correspondingly increased.

At still larger cloud sizes the slope of the energy spectrum decreases and a maximum energy level occurs at some particular eddy size. For still larger eddy sizes little additional energy is added to that already available for diffusion and the rate of cloud growth decreases.

In accordance with these characteristics of the energy spectrum, particle clouds of large size no longer maintain the  $t^{3/2}$  functional dependence and eventually, at very large cloud sizes, the time dependence becomes  $\sim t^{1/2}$  corresponding to a continuous source at large distances.

These time dependency functions and physical concepts are the boundary rules which theories of the diffusion of clusters must follow. Batchelor's contribution was to point out these functional dependencies but the exact relationships were not derived.

Smith and Hay (1961) have formalized these ideas into a quantitative system for describing the diffusion of particle clusters if the environmental turbulent energy conditions are known. One portion of the system makes use of the detailed turbulent energy spectrum in the diffusion description. From the standpoint of practical use of the system, the principal interest lies in an approximate system which is said to be valid for cloud sizes throughout most of the inertial subrange and extending to cloud sizes several times larger than the turbulence scale  $L$  where  $L$  has the broad meaning of an average eddy size.

The Smith-Hay approximation essentially computes the rate of growth of the cloud at the time that the cloud size  $\sigma = .655 L$ . The cloud is then assumed to grow at the same rate throughout the regime for which the approximation applies.

Under the assumptions of the approximation the rate of growth of the cloud is given by:

$$\frac{d\sigma}{dx} = 3i^2 \quad \text{where } \sigma \text{ is a measure of the cloud size, } i \text{ is the}$$

turbulent intensity (see previous section) measured by a suitable instrument,

and  $x$  is the downstream distance. In this usage,  $i$  must include all of the turbulent energy, regardless of eddy size. In the Dallas Tower studies  $i$  is equivalent to  $\sigma_{180}$  (see Appendix B, Section D).

The Smith-Hay treatment clearly indicates the importance of direct measurements of turbulence in describing the diffusion growth of a cluster. The practical problems of obtaining a full turbulent energy spectrum for each diffusion case of interest almost prohibit the use of the detailed Smith-Hay formulation in operational problems. It is consequently of considerable concern to determine the reliability of the  $3i^2$  approximation.

The use of the  $3i^2$  approximation in predicting tower and ground dosages is discussed in the following section.

### C. The Diffusion Model

#### 1. Tower Dosage

Vertical sampling at various levels on the tower affords an excellent opportunity for measuring vertical cloud growth at some distance (or time) after release from the aircraft. Following the Smith-Hay approximate formula for the growth of clusters, the **vertical growth of the cloud should be given by:**

$$\frac{d\sigma_z}{dx} = 3i^2 \quad \text{where } \sigma_z \text{ is the vertical cloud size, } x \text{ is} \quad (1)$$

the downwind distance, and  $i$  is the intensity of vertical turbulence.

The cluster diffusion model is developed for turbulence which is homogeneous in time and in space. The latter is not a good approximation for many releases made at low levels since the turbulent intensity changes markedly with height close to the ground. As a consequence, the model would be expected to apply best to those cases when the vertical spread of the cloud on the tower was not too great.

The Smith-Hay model also applies up to cloud sizes which are "within an order of magnitude of the length scale of the turbulence". For the Dallas tests, the cloud size measured on the tower was generally within a factor of two or three of the turbulence length scale.

#### 2. Ground Dosage

Although the source in the Dallas Tower tests consists of an instantaneous line release, it is useful in the development of the theoretical ground dosage pattern to consider also a continuous source at the same time. In addition, the discussion of both source

configurations simultaneously provides valuable insight into the mechanics of the diffusion and suggests a method of approach for source types other than the aircraft line release.

There have been two recent practical attempts to describe the diffusion from a continuous point source in terms of measured atmospheric parameters rather than the previously used diffusion coefficients of the Sutton type. Meade (1960) has developed a system for describing the spread of the cloud in terms of various combinations of wind speed, insolation, and cloud cover. Pasquill (1961) has presented a similar system but with the additional option of describing the cloud spread by measured turbulence parameters rather than through the indirect variables of wind speed, insolation, and cloud cover.

Pasquill forms an expression for the ground concentration downwind of a continuous point source located at a level  $H$  above the ground as:

$$X = \frac{Q}{\pi \sigma_y \sigma_z u} e^{-\left(y^2/2\sigma_y^2 + H^2/2\sigma_z^2\right)} \quad (2)$$

where  $X$  is the concentration,  $Q$  is the source strength,  $\sigma_y$  and  $\sigma_z$  are cloud sizes at the point where the concentration is being computed,  $u$  is the wind velocity, and  $y$  is the horizontal crosswind distance from the centerline axis of the plume.

An analogous expression for the concentration at a downwind location can be found for a continuous line source located at a level  $H$  above the ground:

$$X = \frac{2 Q' e^{-H^2/2\sigma_z^2}}{\sqrt{2\pi} \sigma_z u} \quad (3)$$

where the source strength,  $Q'$ , is now given in quantity per unit time per unit length along the line.

As pointed out by Pasquill this expression for the concentration from the continuous source is equivalent to the total dosage received at the same point if the source strength,  $Q^*$ , expresses the total quantity released per unit length along the line rather than the rate of release. With these changes Equation (4) gives the total dosage at any downwind point on the ground from an instantaneous line source.

$$D = \frac{2Q''}{\sqrt{2\pi} \sigma_z u} e^{-H^2/2\sigma_z^2} \quad (4)$$

The relations between the parameters for the instantaneous and continuous line source cases are shown in the following table:

	Continuous	Instantaneous
Source Strength	$Q'$	$Q''$
Source Units	$\frac{\text{particles}}{\text{length-time}}$	$\frac{\text{particles}}{\text{length}}$
Sampling Parameter	Concentration, $X$	Dosage, $D$
Sampling Units	$\frac{\text{particles}}{\text{length}^3}$	$\frac{\text{particles-time}}{\text{length}^3}$

It is now assumed that the instantaneous line source cloud grows vertically in the same manner as the cluster whose growth is described by Equation (1). Thus, for the conditions under which this approximation can be assumed to hold, Equation (4) becomes:

$$D = \frac{2Q''}{\sqrt{2\pi} (3i^2 x) u} e^{-H^2/2(3i^2 x)^2} \quad (5)$$

This expression gives the ground dosage at any point  $x$  downwind of the instantaneous line source release. For the continuous line source case the vertical spread of the cloud,  $\sigma_z$ , is given by  $\sigma_\phi x$  (Hay-Pasquill (1959)) where  $\sigma_\phi$  is the standard deviation of wind direction suitably measured by a fast-response bivanometer or other sensor. Thus  $\sigma_\phi x$  would be substituted in Equation (3) for  $\sigma_z$  in the continuous case.

Equation (5) may be used to find the location and magnitude of the maximum ground dosage for comparison with the test results. If Equation (5) is differentiated with respect to  $x$  and the resulting expression set equal to 0 and solved for  $x$ , the result is the distance from the release line to the point of maximum ground dosage:

$$x_{\max} = \frac{H}{3i^2} \quad (6)$$

If Equation (6) for the location of the maximum dosage is substituted in Equation (5), the dosage at this location may be found as:

$$D_{\max} = .485 \frac{Q''}{uH} \quad (7)$$

Equations (5), (6), and (7) provide a simple model which can be used to explain the observed test results. However, there are certain limitations and assumptions involved in the model which will be summarized in the next section.

#### D. Limitations of the Diffusion Model

##### 1. Turbulence Scale

The approximation of:

$$\frac{d\sigma_z}{dx} = 3i^2$$

is expected to apply to cloud sizes of the same order of magnitude as the turbulence scale  $L$ . For larger cloud sizes, according to Smith-Hay, the cloud grows at a slower rate  $\propto t^b$  where  $b < 1$ . At this stage the growth regime becomes more analogous to a continuous source cloud.

##### 2. Homogeneous Turbulence

The model of ground dosages (Equation (5) of the previous chapter) assumes homogeneous turbulent conditions from the release height to the ground. This is a generally poor assumption and an "effective" turbulence must be used in the formula to represent an average of the turbulent conditions encountered between the release height and the ground. An effective turbulence value may be computed in several ways but must, in some manner, include a weighting factor which permits the layers of low turbulence values to contribute in greater measure to the effective turbulence than the higher values. This requirement is necessary because the cloud spends much of its travel time in the low turbulence layers but moves relatively quickly through the higher turbulence layers.

A simple system for computing the effective turbulence is shown diagrammatically in Fig. 2. Turbulence values ( $\sigma$ ) are measured at five points,  $L_1, L_2, L_3, L_4, L_5$ . The average turbulence in the layer between  $L_1$  and  $L_2$  may be expressed as  $\sigma_1 + \sigma_2/2$ , etc. An averaging system which weights the low turbulence layers more heavily and also

includes the depth of the layer over which the average turbulence acts is:

$$\frac{H}{i_e} = \frac{2h_1}{\sigma_1 + \sigma_2} + \frac{2h_2}{\sigma_2 + \sigma_3} + \frac{2h_3}{\sigma_3 + \sigma_4} + \frac{2h_4}{\sigma_4 + \sigma_5} + \frac{h_5}{\sigma_5}.$$

where  $h_1$  = the depth of the layer bounded by the points  $L_1$  and  $L_2$ , etc., and  $H = h_1 + h_2 + h_3 + h_4 + h_5$ . In effect, as shown in Fig. 2, the broken, dashed line is replaced by an "effective" turbulence angle, represented by the solid line. This equation may be used to compute  $i_e$  (total turbulence intensity) in the Dallas Tower tests if  $\sigma$  values read by the  $\sigma_{180}$  meter are used in the computations. As pointed out in Appendix B,  $\sigma_{180}$  includes virtually all of the turbulent energy present in the Dallas measurements and thus corresponds to  $i$ , the turbulent intensity, as defined by Smith and Hay (1961).

It is to be noted in the above equation that the last layer (lowest 30 feet) is considered to have a  $\sigma$  value equal to the value at 30 feet. Since the depth of the layer is so small this assumption does not cause any appreciable error in calculating  $i_e$ . Effective sigmas computed in this manner for all tests are given in Part III of Volume II.

### 3. Average Wind

The model of ground dosages (Equation (5) of the previous chapter) contains a horizontal wind velocity,  $u$ , which is assumed constant from the release height to the ground in the same manner as the turbulence is assumed constant.

A simple average wind has been computed by weighting the layer depths (Fig. 2) appropriately as

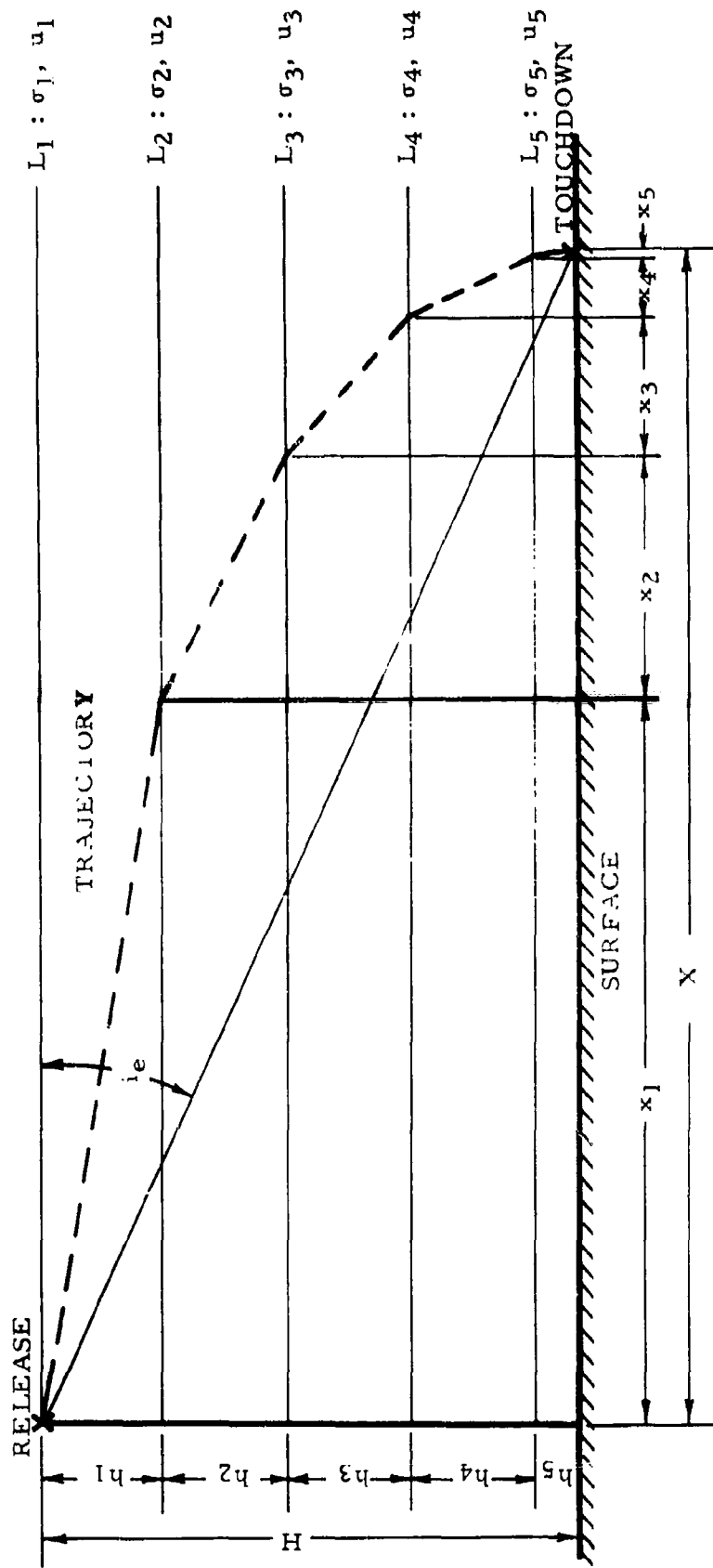
$$\bar{H}\bar{u} = \frac{h_1(u_1 + u_2)}{2} + \frac{h_2(u_2 + u_3)}{2} + \frac{h_3(u_3 + u_4)}{2} + \dots$$

where  $\bar{u}$  represents the average wind in the layer of depth  $H$  while  $u_1, u_2$ , etc. are measured velocities at the various levels  $L_1, L_2$ , etc.

Resulting average winds are shown in Part III of Volume II.

### 4. Time Homogeneity of Turbulence

Another assumption implicit in Equation (5) of the previous chapter is the homogeneity in time of the turbulence characteristics. Successful application of the model would require that the statistical character



CALCULATION OF EFFECTIVE TURBULENCE  $\sigma$  ( $i_e$ )

Fig. 2

of the turbulence should not change appreciably over the time interval necessary for the cloud to move to the end of the rotorod line (about 1-3 hours).

In most cases, turbulent intensity changes during such a time interval were relatively small. However, marked time changes occurred on Trial 19 (thunderstorms in the vicinity) and on Trial 36. In the latter case, low stratus clouds formed at the tower about 45 minutes after the release. The turbulent intensity increased very rapidly from a low value prior to the cloud formation to an implication of moderate turbulence at all levels below the cloud base. In the remainder of the trials the turbulent levels could be considered as steady during passage of the cloud along the rotorod line, particularly since spatial variations in turbulence along the line were likely to have been more important than the time variation at the tower.

## V. TEST RESULTS

### A. Introduction

A general summary of the meteorological conditions and sampling results appears in Volume II. Part I describes the synoptic situation existing on all test nights. Parts II and III give the geostrophic winds, average winds, and effective turbulence sigmas. Figures II-1 through II-74 summarize the data obtained during each test and present vertical profiles of wind speed, wind direction, vertical velocity variance, sigma, Richardson number, and stability together with the release height and vertical and horizontal dosage distributions. The following sections of this chapter are an analysis of the data appearing in Volume II.

### B. The Turbulence Environment

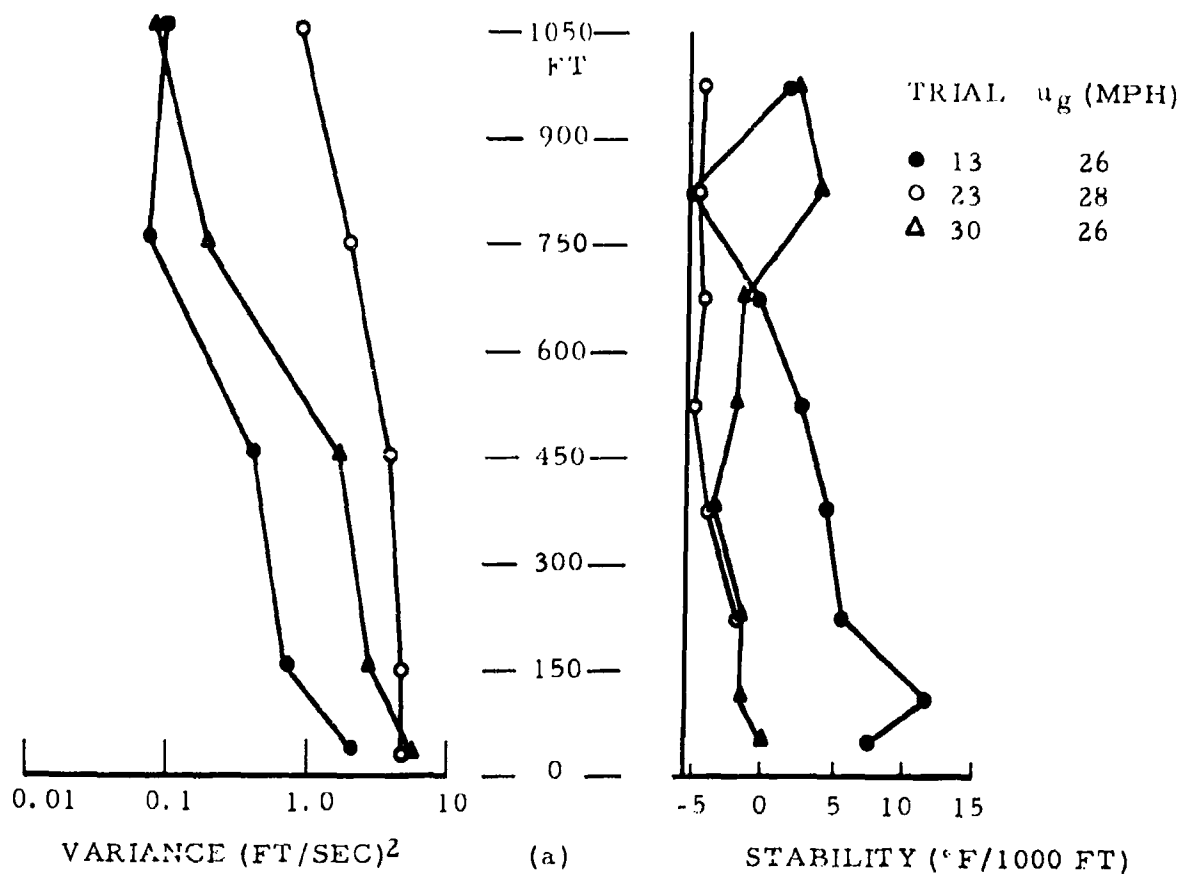
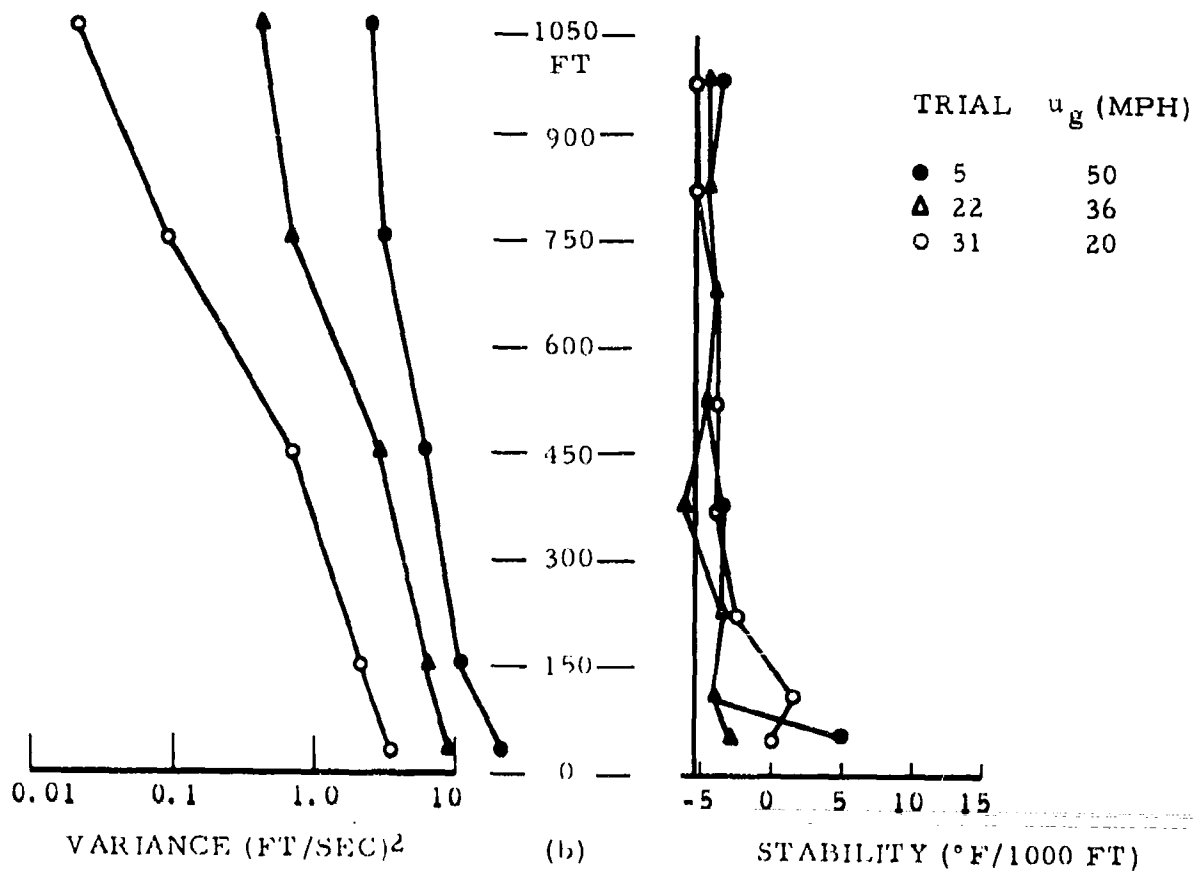
#### 1. Effects of Stability and Geostrophic Wind on Vertical Velocity Variance

During nighttime (non-convective) conditions the principal source of turbulent energy is ground roughness. Since the vertical temperature lapse rate is usually stable at night, the turbulent energy decreases in magnitude from the ground levels upward. Fig. 3a illustrates this process by comparing three tests with similar geostrophic wind velocities but varying temperature stabilities. Trial 13 with temperature inversion conditions to 600 feet shows the lowest values of vertical variance through these layers. Trials 23 and 30 had similar temperature stabilities in the lowest 450 feet but above this level the stability for Trial 30 was considerably greater than Trial 23. The vertical variances for the two tests are similar in the lowest 450 feet but the variance for Trial 30 decreases more rapidly above this level as a result of the greater temperature stability.

Fig. 3b shows the effect on vertical variance of varying the geostrophic wind velocity for three cases of similar temperature stability. Increasing geostrophic wind leads to increasing variance at all levels although the variance increases are greater at high levels. For this case of slight temperature stability, the effect of increasing geostrophic wind is to cause a more uniform turbulence level as a function of height throughout the lowest 1000 feet.

#### 2. Vertical Velocity Variance and Richardson Number

Fig. 4 shows the relation between Ri numbers and vertical variance for the levels 150 feet and 450 feet for all tests. The Ri numbers were calculated from temperature and wind profiles determined by 30-300 foot data and 300-600 foot data, respectively, while



DEPENDENCE OF VARIANCE ON GEOSTROPHIC WIND AND STABILITY

Fig. 3

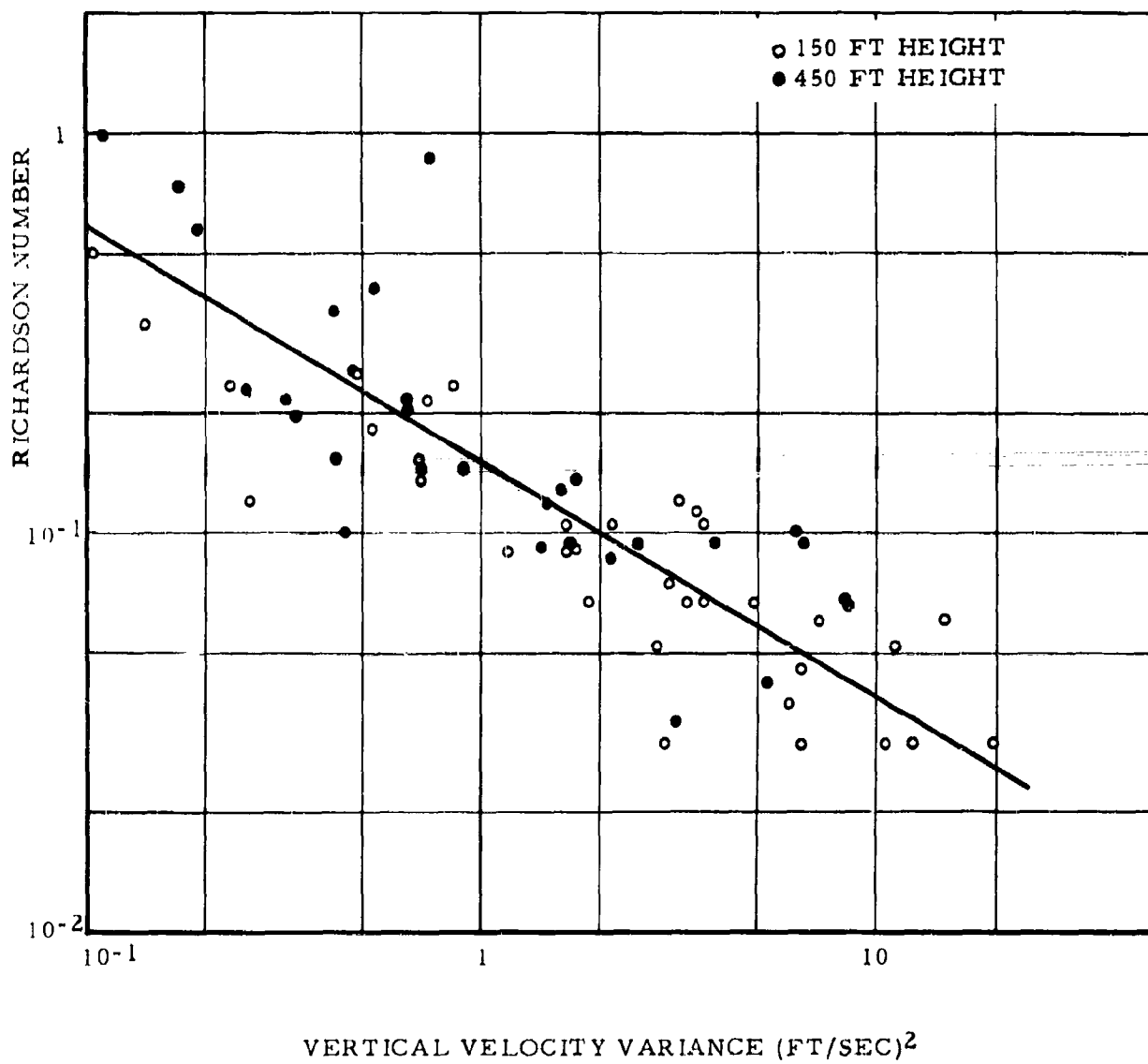


Fig. 4

the vertical variance was measured directly at 150 and 450 feet. It is apparent from Fig. 4 that nearly all of the 150 foot and most of the 450 foot data are associated with  $Ri$  numbers of .3 or less where continual turbulence generation would be expected. In this range there appears to be a linear relationship with log-log coordinates between  $Ri$  number and vertical velocity variance.

Figs. 5 and 6 show similar plots for the 750 foot and the 1050 foot levels. For these levels Richardson numbers greater than .3 are frequent, and it is clear that the relationship between  $Ri$  and vertical velocity variance becomes much less well defined. The straight line relationship shown in Fig. 4 for 150 and 450 feet is included for comparison in Figs. 5 and 6, and it is seen that this relationship is useful only to  $Ri$  numbers of around .3. For larger  $Ri$  numbers a new slope appears to be required although the scatter of the points is very large.

These figures indicate that, for  $Ri$  numbers less than about .3, a measure of the Richardson number provides an adequate description of the concurrent turbulence level. For larger Richardson numbers this is no longer true. At these large  $Ri$  numbers turbulence is not being generated continually under these conditions and the existing turbulence must be primarily turbulence which has been generated elsewhere and transported to the area where it is measured without having been damped out. Thus the turbulence intensity might have a wide range of values and not necessarily be associated with measured wind and temperature profiles.

To assure transport of material downward from an elevated release, it seems essential that the release be made in a layer where turbulence is being continually generated throughout the layer. According to the above, this requirement would be satisfied for layers in which the Richardson number does not exceed .3 at any level. For releases at higher levels, the figures indicate that turbulence may or may not be present between the ground and release level, and consequently the particle cloud may or may not reach the ground in substantial quantity. Even if substantial turbulence is measured at the higher levels under the conditions of  $Ri > .3$  it cannot be assumed that this turbulence is coupled mechanically with the lowest turbulent layers. The measured turbulence may be in an isolated layer, separated from the lower layer by a substantial quiet region.

### 3. Depth of Turbulent Layer

If the layer immediately adjacent to the ground in which  $Ri < .3$  is used as a criterion for the "turbulent" layer, the depth of this layer may be found from vertical profiles of the Richardson number. These depths are shown in Table III.

TABLE III  
DEPTHS OF TURBULENT LAYER

<u>Test</u>	<u>Depth of Turbulent Layer</u>	<u>Release Height</u>
1*	less than 150 ft.	380
2*	250	380
3	750	380
4	1050	680
5	1000	680
6	more than 1050	380
7	more than 1050	680
8	more than 1050	980
9*	275	680
10*	300	680
11	450	380
12*	less than 150	980
13	400	450
14	600	450
15	600	600
16*	580	750
17	900	600
18	850	450
19	620	450
20*	560	750
21	800	750
22*	700	1050
23*	880	1050
25	500	450
26	500	450
27	500	450
28	920	750
29	750	750
30	750	450
31*	550	1050
32*	550	750
33*	300	450
34*	300	450
35*	300	450
36*	200	450

For tests marked with an (\*) the releases were made at a height substantially above the top of the turbulent layer. In these cases the turbulent connection to the ground is uncertain, regardless of turbulent measurements made at the release height itself. It will

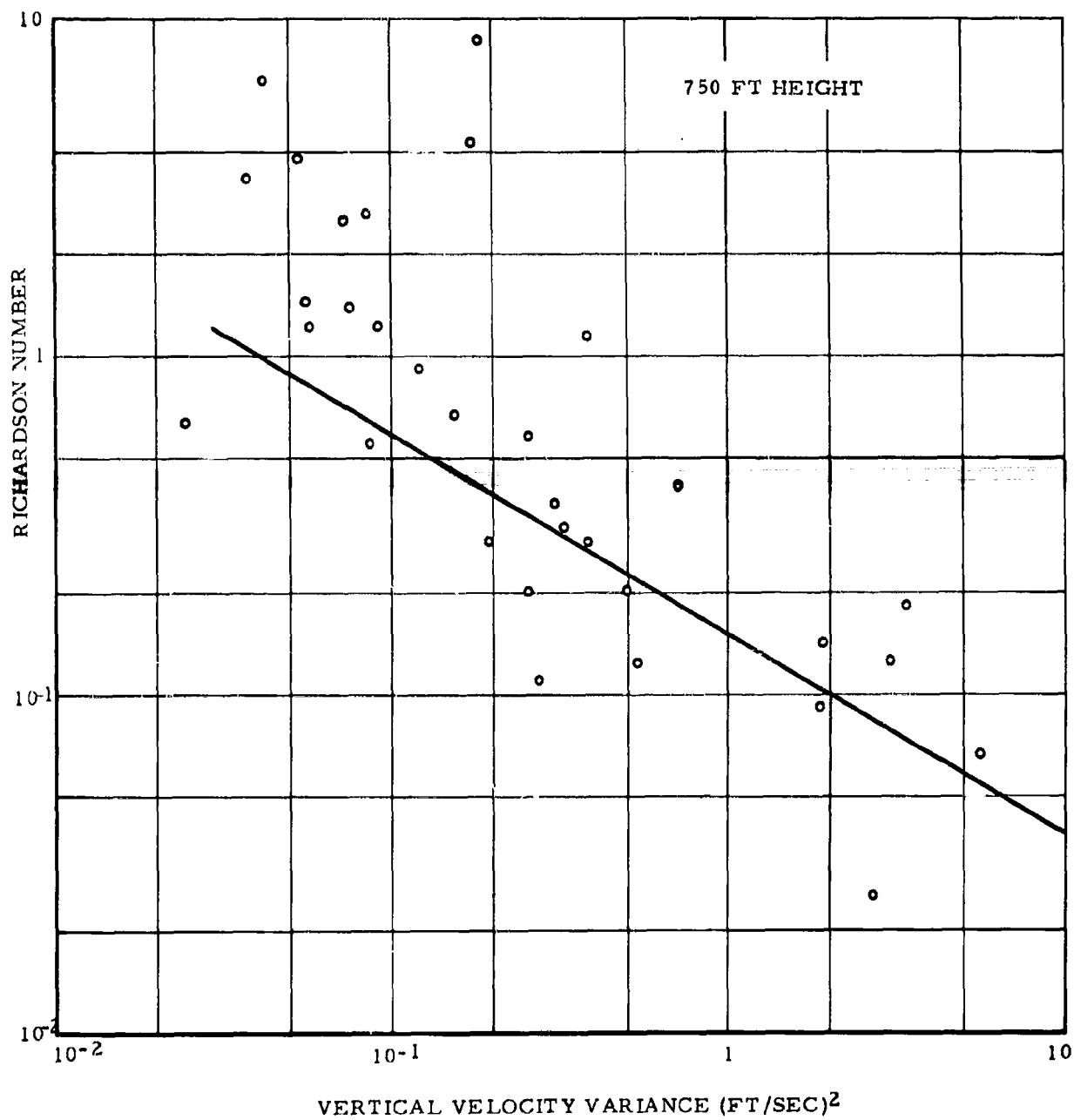
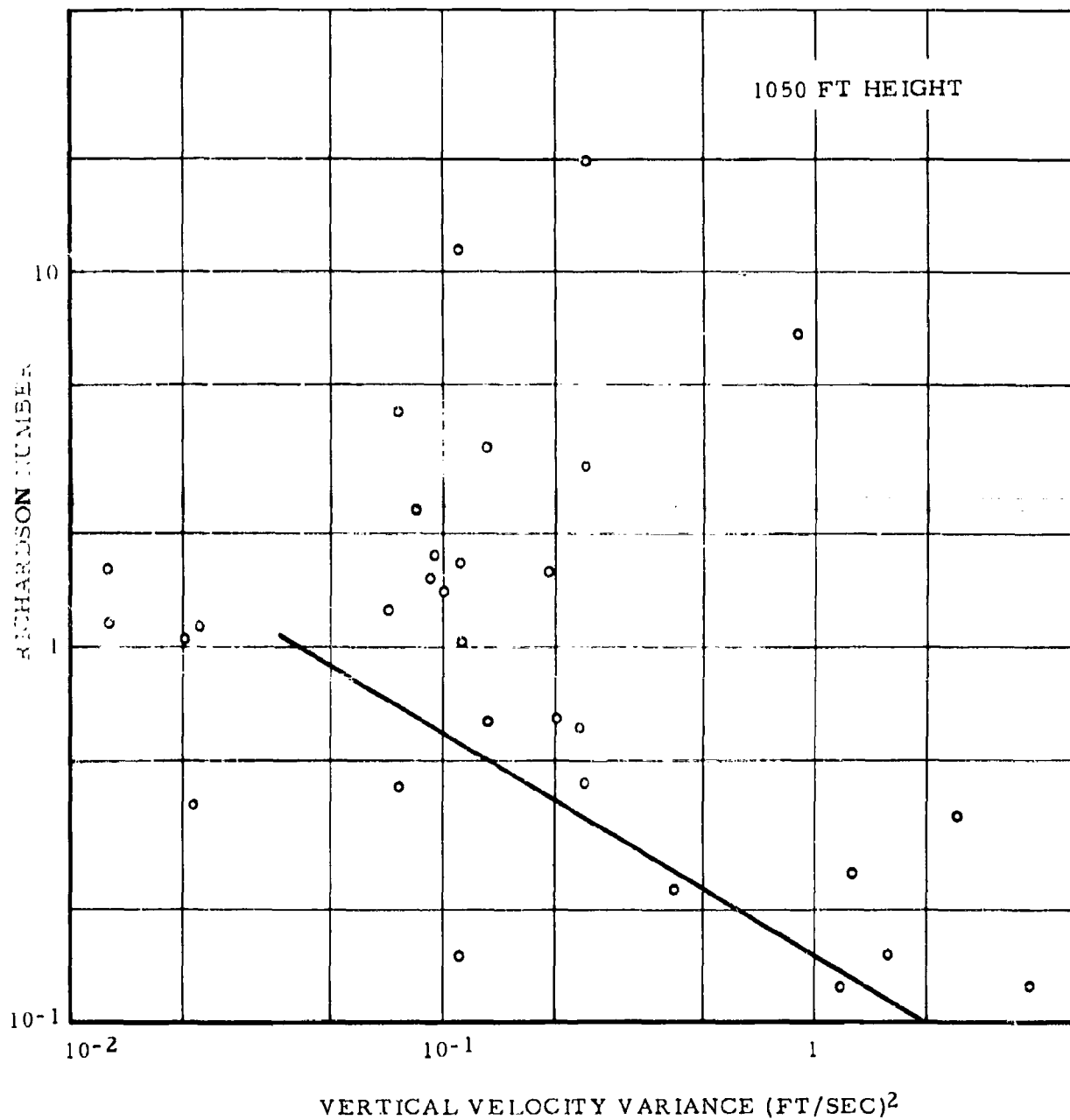


Fig. 5



be shown in a later section that the test results in terms of ground dosage are considerably more erratic for these cases than for the remainder of the tests where releases were made within the turbulent layer.

Table IV shows the distribution of turbulent layer depths for the various tests:

TABLE IV

<u>Depth of Turbulent Layer</u>	<u>No. of Cases</u>
400 ft. or less	10
400-600 ft.	10
600-800 ft.	6
more than 800 ft.	9

This distribution indicates that releases should be kept below 600 feet in most cases in the Texas area in order to avoid the erratic character of the ground dosages associated with release heights at higher Ri numbers. Deepest turbulent layers (Trials 4-8) occur with strongest geostrophic winds (over 50 mph) when the turbulent intensity is high throughout an extensive layer.

#### C. Vertical Diffusion

##### 1. Particle Budget Calculations

If the particle cloud does not spread vertically beyond the upward limit of the tower, it is possible to compute the total number of particles per unit length along the release line from the dosages measured as the cloud passes the tower. These may be compared with the total number of particles released by the aircraft. The technique for making these particle budget calculations is given in Dugway Technical Memorandum DPGTM 1045 which describes the "Field Calibration of the L-23 FP Disseminator". Results of the calculations for the Dallas tests are given in Tables V and VI for Trials 1-23 and Trials 25-37 respectively. The percentage recoveries shown have been compiled on the basis of an initial release of  $1.24 \times 10^{10}$  particles per gram.

Table V shows an average percentage recovery of about 28 per cent excluding one unreasonable value of 282 per cent in Trial 6. The figure of 28 per cent can be compared with the average of 39 per cent obtained in five calibration trials at Dugway with the same disseminator. (Technical Memorandum DPGTM 1045 and errata supplement.) The

relatively poor agreement between the first two test series and the calibration trials is apparently due to poor resolution of the vertical cloud distribution on the Dallas tower. Under the Texas conditions of low turbulence and small vertical cloud sizes, it appears that large numbers of particles (near the cloud center) passed between samplers on the tower and were not adequately sampled with the 150 foot vertical spacing used.

This inadequate sampling of the center of the cloud creates an additional problem in measuring the vertical cloud size as it passes the tower. If a true measure of the center of the cloud is not obtained the vertical cloud distribution will appear less "peaked" and the vertical cloud size, measured by fitting a normal distribution to the observations will appear larger than it should if the cloud were reliably sampled. This has been corrected for by adding sufficient particles at intermediate (unobserved) levels on the tower to make the percentage recovery more nearly 39 per cent. Vertical cloud sizes were then computed from this reconstructed vertical cloud distribution.

TABLE V

PARTICLE BUDGET CALCULATIONS

<u>First Test Series</u>		<u>Second Test Series</u>	
<u>Trial</u>	<u>% Recovery</u>	<u>Trial</u>	<u>% Recovery</u>
1	6.8	13	41.8
2	73.9	14	19.2
3	3.0	15	22.6
4	11.1	16	39.8
5	17.6	17	37.3
6	282.	18	36.3
7	49.	19	1.9
8	13.4	20	2.3
9	17.5	21	45.1
10	42.8	22	40.4
11	21.5	23	21.5
12	56.9		
Average 49.6%		Average 28.0%	
Average 28.5% (excluding Test 6)			

Table VI shows the results of obtaining better sampling on the tower by the addition of enough samplers to give 50 foot resolution. The

average percentage recovery of 44 per cent is in line with the calibration value of 39 per cent. Vertical cloud sizes for the third test series were therefore not corrected for inadequate sampling and the computed vertical cloud sizes for this series should be given more consideration than those of the first two test series.

TABLE VI  
PARTICLE BUDGET CALCULATIONS

<u>Third Test Series</u>			
<u>Trial</u>	<u>% Recovery</u>	<u>Trial</u>	<u>% Recovery</u>
25	47.5	32	37.9
26	32.5	33	49.2
27	73.6	34	25.6
28	21.8	35	54.1
29	65.5	36	27.9
30	58.9	37	52.5
31	31.0		

Average 44.5%

## 2. Computation of Vertical Cloud Size

During the course of particle budget calculations the total number of particles passing the tower in various layers was computed. If the total number of particles passing the tower is obtained as a sum of the various layers, the percentage of the total passing the tower in the lowest 100 feet, 200 feet, 300 feet, etc. can be calculated. An example of the calculations for Trial 28 is plotted in Fig. 7. In this figure, approximately 7 per cent of the particles passed the tower in the lowest 400 feet, 28 per cent in the lowest 600 feet, etc. The coordinates of the figure are height vs. cumulative percentage. On the type of coordinate scales shown, a normal or Gaussian width distribution becomes a straight line. Fig. 7 shows that the distribution for Trial 28 did, in fact, closely approximate a Gaussian distribution.

A measure of the vertical size of the cloud may be obtained on the assumption of a Gaussian distribution. One standard deviation ( $\sigma$ ) on each side of the 50 per cent (mid-point) value of the cloud falls at 16 per cent and 84 per cent on the cumulative percentage scale. The vertical height on the tower between 16 per cent and 84 per cent thus represents a distance of  $2\sigma$ .

Table VII shows the vertical cloud sizes computed in this manner for all of the tests. For some of the Trials 1-23 the sizes in parentheses show the original values obtained before correcting the particle recovery to near 39 per cent.

In general, the cloud distributions on the tower approximate a Gaussian distribution to a reasonable degree. The principal deviations tend to occur near the ground where the clouds are drawn downward by increased turbulence in the lower layers. The technique of measuring  $\sigma$  as one standard deviation on either side of the position of the center of the cloud tends to minimize the errors introduced near the edge of the cloud since these do not contribute greatly to cumulative percentage values. The vertical cloud sizes measured in this manner thus provide representative values as long as the particle recovery is sufficiently near the 39 per cent value to assure that the cloud has been effectively sampled.

TABLE VII  
TOWER MEASUREMENT OF VERTICAL CLOUD SIZE  
(CLOUD  $\sigma$ )

<u>Trial</u>	<u>Vertical Size</u>	<u>Trial</u>	<u>Vertical Size</u>
1	25 (33) ft.	19	55 ft.
2	23	20	90
3	22 (31)	21	115
4	40 (105)	22	60
5	48 (76)	23	178
6	67	25	110
7	77 (136)	26	78
8	38 (111)	27	95
9	50 (60)	28	128
10	70 (61)	29	130
11	60 (96)	30	105
12	47	31	163
13	40	32	30
14	78	33	75
15	75	34	40
16	75	35	95
17	80	36	68
18	165	37	123
		38	90

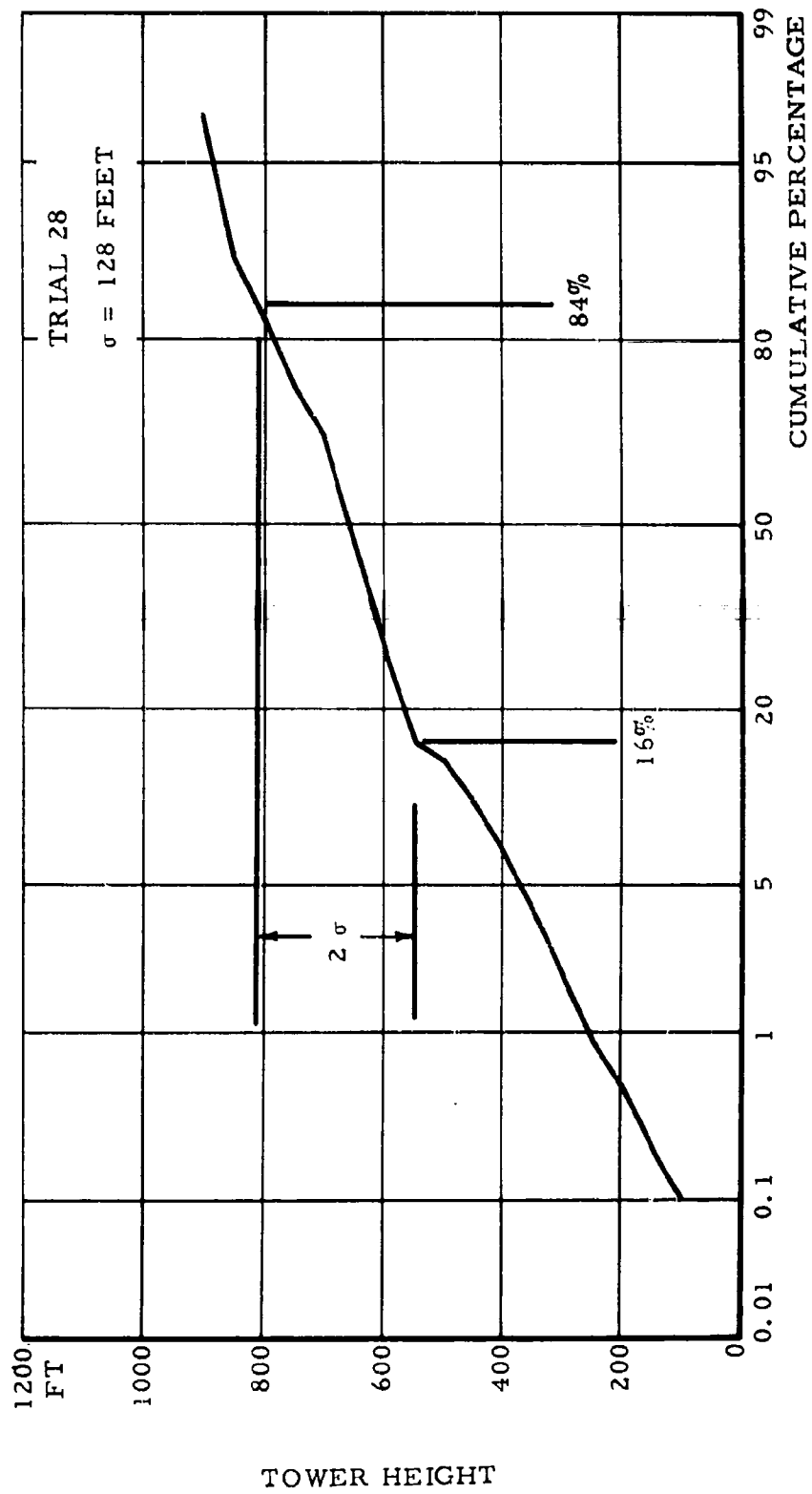


Fig. 7

### 3. Mean Height of the Cloud Center

It might be expected that the height of the cloud center passing the tower would closely approximate the height of release for the relatively flat terrain characteristic of the Dallas area. There were a number of cases, however, where substantial mean vertical displacements of the cloud center were observed, even in relatively short distances. Table VIII shows release height of the cloud center for those tests where these two heights could not be considered to be the same.

Trial 8 shows the most striking change in mean height, a decrease of 500 feet in about one mile of travel. Test Series 3, where vertical sampling resolution was 50 feet, shows clear and unequivocal changes in the mean cloud position. Trial 31 showed particular complications with two distinct peaks about 350 feet apart. The results of this complex distribution are reflected in the cloud  $\sigma$  of 163 feet shown in the previous section for Trial 31. This width has no real meaning since the usual Gaussian distribution was changed into a bi-modal distribution.

These vertical displacements, frequently quite substantial, must be attributed to wave motions of a non-diffusive nature. These commonly occur under stable conditions, particularly in rolling terrain. In the case of Trial 8, the effect of the vertical displacement on ground dosages is to cause arrival at the ground at an earlier time than would have otherwise been expected.

TABLE VIII  
CHANGE OF HEIGHT OF CLOUD CENTER

<u>Trial</u>	<u>Release Height</u>	<u>Height of Center</u>	<u>Release Distance</u>
7	680 ft.	450 ft.	1.05 miles
8	980	450	1.1
11	380	250	2.1
14	450	300	5.2
15	600	450	6.3
17	600	450	4.7
19	450	150	2.3
26	450	300	5.5
31	1050	1250 and 900	6.3
34	450	550	6.5
36	450	500	6.25
38	450	350	4.12

#### 4. Comparison of Observed and Computed Vertical Cloud Sizes

It was quickly seen from the results of the first Dallas test series that the vertical cloud sizes computed as indicated above were substantially greater than predicted by the expression:

$$\frac{d\sigma_z}{dx} = 3i^2.$$

Table IX shows a comparison of observed vertical cloud sizes and calculated sizes ( $3i^2$ ) for Test Series 3 when sampling resolution was sufficient to define the tower vertical cloud sizes accurately. The observed tower vertical cloud sizes are seen to be substantially larger than the computed sizes in all cases.

TABLE IX

#### OBSERVED VS. COMPUTED TOWER CLOUD SIZES

<u>Trial</u>	<u>Observed</u>	<u>Computed (<math>3i^2</math>)</u>
25	110 ft.	60 ft.
26	78	26
27	95	24
28	128	20
29	130	17
30	105	55
31	163	2
32	30	2
33	75	5
34	40	2
35	95	12
36	68	3
37	123	9
38	90	17

#### 5. Effect of Aircraft Wake on Vertical Cloud Size

The differences between observed and computed vertical sizes are so large as to require considerable re-examination of the entire problem of aircraft releases. One of the assumptions that does not appear to be valid is that the aircraft release can be considered as a point source.

The aircraft, in motion through the air, leaves a wake behind it consisting of a pair of line vortices, horizontal and parallel to the flight path. The characteristics of this vortex field are discussed in Appendix C. A few hundred feet behind the aircraft the vortex field is enclosed in a vertical size of about 50 ft. for the L-23. Material released into the wake would be carried rapidly around the vortex field and quickly assumes a comparable vertical size. At this stage the vertical size of the cloud, measured in a manner comparable to the subsequent tower vertical size calculations would be about 15 feet ( $\sigma$ ). This figure was determined from L-23 calibration data taken at Dugway after a travel distance of about 100 yards from the release point. As a consequence, the particle cloud begins its diffusion growth with this initial size rather than as a point source.

After about a minute, the pair of line vortices breaks up into large turbulent eddies and the wake energy, transformed into turbulent energy, is added to the already existing diffusing power of the outside air. Thus, after the initial, rapid increase in cloud size ( $\sigma$ ) to about 15 feet, the rate of growth of the cloud should be somewhat greater than calculated from bivariate turbulence data as a result of the added effect of the turbulent wake energy.

Two general comments can be made concerning these wake effects:

- 1) The wake effects will be relatively more important in cases with low natural atmospheric turbulence levels.
- 2) The wake effects will account for a larger proportion of the total cloud growth for short release distances. At long distances the wake effect becomes negligible compared to natural turbulence effects.

The initial attempt made to account for the effect of aircraft wake on vertical cloud growth in the Dallas data involved subtracting the initial cloud size ( $\sigma = 15$  ft.) from the final measured tower size and attributing the difference to atmospheric turbulent growth. Results of this study are shown in Figs. 8a and 8b. These figures are a plot of turbulent intensity,  $i$ , vs. the square root of cloud growth  $\sqrt{dz/dx}$  from release to the time of tower passage. The approximation:

$$\frac{d\sigma_z}{dx} = 3i^2$$

is shown as a dashed line. It should be noted that computed cloud sizes for Test Series 3 should be considered to be more accurately

defined than for Test Series 1 and 2. This figure is identical in form to that used by Smith-Hay (1961) and thus may be readily compared.

Figs. 8a and 8b again show that the observed vertical cloud sizes are consistently larger than the  $3i^2$  approximation. It is also seen that the comparison with the  $3i^2$  approximation becomes increasingly poor for lower values of  $i$ .

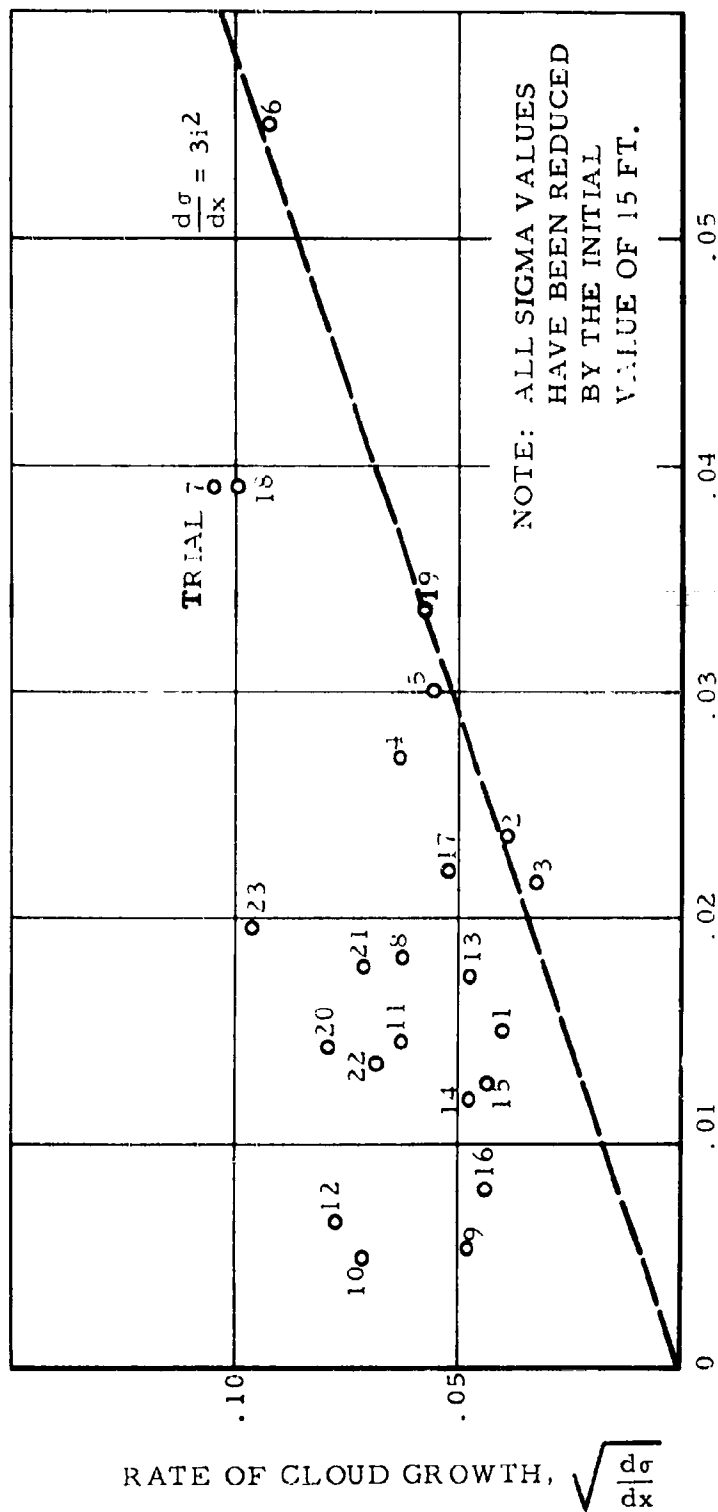
A comparison of Figs. 8a and 8b with the similar plot of Smith-Hay (1961) shows that only three of their reported tests fall in the turbulent intensity range of 0 to .05 shown in Figs. 8a and 8b. All three of these English tests also result in larger observed vertical cloud sizes than would be calculated from the  $3i^2$  approximation. Their reported agreement with this approximation is the result of tests made under conditions of greater turbulent intensity (up to  $i = .20$ ). This is in accordance with Figs. 8a and 8b which imply better agreement with the  $3i^2$  approximation for greater turbulent intensities. Thus both the Dallas and English data suggest a consistent deviation from the  $3i^2$  approximation for low values of  $i$  and a reasonable agreement with observed vertical cloud sizes for larger values of  $i$ .

The remaining effect of the aircraft, discussed above but not included in Figs. 8a and 8b, is the turbulent energy added to the cloud growth due to motions in the wake itself. As pointed out above, this additional energy should influence the cloud growth to a greater extent for short rather than for long release distances.

As a consequence, the data of Figs. 8a and 8b were stratified according to release distances with the results shown in Figs. 9a and 9b. These figures show the cloud growth data in two groups; a) for 1-2 mile release distances, and b) for approximately 6 miles distance. There were insufficient numbers of cases to produce similar graphs for other distances.

By the methods described in Appendix C, the combined effects of vortex wake energy and natural turbulent energy have been plotted as dashed lines in Figs. 9a and 9b. It is seen that the agreement with observations is better than with the  $3i^2$  relation, but, more important, character of the observed deviation is accounted for by the vortex wake energy, i. e., greatest deviations occur at low values of natural turbulence.

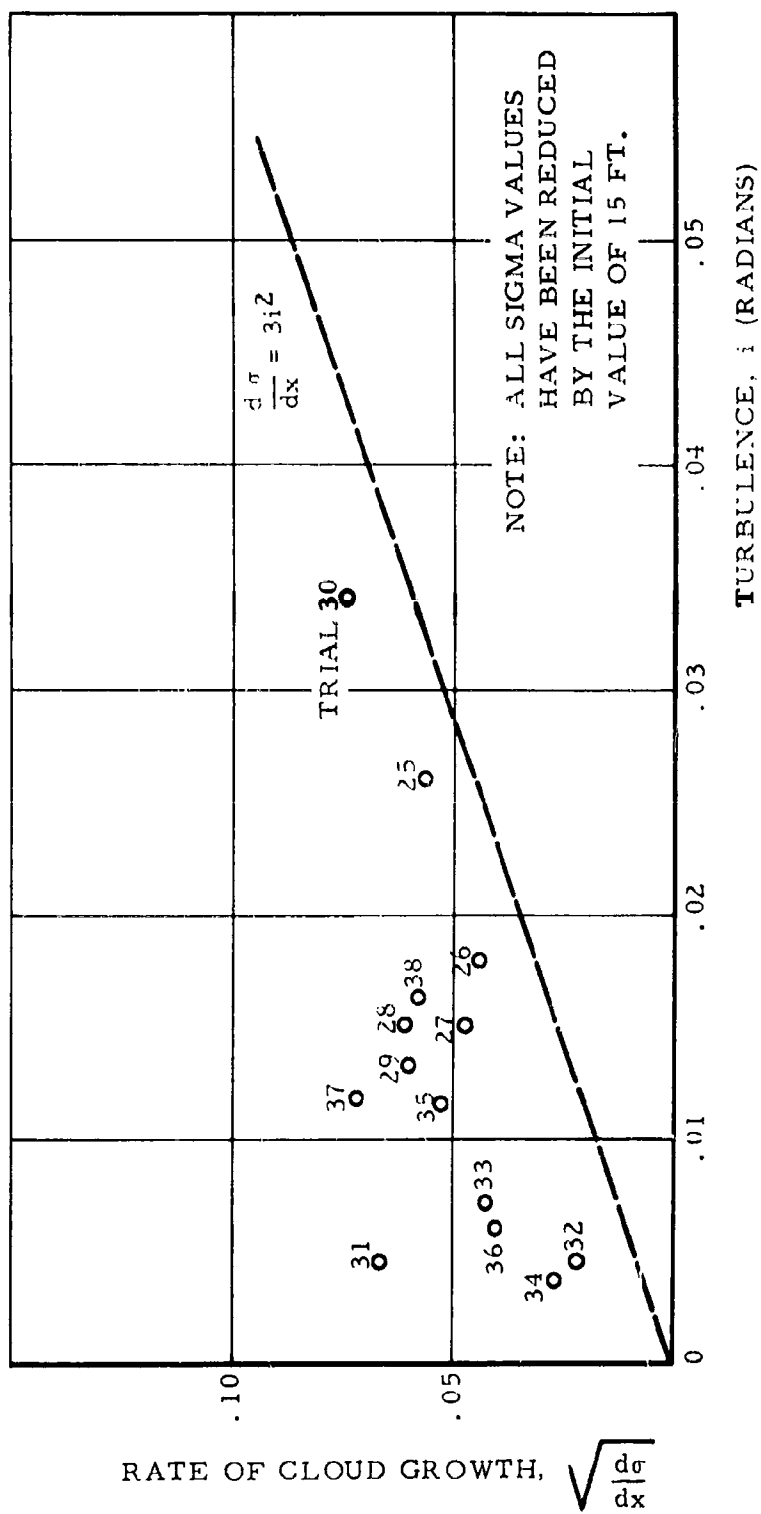
The agreement between the dashed lines and the plotted points is partly fortuitous. The effect of dissipation of the vortex wake energy is not included in Figs. 9a and 9b but, on the other hand, skin friction and propeller effects add greater turbulent energy to the wake than has been used in computing the dashed lines shown in the figures (see Appendix C).



TURBULENT INTENSITY VS. VERTICAL CLOUD GROWTH TO TOWER

TEST SERIES 1 AND 2

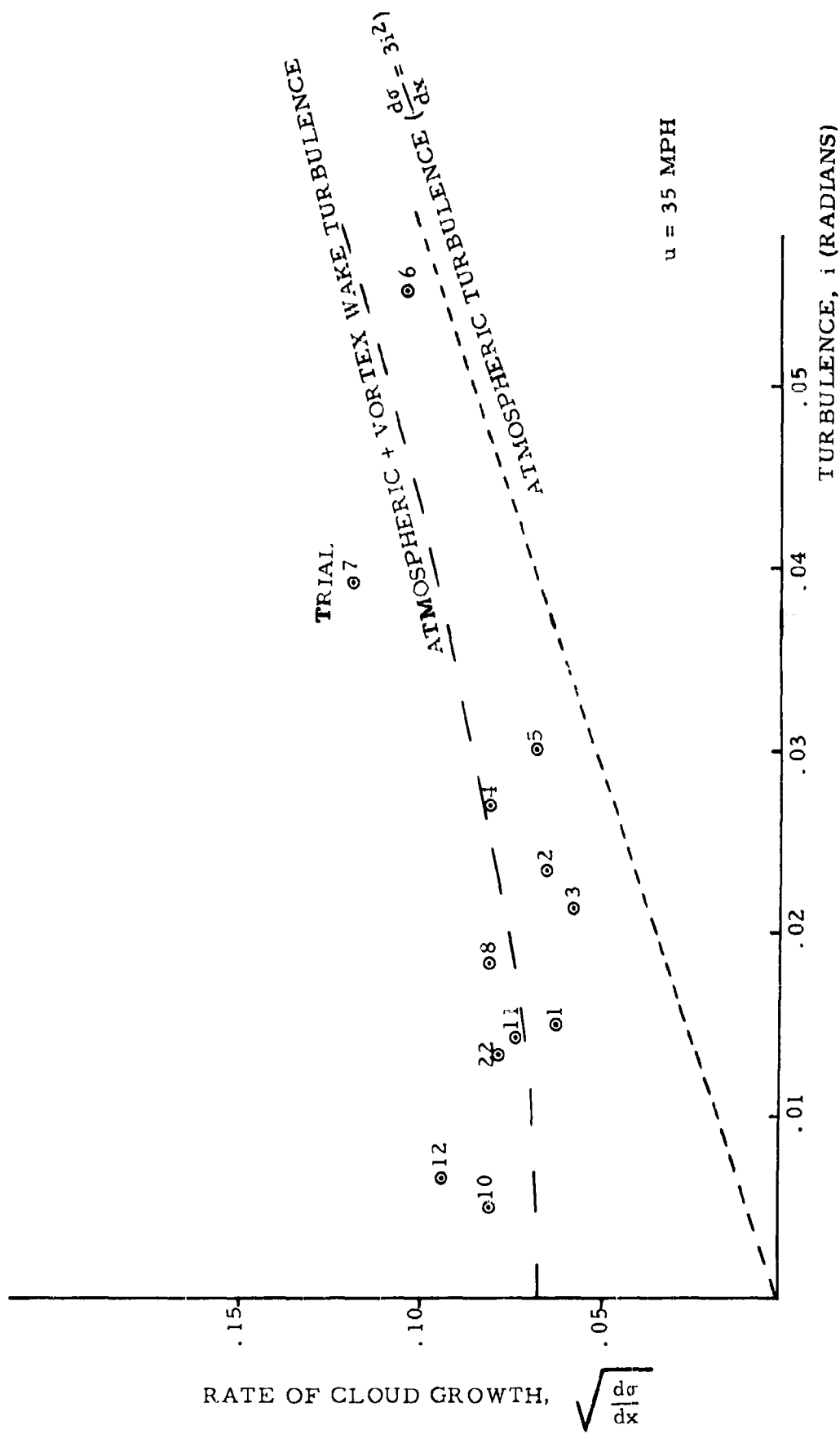
Fig. 8a



TURBULENT INTENSITY VS. VERTICAL CLOUD GROWTH TO TOWER

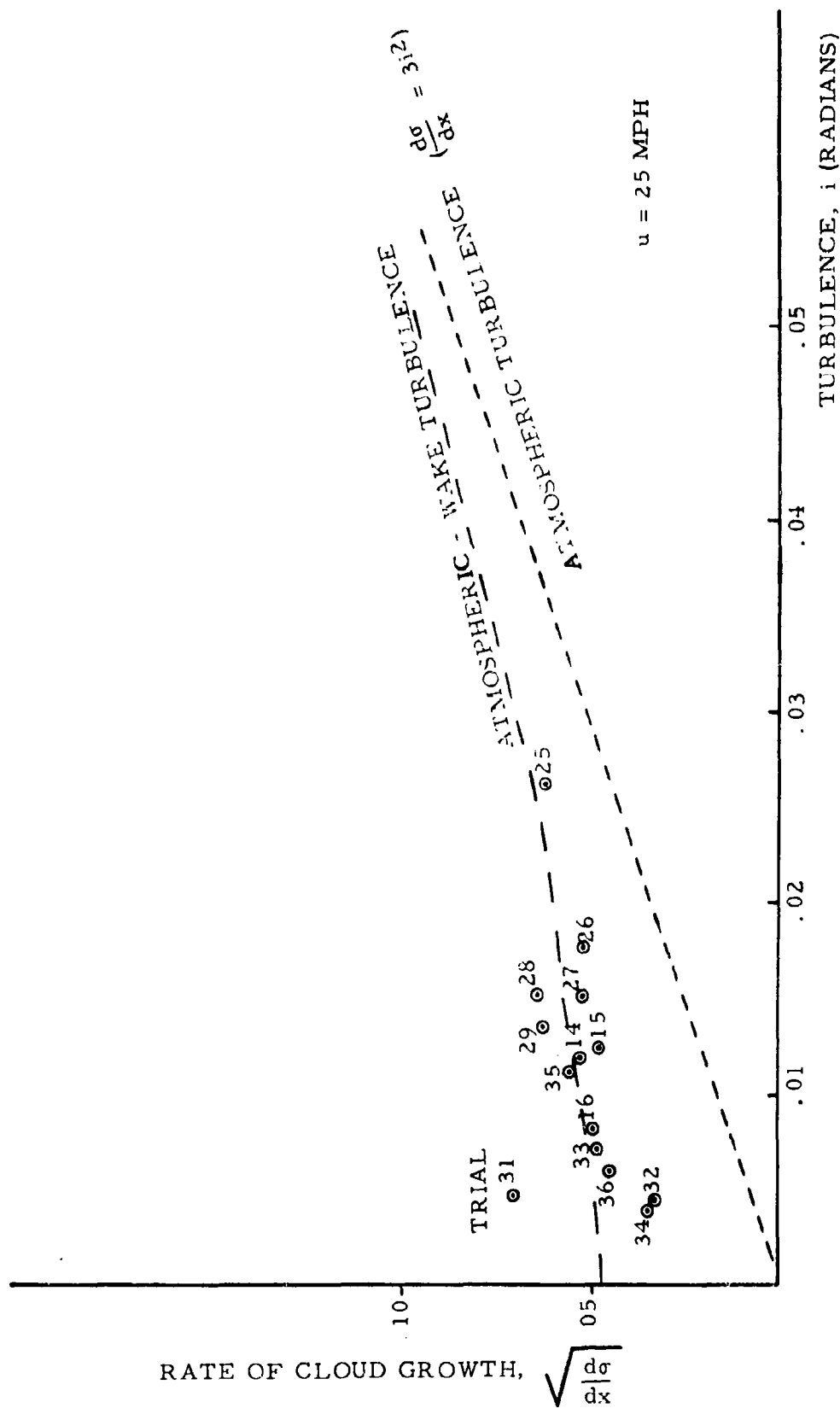
TEST SERIES 3

Fig. 8b



EFFECT OF VORTEX WAKE TURBULENCE ON CLOUD GROWTH (1-2 MILES FROM RELEASE)

Fig. 9a



EFFECT OF VORTEX WAKE TURBULENCE ON CLOUD GROWTH (6 MILES FROM RELEASE)

Fig. 9

## 6. Summary

The rate of vertical growth of the cloud as measured at the tower exceeds the value calculated from:

$$\frac{d\sigma_z}{dx} = 3i^2, \text{ particularly at low levels of natural}$$

turbulent intensity.

If reasonable allowance is made for the effects of turbulent wake energy produced by the aircraft itself, the measured cloud growths can be explained qualitatively by the combined effects of turbulent wake and natural atmospheric turbulent energy. However, it has not been possible to compute the entire turbulent wake effect quantitatively and it must be concluded that the  $3i^2$  relation, used in conjunction with effects of the aircraft itself, produces a reasonable result but that the validity of the relation has not been adequately demonstrated.

### D. Downwind Ground Sampling

#### 1. Maximum Dosage

Formulas for calculating ground dosage and distance from release to the maximum dosage are:

$$D_{\max} = .485 \frac{Q}{uH},$$

$$x_{\max} = \frac{H}{3i_e^2}$$

and are discussed in an earlier section.

In accordance with the discussion of Section V. A., the trials have been divided into: 1) releases within the turbulent layer ( $Ri < .3$ ); 2) releases above the turbulent layer; and 3) trials where dilution from the ends of the release line (unfavorable wind direction) affected the sampler line before the true maximum dosage was reached or those trials when no substantial dosages were observed on the sampling line. The Tables XI, XII, and XIII summarize the maximum dosage results for these three categories.

TABLE XI

COMPARISON OF OBSERVED AND CALCULATED DOSAGE  
RELEASES WITHIN THE TURBULENT LAYER ( $R_i < .3$ )

<u>Trial</u>	<u>Maximum Dosage *</u>			<u>Distance to Maximum Dosage</u>	
	<u>Observed</u>	<u>Calculated</u>	<u>% Obs/Calc</u>	<u>Observed</u>	<u>Calculated</u>
4	550	325	169%	18 miles	9 miles
5	450	320	141	11	11
6	600	604	99	9	3
7	500	313	160	9	8
11	700	747	94	11	9
17	800	400	200	8	15
18	1000	568	176	9	4
21	450	403	112	15	29
25	900	947	95	13	7
26	800	838	95	11	34
27	650	773	84	8	12
28	650	440	148	27	27
29	200	408	49	30	25
30	800	750	107	25	6

Avg. 123%

\* Dosages in particle-minutes/ft<sup>3</sup> and corrected to uniform release rate of 2.5 lbs/mile ( $1.24 \times 10^{10}$  particles/gram).

TABLE XII

COMPARISON OF OBSERVED AND CALCULATED DOSAGE  
RELEASES ABOVE THE TURBULENT LAYER ( $R_i > .3$ )

<u>Trial</u>	<u>Maximum Dosage*</u>			<u>Distance to Maximum Dosage</u>	
	<u>Observed</u>	<u>Calculated</u>	<u>% Obs/Calc</u>	<u>Observed</u>	<u>Calculated</u>
9	200	445	45%	22 miles	154 miles
20	1200	352	341	22	22
22	600	207	290	29	72
23	250	234	107	27	34
35	1800	945	190	18	9
36	800	1275	63	26	17

\* Dosages in particle-minutes/ft<sup>3</sup> and corrected to uniform release rate of 2.5 lbs/mile ( $1.24 \times 10^{10}$  particles/gram).

TABLE XIII

TRIALS FOR WHICH COMPARISONS ARE UNAVAILABLE

<u>Trial</u>	<u>Remarks</u>
1	Did not reach ground in 30 miles
2	Maximum not on sampler line
3	Maximum not on sampler line
8	Maximum not on sampler line
10	Did not reach ground in 30 miles
12	Maximum not on sampler line
13	No rotorod ground sampling
14	No rotorod ground sampling
15	No rotorod ground sampling
16	Did not reach ground in 30 miles
19	Maximum not on sampler line
31	Did not reach ground in 30 miles
32	Did not reach ground in 30 miles
33	Maximum not on sampler line
34	Did not reach ground in 30 miles

There is frequently considerable difficulty involved in determining the distance to the maximum dosage location from the observed ground dosage because of the erratic, variable nature of the ground dosage pattern during some of the tests. In view of this difficulty, the agreement between observed and calculated dosages and distances shown in Table XI for releases within the turbulent layer is considered to be good. In Table XII the agreement is considerably poorer and, in particular, the variability of the calculated-observed comparison is very much greater than in Table XI.

2. Cloud Touchdown Distance

The location of the initial appearance of the cloud at ground levels can be considered as another measure of the ground dosage characteristics. While the cloud is in the air, still diffusing downward, a common description of the edge of the cloud is the vertical distance from the center of the cloud to the point where the concentration has fallen to 1/10 of a value at the center of the cloud. Under the usual assumption of a Gaussian particle distribution in the vertical this 1/10 value occurs at an angular distance of  $2.15\sigma$  from the center of the cloud as measured from the source. When the line described by this angular deviation touches the ground, a reasonable description of the initial appearance of the cloud at the ground will have been achieved.

If H is the release height, the horizontal distance from the release to the first appearance of the cloud on the ground is given by:

$$\text{Touchdown distance} = \frac{H}{6.45 i_e^2} .$$

This formula expresses the principle that a cloud spreading at the rate of  $3 i_e^2$  (Smith-Hay) has a cloud edge whose angle is 2.15 times  $3 i_e^2$ . The principal difficulty in verifying this expression lies in the problem of determining the observed distance for comparison. In some cases the ground dosage increases abruptly as a function of downwind distance and the appropriate touchdown distance can be obtained easily. In other cases, however, the initial appearance of the cloud is erratic and subject to local turbulence effects and the appropriate distance is not easily determined.

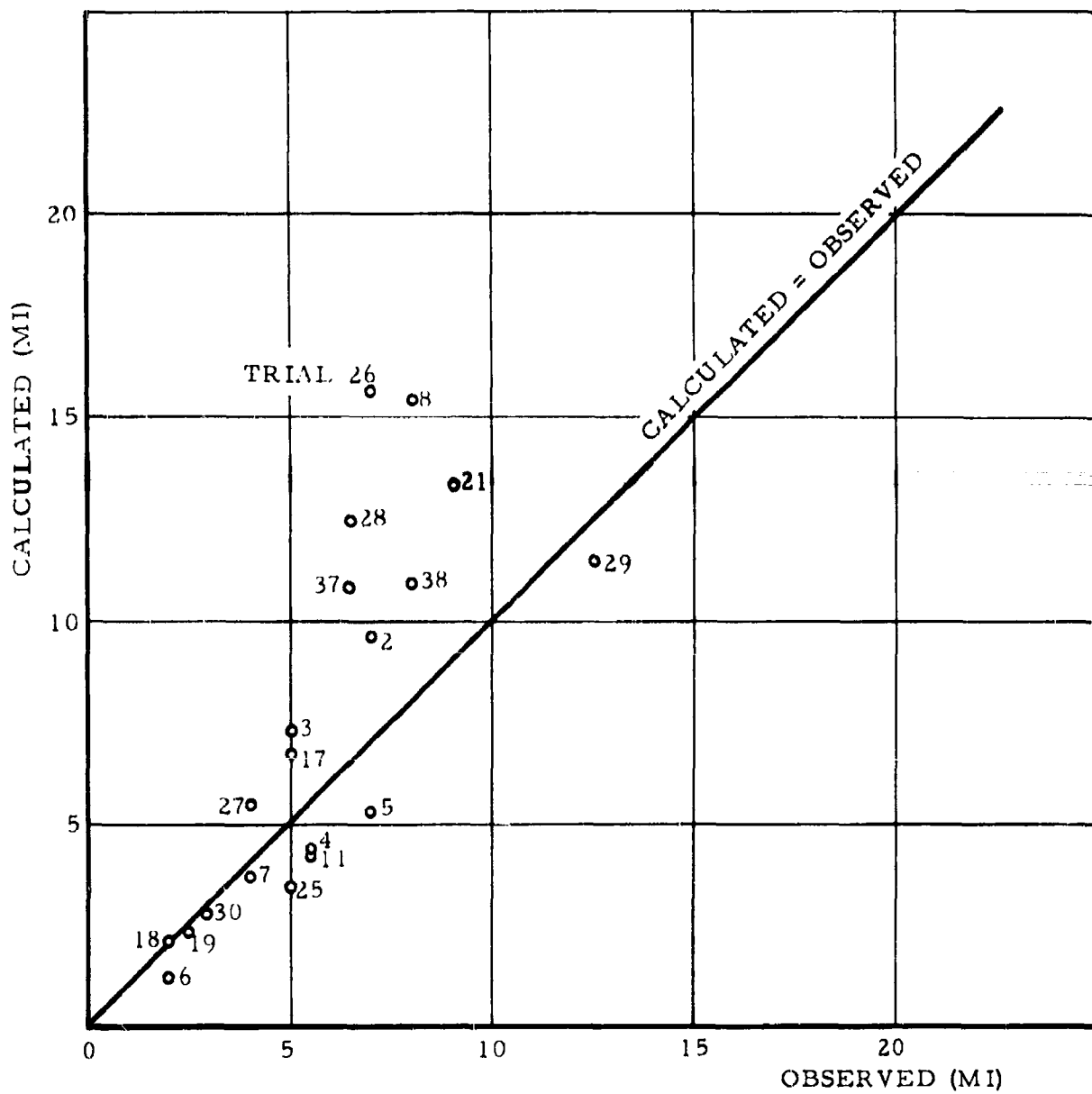
Fig. 10 shows a comparison of observed touchdown distances and computed distances obtained from the above expression. In view of the difficulties involved, the agreement is considered to be good up to distances of 5-10 miles from the release. The principal deviations at 7-10 miles (observed) occur as a result of downward deflection of the mean cloud center (Trials 8, 26, 28).

Fig. 10 includes only the trials shown in Table XI for which releases were made within the turbulent layer. For the remainder of the tests the agreement between observed touchdown distances and those computed from the model becomes quite erratic. This behavior is similar to that described in the previous paragraphs for maximum dosage.

For releases within the turbulent layer, therefore, it is concluded that the  $3 i_e^2$  approximation provides a useful means of predicting the location of the initial appearance of the cloud at the ground.

### 3. Downwind Dosage Distribution

The downwind ground dosage distribution for the 30-mile sampling line has been computed from the simple diffusion model given in Equation (5):



CALCULATED VS. OBSERVED TOUCHDOWN DISTANCES

Fig. 10

$$D = \frac{2Q}{3 i_e^2 x u \sqrt{2\pi}} e^{-H^2/18 i_e^4 x^2}$$

which was described in an earlier section. These distributions have been computed for all tests for which appreciable ground dosages were received on the sampling line but excluding the cases where the cloud drifted across the line due to changes in mean wind direction. Results of the computations are shown in Figs. 11, 12, and 13, and are compared to observed distributions. In general, the agreement between observed and computed distributions is considered satisfactory.

One difficulty in the use of the model is that it assumes a spreading of the cloud upward from the release height at the same rate that the downward spreading occurs. In the stable nighttime conditions of Texas the turbulence decreases markedly with height above ground and the rate of spreading upward is thus overestimated by the model. In reality, a turbulent layer top is usually observed above which appreciable diffusion no longer occurs.

The model, therefore, predicts more dilution of the cloud (greater downwind decrease in ground dosage) than might actually be expected to occur. The principal need for further development of the model is to develop a technique for handling this difficulty which essentially arises from the decrease of turbulent intensity with height.

There are several general comments which can be made concerning the character of the ground dosage distributions:

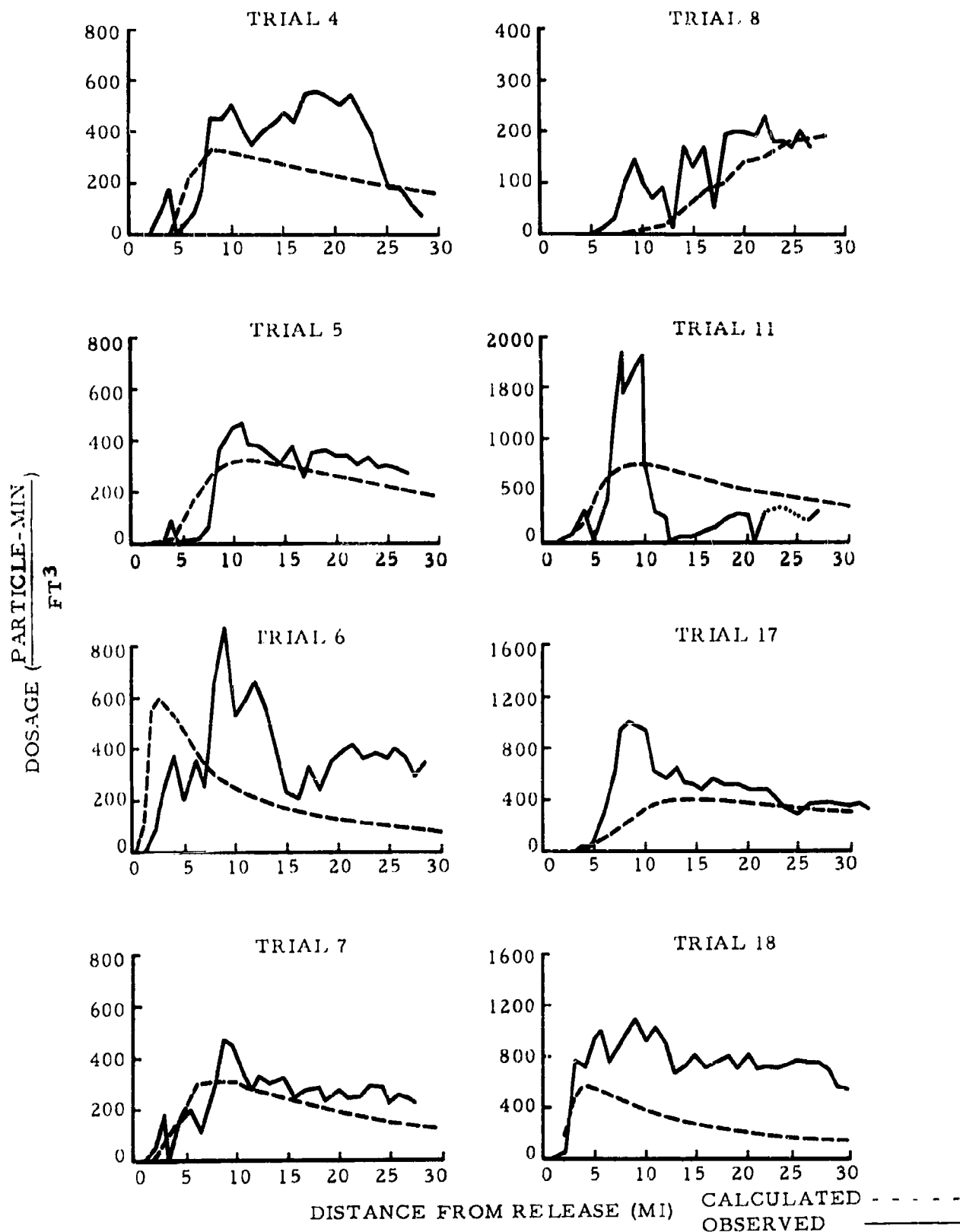
- 1) The dosage distribution along the sampler line for a given test shows much greater erratic variations for the third test series. This is the result of the lighter turbulence conditions and inhomogeneous mixing of the particle cloud. These conditions are particularly apparent for Trials 25, 26, 27, 30, 35, 37, and 38 -- all with 450 foot releases. For 750 foot releases the particle cloud is usually mixed to a greater extent and the erratic nature of the distribution is not so striking.
- 2) Under the light turbulence conditions in the Dallas area, releases at about 1000 feet either produce light dosages within the first 30 miles or none at all. For releases at about 700 feet, larger dosages are observed, the downwind distributions are relatively free from variation, but on a number of occasions (4) the cloud did not reach the ground at all.

- 3) For releases made near 400 feet the cloud usually reaches the ground, but dosage distributions downwind are likely to have erratic variations and the maximum ground dosage is likely to be large compared with the remainder of the 30 mile line.
- 4) Of a total of 9 trials without appreciable dosage amounts observed on the 30-mile sampling line, three involved releases at about 400 feet, four at about 700 feet, and two at about 1000 feet. In all cases the turbulence at release height was very light and very little diffusion occurred at the release height within the time spent in passing over the sampler line. In all of these cases there was considerable turbulence at some lower level and a somewhat lower release would have been much more successful.
- 5) By computing effective turbulent intensities ( $i_e$ ) for various release heights for all tests, it is possible to obtain an estimate of the optimum release height in the Dallas area. If the requirement is imposed that the cloud reach the ground within 15 miles of the release line, releases from 450 feet would have been successful in 86 per cent of the cases, in 37 per cent of the cases if all releases had been at 750 feet, and in only 3 per cent of the cases for 1050 foot releases.

#### E. Crosswind Ground Sampling

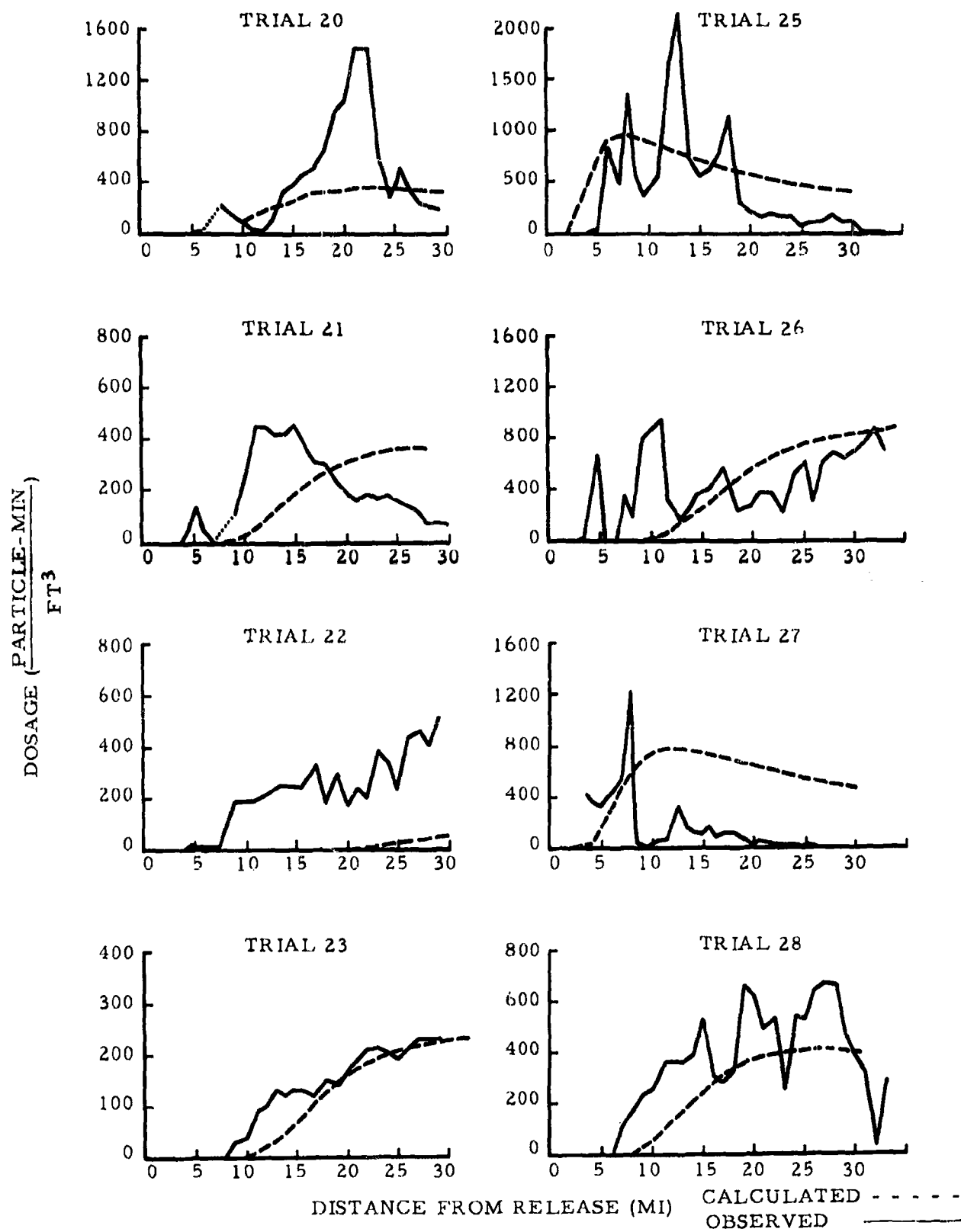
In a number of the trials (Trials 21-33) a crosswind sampling line was set up at a distance of about 25 miles downwind from the Dallas Tower. This line extended in an east-west direction for 12 miles on either side of the main sampling line. Rotorod samplers were spaced at two-mile intervals along this crosswind sampling line. The principal value of the crosswind line was to determine whether horizontal dilution from the ends of the release line affected the far downwind end of the main sampler line. The results of the crosswind sampling line may also be used to investigate the problem of the required release length to obtain specified downwind area coverages.

Fig. 14 shows a plan view of the downwind and crosswind sampler lines for Trial 23. The release line is shown as well as the wind direction at release height. At the downwind distance of the crosswind line location, dosages along the main sampler line and the crosswind line are seen to be relatively uniform except for marked decreases in dosage near the eastern end of the crosswind line. It is in this eastern region where an estimate of the inward dilution from the end of the release line can be made.



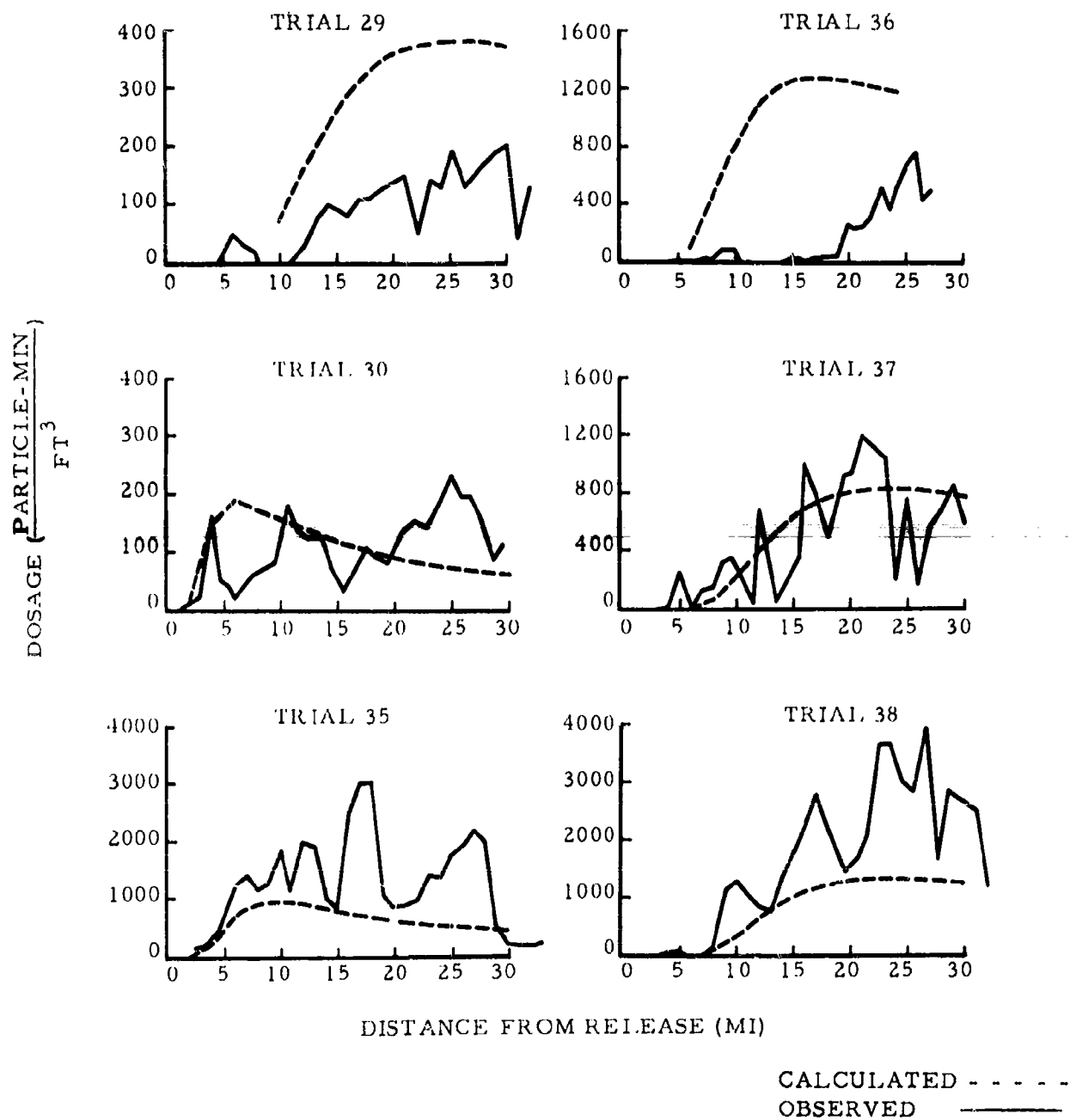
COMPARISONS OF CALCULATED AND OBSERVED DOSAGES

Fig. 11



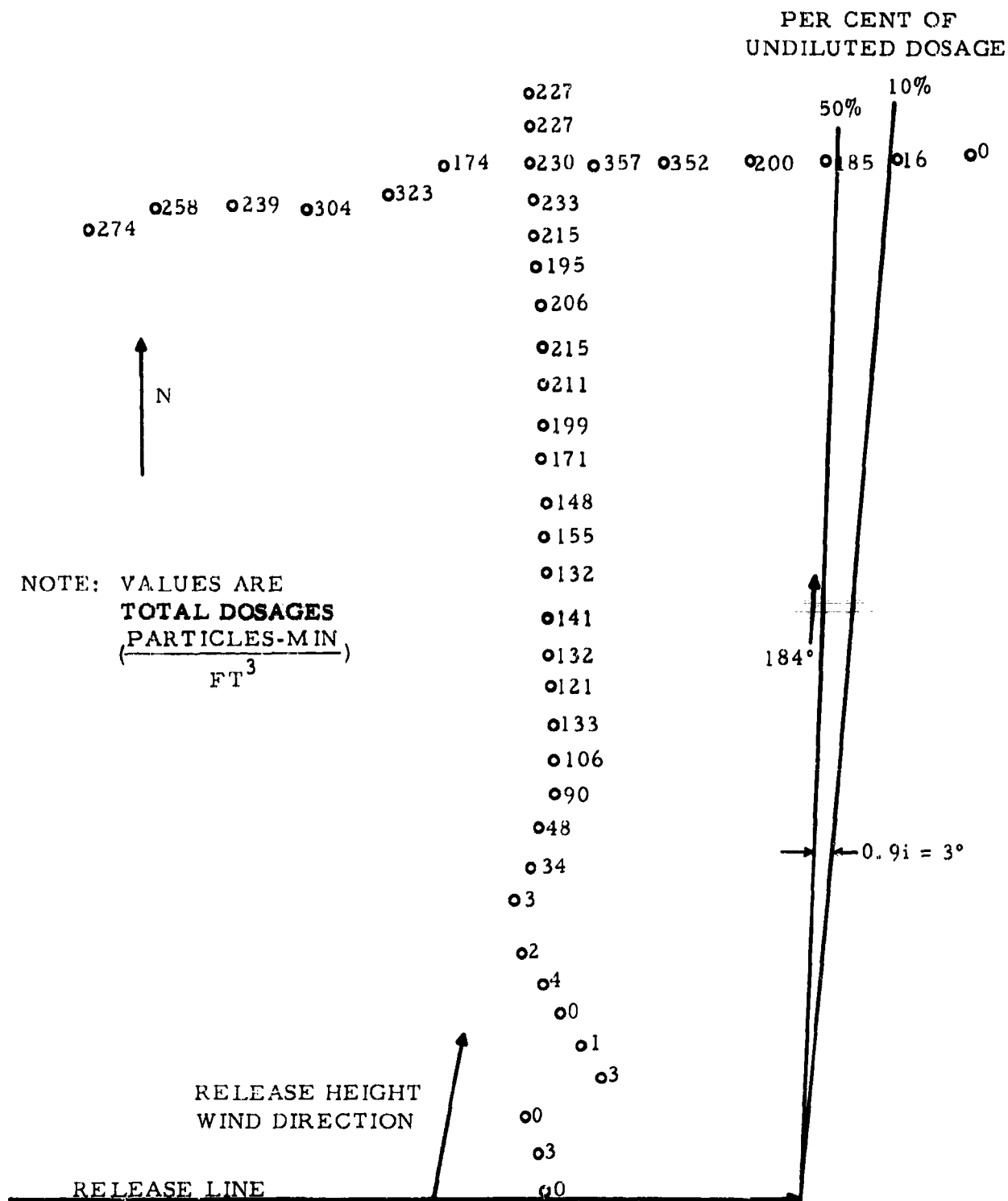
COMPARISONS OF CALCULATED AND OBSERVED DOSAGES

Fig. 12



COMPARISONS OF CALCULATED AND OBSERVED DOSAGES

Fig. 13



DOWNWIND AND CROSSWIND SAMPLING, TRIAL 23

Fig. 14

Fig. 15 shows the method of calculating the horizontal dilution of the cloud for the Dallas tests. In Fig. 15a the situation at the release line itself is shown without any dilution. In Figs. 15b and 15c dilution has occurred in an increasing manner. The result is a net transport of particles outward and a net loss from the previously undiluted end of the release line. It is assumed that this transport of material takes place in a manner which leads to a Gaussian-type curve from the undiluted region of the line outward as shown. Under these conditions the location of the 50 per cent dosage value (Point B) is  $1.25\sigma$  from the point of maximum dosage (Point A -- no dilution).  $\sigma$  may be measured in terms of distance along the release line or in terms of angular distance from the end of the release line itself. This 50 per cent dosage value gives the mean position of the edge of the release line.

At another point on the crosswind line the dosage has decreased to 10 per cent of the undiluted value (Point C). Under the Gaussian assumptions this occurs at a distance of  $2.15\sigma$ . Thus, if the Points B and C (50 per cent and 10 per cent of the undiluted dosage) are located on the crosswind line, the angular difference between these two points is  $0.9\sigma$ .

This method is illustrated in Fig. 14 for Trial 23. In this case, the mean cloud edge can be measured at  $184^\circ$  azimuth (from North) and  $0.9\sigma$  is given as  $3^\circ$ . By comparison with measured meteorological parameters, the mean wind direction between release height and ground levels on the tower was also  $184^\circ$ . The horizontal turbulence  $\sigma$  was measured at the 450 foot level in this test at  $3.2^\circ$  which corresponds very closely to the cloud spread  $\sigma$  of  $3/0.9$  or  $3.3^\circ$ .

Table XIV shows a summary of measured mean cloud edges and horizontal cloud spreads compared to observed meteorological values.

In Trials 31-33, insufficient amounts were observed on the crosswind line for an adequate determination of the horizontal cloud spread.

With the exception of Trials 21 and 25, the table shows that the mean cloud edge, computed in the manner shown in Fig. 14, closely approximates the mean wind direction measured on the tower between the ground and the release height. For Trials 21 and 25 there were no levels on the tower with wind directions as suggested by the mean cloud edge and it must be assumed that the wind direction changed downwind of the tower and that the tower measurements were not representative of the entire sampler line.

Likewise, the spread of the cloud measured as shown in Fig. 14 closely approximates the horizontal turbulence  $\sigma$  as measured on the tower at 450 ft. Again, the agreement for Trials 21 and 25 is relatively poor.

TABLE XIV

COMPARISON OF HORIZONTAL DILUTION WITH  
OBSERVED METEOROLOGICAL VALUES

<u>Trial</u>	<u>Release Height</u>	<u>Mean Cloud Edge</u>	<u>Mean Wind Direction</u>	<u>Cloud Spread</u>	<u>Horizontal Turbulence <math>\sigma</math></u>
21	750 ft.	163° azimuth	189° azimuth	5.0°	1.9 at 450 ft.
22	1050	173	178	3.3	2.6
23	1050	184	184	3.3	3.2
25	450	147	174	8.3	2.1
26	450	172	161	2.2	1.6
27	450	217	205	2.2	1.4
28	750	163	165	3.3	2.4
29	750	182	185	3.9	3.0
30	450	199	187	5.6	2.4

It should be noted that the agreement in cloud spread rate is with a measured turbulence,  $\sigma$ , not with a growth rate of

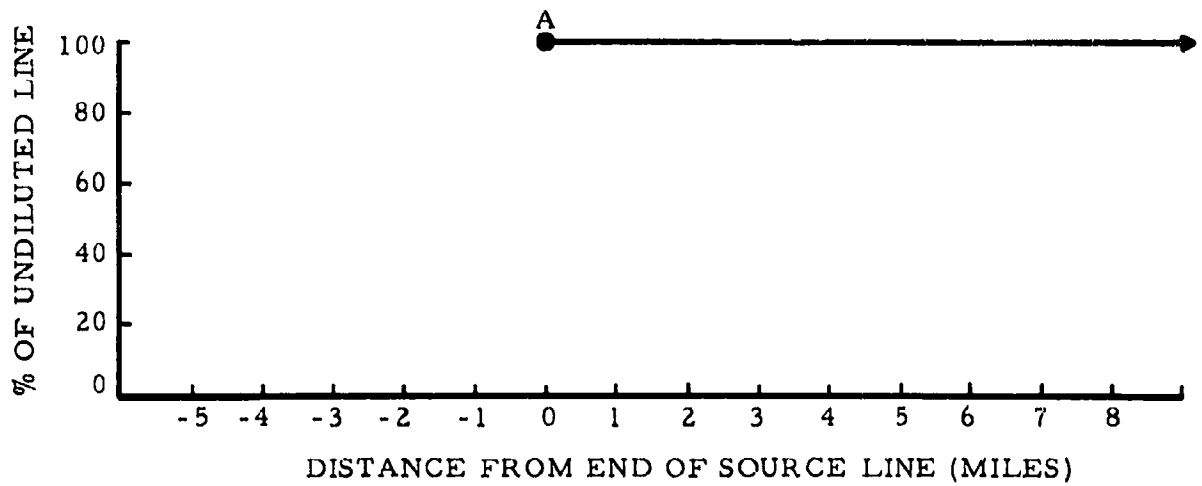
$$\frac{d\sigma}{dx} = 3i^2 \text{ as has been found useful for vertical cloud growth}$$

measurements. Table XIV indicates that the dilution in the horizontal direction takes place at a faster rate,  $\sigma$ , corresponding to the spreading rate found by Hay and Pasquill (1959) for a continuous source-type cloud. This occurs because the cloud is quite large (compared to the turbulence scale) in the horizontal direction as is a continuous source. In the vertical dimension the cloud size at release is small compared to the turbulence scale and the cloud grows initially as a point source in the vertical direction.

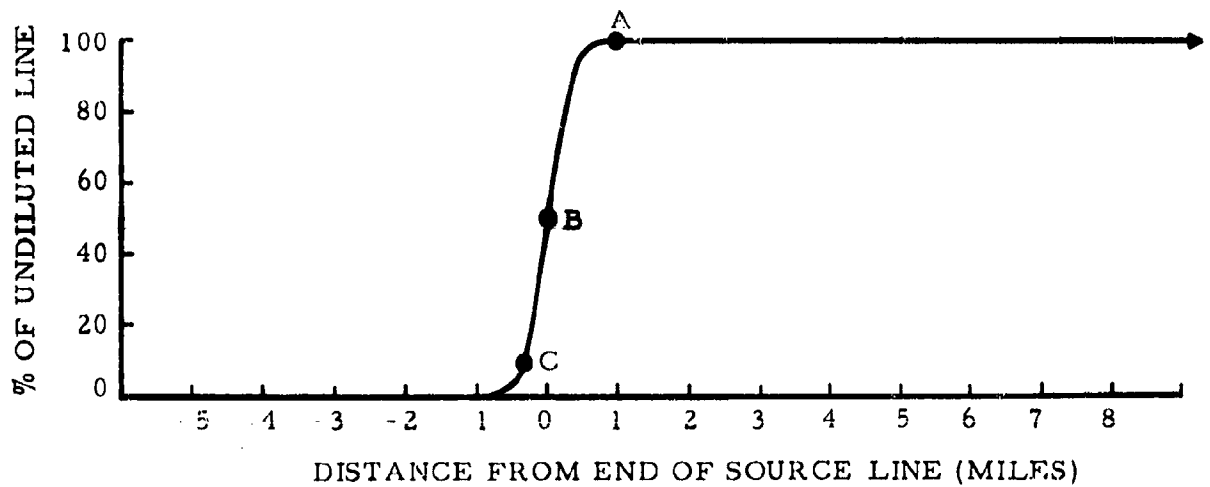
Horizontal turbulence  $\sigma$ 's have been compared with vertical  $\sigma$ 's at the same level and for the same time interval for 38 cases in the Dallas tests. This comparison is shown in Table XV. The average ratio of horizontal to vertical turbulence was:

$$\frac{\sigma_H}{\sigma_v} = 1.45.$$

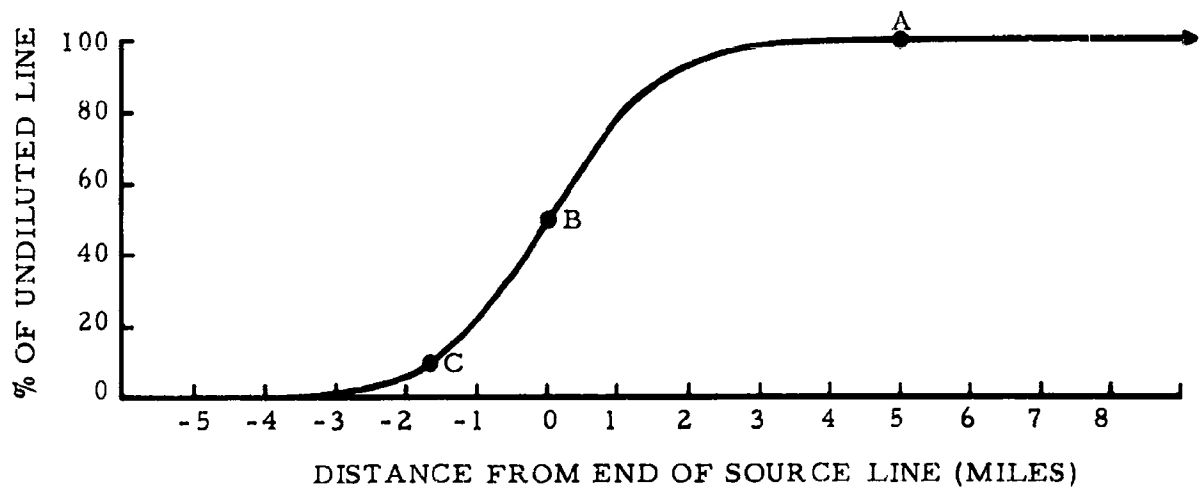
Most of these cases were measured at the 450 foot or 750 foot levels and there was no apparent variation in this ratio with height in these cases. For lower heights the turbulence might be expected to be more isotropic and the value of this ratio might be expected to be somewhat lower.



a. UNDILUTED LINE



b. INITIAL DILUTION



c. LATER STAGE OF DILUTION

DILUTION AT END OF LINE SOURCE

Fig. 15

TABLE XV

COMPARISON OF HORIZONTAL AND VERTICAL TURBULENCE

<u>Test</u>	<u>Height (ft)</u>	<u><math>\sigma_H/\sigma_v</math></u>	<u>Test</u>	<u>Height (ft)</u>	<u><math>\sigma_H/\sigma_v</math></u>
1	1050	2.9	19	450	1.2
2	150	2.0	20	450	1.1
3	150	1.6	21	450	1.0
4	750	1.4	22	450	1.1
5	750	1.6	23	450	1.0
6	750	1.4	25	450	1.4
7	750	1.0	26	450	1.4
8	750	1.4	27	450	1.6
9	750	2.1	28	450	1.1
10	750	2.9	29	450	1.2
11	750	2.0	30	450	1.1
11	150	1.1	31	450	1.1
12	750	4.6	32	450	1.2
13	450	.9	33	450	1.6
14	450	1.3	34	450	2.9
15	450	1.1	35	450	1.1
16	450	1.8	36	450	2.2
17	450	1.2	37	450	1.5
18	450	1.1	38	450	1.4

These results suggest that horizontal dilution may be calculated from the horizontal turbulence measurement in the layer between release height and the ground. In the absence of this measurement, a value of 1.45 times the effective vertical turbulence,  $i_e$ , will provide a reasonable estimate of the horizontal turbulence. With the horizontal turbulence  $\sigma$  obtained, the angular extent of horizontal dilution (to the undiluted portion of the cloud) should amount to  $1.25\sigma_H$ , measured inward from the mean wind direction in the layer from the ground to release height.

F. Estimation of Effective Turbulent Intensity  $i_e$

It has been shown that the maximum ground dosage, distance to the maximum dosage and general character of the downwind dosage distribution may be obtained from the effective vertical wind variation ( $i_e$ ) computed from measurements of turbulence in the layer below the release height. If turbulence measurements are not available it is useful to see if  $i_e$  can be estimated from the more common measurements of vertical temperature and velocity profiles.

Since  $i_e$  refers to conditions throughout the layer from the release height to the ground, some representation of mean temperature and wind conditions throughout the layer should be related to  $i_e$ . Fig. 16 shows the ratio of average lapse rate to (average wind velocity)<sup>2</sup> plotted against  $i_e$  for release heights of 450, 750, and 1050 feet. Both average lapse rate and average wind velocity are measured between the ground and release height. This ratio is similar in form to the Richardson number but is somewhat easier to calculate and may express the functional relationship with  $i_e$  equally well. It has been used extensively by various workers (e.g. Barad (1959)). The precise position of the lines which have been fitted by eye to the data in Fig. 16 is likely to depend on the particular terrain involved and the lines shown should be used only for relatively flat terrains similar to the Dallas area.

Fig. 17 shows the relation between  $i_e$  and distance to maximum ground dosage for release heights of 450, 750, and 1050 feet. The lines have been computed from the formula for distance to maximum dosage:

$$x_{\max} = \frac{H}{3 i_e^2}$$

discussed in earlier sections.

Also in an earlier section it was shown that the maximum dosage could be expressed as:

$$D_{\max} = \frac{.485Q}{uH}$$

This function is plotted as  $Q/D_{\max}$  (required source strength per unit dosage) in Fig. 18.

The set of three figures (16, 17, 18) provide the information necessary to compute maximum ground dosage and distance to maximum ground dosage for a variety of release and meteorological conditions. The charts apply only to relatively flat terrain similar to the Dallas area. The extent to which these figures will require modification over terrain with different roughness characteristics will be the subject of a later study.

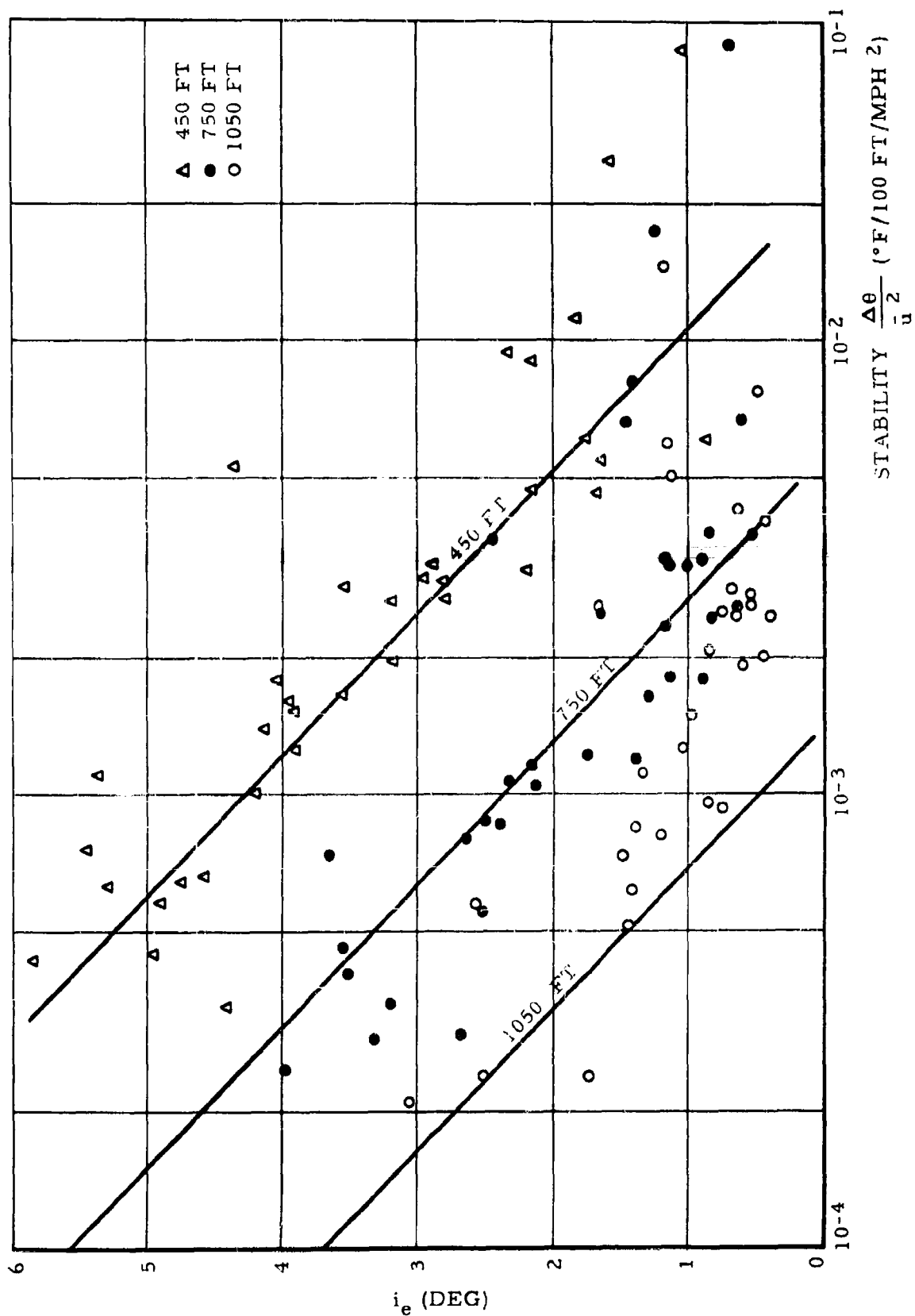
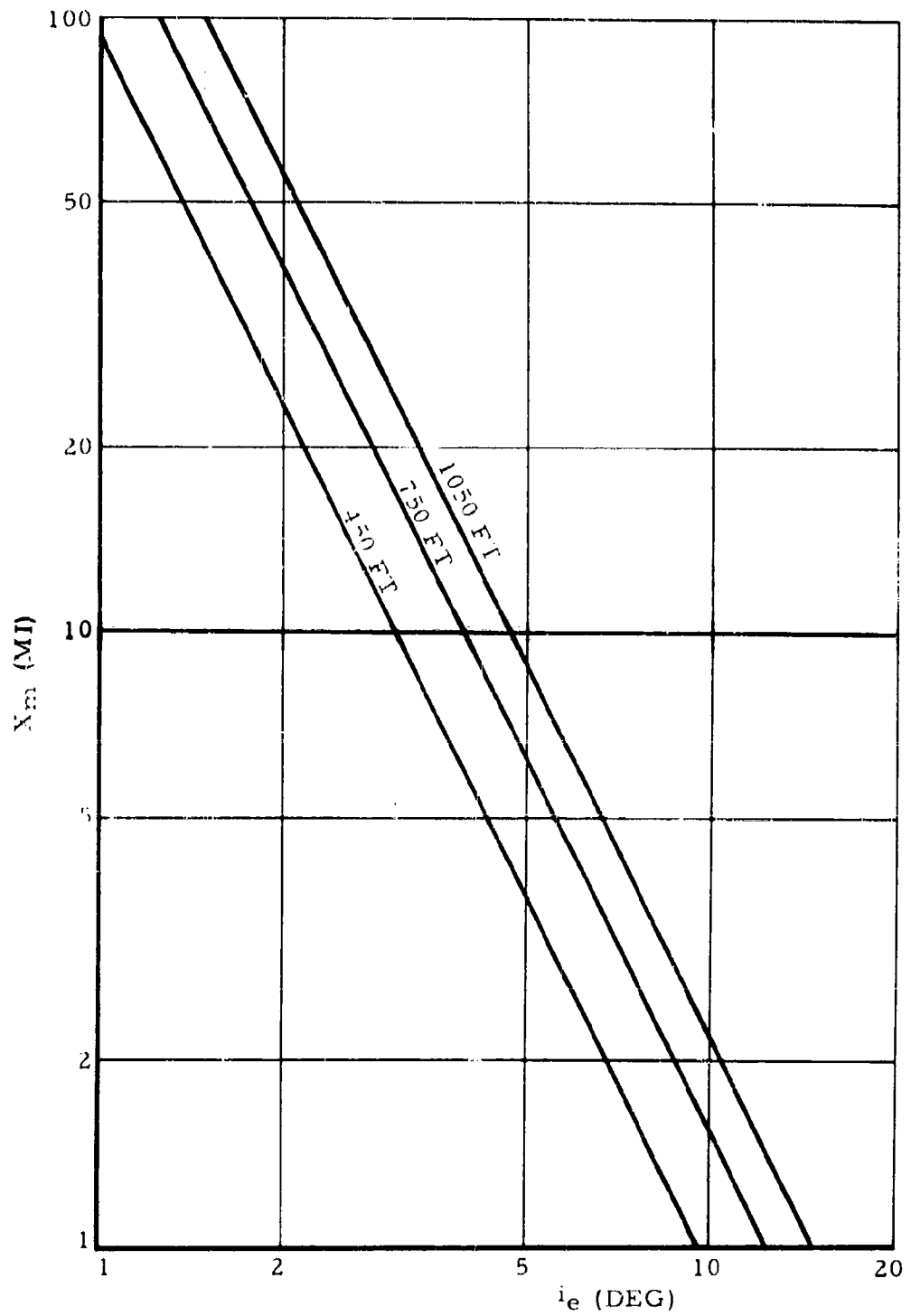
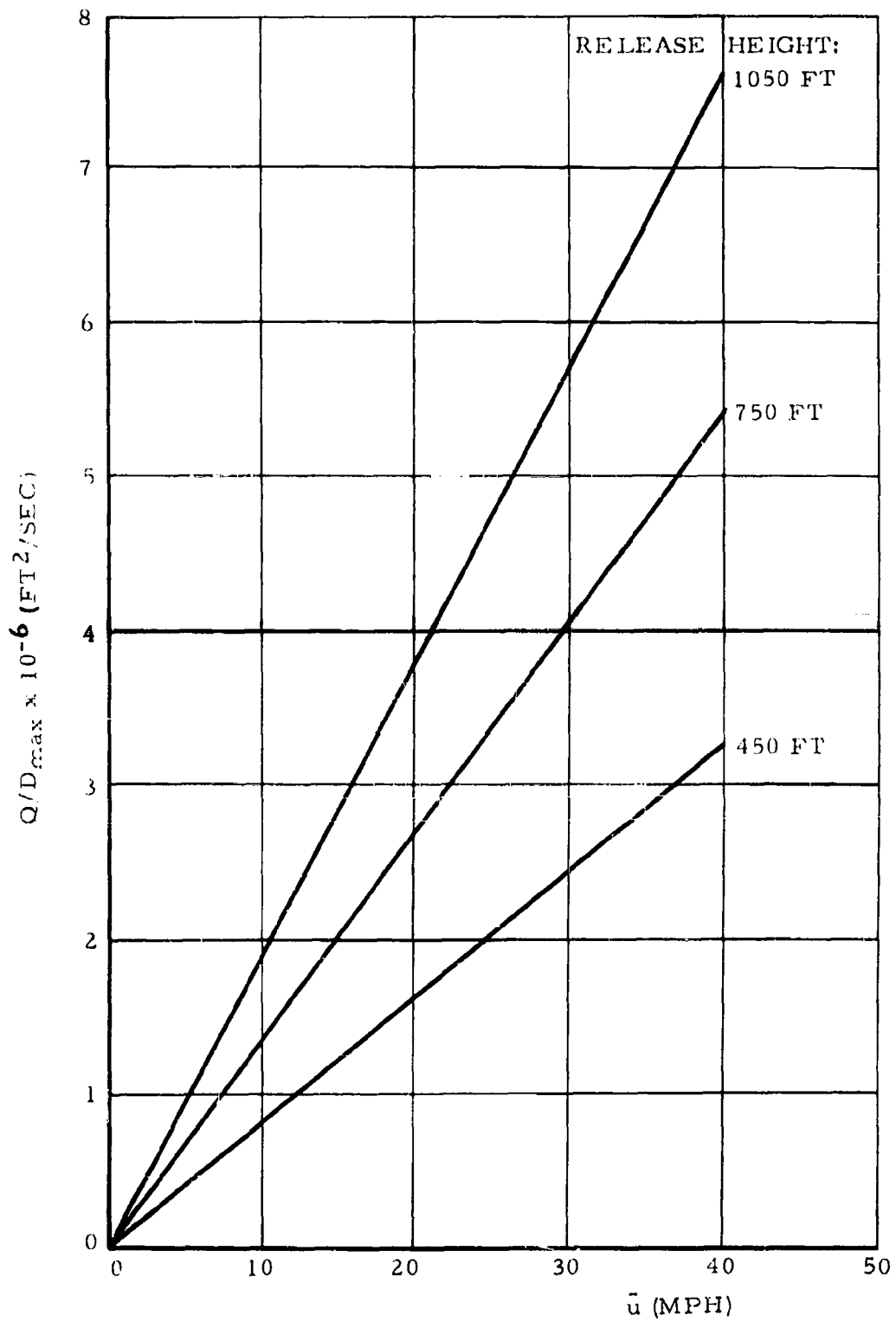


Fig. 16



DISTANCE OF MAXIMUM DOSAGE FROM RELEASE VS. EFFECTIVE SIGMA

Fig. 17



REQUIRED RELEASE RATE/UNIT MAXIMUM DOSAGE VS.  
AVERAGE WIND SPEED

Fig. 18

## VI. CONCLUSIONS

1. The vertical rate of growth of the aerial line source cloud can be expressed as  $d\sigma_z/dx = 3i^2$  where  $\sigma_z$  is a measure of the vertical cloud size,  $x$  is the downwind distance, and  $i$  is the turbulent intensity (in radians) measured as an angular displacement from the mean wind direction. This expression appears to be useful through a wide range of cloud sizes ( $\sigma$ ). In light atmospheric turbulence conditions and/or short release distances, it may be necessary to add the effect of the aircraft wake to obtain a reasonable explanation of the total cloud growth.
2. This rate of growth ( $3i^2$ ) leads to a model of ground dosage given by:

$$D = \frac{2Q}{3i_e^2 x u \sqrt{2\pi}} e^{-H^2/18i_e^4 x^2} \quad \text{where } D \text{ is the ground}$$

dosage at a distance  $x$  from the release,  $Q$  is the source strength,  $H$  is release height,  $u$  is mean velocity in the layer from ground to release height. A weighted average turbulent intensity ( $i_e$ ) and wind ( $u$ ) have been computed for this layer from observed turbulence and wind data. Maximum ground dosage and distance from the release to maximum dosage may be computed from the model given above.

3. Agreement between observed ground dosages and dosages computed from the model is good for releases made within a layer described by a Richardson number  $< .3$  from the ground to release height. For this situation, maximum dosage observed at the ground averaged 23 per cent greater than predicted by the model for the 14 tests which satisfied this criterion.
4. When the release was made at a level above the layer of  $Ri < .3$  observed variations from the dosage predicted by the model were very large and in some instances the cloud did not reach the ground appreciably along the 30 mile line.
5. Dilution of the cloud from the ends of the release line was measured in nine of the tests where adequate sampling was available along a crosswind line near the downwind end of the main sampler line. It was found that the cloud dilutes laterally at a rate corresponding to  $\sigma_H$ , the horizontal turbulence measurement at an intermediate level such as 450 feet. Comparison with concurrent vertical turbulence data indicates that  $\sigma_H$  averages about  $1.4\sigma_v$  for the conditions observed in the Dallas tests, where  $\sigma_v$  is the vertical turbulence measured at the same time and location. The dilution rate indicated

above corresponds to the dilution of a continuous source cloud and the long release line approximates this type of source in the horizontal direction.

6. Vertical growth of the cloud, measured by vertical sampling along the tower, was consistently greater than would be expected from the expression:  $d\sigma_z/dx = 3i^2$ . One of the reasons for the discrepancy is that the cloud has an appreciable initial size rather than beginning its diffusional growth as a point source. This initial size is the result of the aircraft vortex action immediately behind the airplane and has been estimated at  $\sigma = 15$  feet from Dugway calibration tests.
7. In addition to causing an appreciable initial cloud size, the aircraft also introduces turbulent wake energy into the air volume containing the particle cloud. The subsequent growth of the cloud appears to be the result of the combined effect of the wake energy and the natural atmospheric turbulent energy.
8. In many operating situations,  $i_e$ , the effective turbulence in the layer from the ground to release height can be reliably estimated without direct measurements of turbulence from the ratio of temperature gradient in the layer to average wind speed squared ( $\Delta\theta/\bar{u}^2$ ). The exact relation between this quantity and  $i_e$  will be a function of the terrain, at least in the lowest levels above the ground.
9. Calculations of  $i_e$  for all tests have been used to estimate the potential effectiveness of releases at 450, 750, and 1050 feet, regardless of actual release height, for all tests. If a criterion is assumed which requires that the particle cloud reach the ground in reasonable quantity in the first 15 miles the following table summarizes the results:

	<u>Would Reach Ground in 15 miles</u>	<u>Would Not Reach Ground</u>
450 feet	30 cases	5 cases
750	13	22
1050	1	34

Effective ground coverage under the Dallas test conditions is thus mainly limited to releases in the lowest 450 feet.

## VII. RECOMMENDATIONS

1. Generalization of the present results to other areas is limited by the lack of test data under rougher terrain conditions. Measured turbulence in the Dallas area was generally light although, on occasion, the geostrophic wind values were quite large. Tests under stronger turbulence conditions will require work over rougher terrain rather than under more extreme weather conditions.
2. Diffusion downward to the ground is severely limited in light wind (light turbulence) conditions. Results in the Dallas area over relatively smooth terrain indicate that a geostrophic wind of 15-20 mph is required before the turbulence is sufficiently strong for a successful release from about 450 feet. Further work is needed in light winds in rougher terrain to determine the limiting conditions for releases in other types of terrain.
3. In the near future, it will become necessary to consider more complex flow fields than those with assumed horizontal homogeneity as in Dallas. This would include the dosage variations associated with windward and leeward slopes, the three-dimensional effects of isolated hills or ridges, etc. When the size of the obstacle becomes comparable to the release height, the mean flow experiences large-scale deflections which cannot be treated by turbulence methods but must be approached by a combined three-dimensional wind flow-turbulence study.
4. The relation of cluster diffusion to turbulence parameters has been clarified to some extent by the English work (Hay-Smith, 1961). However, the maximum cloud size (compared to turbulence scale) to which the simple  $3i^2$  expression may be applied remains somewhat confused. In general, the growth of intermediate size clouds (more than several times the turbulence scale length) does not seem to be adequately expressed by the theoretical work done to date.

The consequences of this problem are that it is not possible, on the basis of present information, to judge how far downwind the simple ground dosage model (Equation (5) ) may be applicable before the cloud size (compared to turbulence scale) becomes too large or the effects of inhomogeneous turbulence become too great.

5. Additional comparative tests of adjacent rotorod and filter samples are required in order that the discrepancies in rotorod efficiencies can be evaluated.
6. The scope of the present analysis has been restricted somewhat by time, contract scope, and financial limitations. Numerous additional

fruitful studies of the data can be made and Volume II of this report has been issued for this purpose. These studies might include: relations between turbulence and synoptic weather parameters, a more realistic method of handling vertical inhomogeneities in turbulence than "effective" turbulence angle, dosage variability along the sampler line, limitations on the downwind distance applicability of the ground dosage formulas shown above, etc.

## ACKNOWLEDGMENTS

Dugway personnel assisted greatly in the field operations, particularly in the conduct of the fluorescent particle sampling. Dissemination, sampling, and assessment of the particles were carried out in a manner which contributed greatly to the success of the program.

Through the kind cooperation of Dr. Morton L. Barad of the Air Force Cambridge Research Laboratories, meteorological data from the television tower observational network were made available in tabulated and punch card form. The Department of Electrical Engineering, University of Texas, operators of the network, provided considerable assistance during the conduct of the field operations. Hill Tower, Inc., operators of the television tower, kindly granted permission to install turbulence sensors and sampling instrumentation on the tower itself. Mr. Oscar Carter of Hill Tower, Inc., was of inestimable value in carrying out the field operations. The U.S. Weather Bureau office at Love Field, Dallas, provided meteorological data and forecast information which was of great help in scheduling the tests as well as in the later analysis.

## VIII. REFERENCES

- Aerosol Laboratory, 1960: Quarterly Report No. 448-3, April-June 1960, p. B-9.
- Barad, M. L., 1959: "Analysis of Diffusion Studies at O'Neill", Adv. Geophysics, 6, Academic Press, pp. 389-398.
- Batchelor, G., 1950: "The Application of Similarity Theory of Turbulence to Atmospheric Diffusion", Quart. Journ. Roy. Met. Soc., 76, 328, pp. 133-147.
- Hay, J. S., and Pasquill, F., 1959: "Diffusion from a Continuous Source in Relation to the Spectrum and Scale of Turbulence", Adv. Geophysics, 6, Academic Press, pp. 345-365
- Jones, J. I. P., and Pasquill, F., 1959: "An Experimental System for Directly Recording Statistics of the Intensity of Atmospheric Turbulence", Quart. Journ. Roy. Met. Soc., 85, 365, pp. 225-236.
- Kolmogoroff, A. N., 1941: "The Local Structure of Turbulence in Incompressible Viscous Fluid for Very Large Reynolds Numbers", Comptes Rendus (Doklady) de l'Academie des Sciences de l'U. S. S. R., 30, pp. 301-305.
- MacCready, P. B., 1962: "Inertial Subrange of Atmospheric Turbulence", Journ. Geophysical Research, 67, No. 3.
- Meade, P. J., 1960: "Meteorological Aspects of the Peaceful Uses of Atomic Energy", Part I, WMO Technical Note No. 33.
- Mitcham, W. S., and Gerhardt, J. R., 1960: Final Report, Contract AF 19(604)-3498, ARD-TR-60-283.
- Pasquill, F., 1961: "The Estimation of the Dispersion of Windborne Material", Met. Mag., 90, No. 1063, pp. 33-49.
- Smith, F. B., and Hay, J. S., 1961: "The Expansion of Clusters of Particles in the Atmosphere", Quart. Journ. Roy. Met. Soc., 87, 371, pp. 82-101.

## APPENDIX A

### COMPARISON OF ROTOROD AND FILTER SAMPLERS

Comparisons of rotorod and filter sampler counts were available from the tower base and three downwind locations. Separation of the samplers at the tower was several feet, while separation at the downwind locations was from less than 1/4 mile to about 1/2 mile. Although about thirty pairs of values were available for comparison, only the sixteen shown below for which filter counts exceeded 100 were used. The average effective sampling rate of the rotorod sampler is determined from the comparison as 32.9 liters/min.

Trial	Location	Filter Rate (liters/min)	Sampler Counts	Rotorod Counts	Ratio: <u>Rotorod</u> <u>Sampler</u>	Rotorod Rate (liters/min)
4	15E*	12.5	198	533	2.69	33.6
4	25E-26E	12.5	186	707-565	3.80-3.04	42.7 avg.
5	15E	12.5	234	560	2.39	29.9
5	25E-26E	12.5	95	492-424	5.18-4.46	60.3 avg.
6	15E	12.5	438	966	2.20	27.5
7	15E	12.5	184	4.7	2.26	28.3
9	22A-24A	12.5	112	191-185	1.70-1.65	20.9 avg.
17	15E	12.5	452	514	1.14	14.3
18	Tower	12.5	301	797	2.65	33.2
18	15E	12.5	138	735	5.32	66.5
22	15E	12.5	118	267	2.26	28.3
25	Tower	6.5	194	968	4.99	32.4
25	15E	6.5	204	925	4.53	29.4
26	15E	6.5	160	522	3.26	21.2
28	15E	6.5	97	325	3.35	21.8
35	Tower	6.5	270	1518	5.62	26.6

\* Refers to Sampler No. 15 on Sampler Line E.

## APPENDIX B

### TURBULENCE MEASUREMENTS AND ANALYSIS

#### A. Turbulence Information and Summary

The fundamental aim of this project has been to relate diffusion to turbulence, by measurement and theory. The turbulence at various tower heights was measured by bivan sensors, recorded on a multi-channel tape recorder, and reproduced in the laboratory for analysis. The bivanes yield only direction information, but this is the parameter on which the diffusion theory is based. Turbulent velocities are perhaps more fundamental when considering the physical basis of the turbulence; if desired, these are obtained to the accuracy needed by multiplying the direction changes (in radians) times the mean velocity.

The diffusion theory under consideration requires some knowledge of the frequency structure of the turbulence. Two points are important: 1) the standard deviation of the turbulence must be known; and 2) there must be some information on the scale of the turbulence. The analysis gear was made somewhat more complex and versatile than would be required solely to handle these two points, because the expected scales were not known before measurements were made and because the additional data can aid in giving better physical insight into the turbulence process.

The primary spectrum analysis tool consisted of three "sigma meters", based on the design of Jones and Pasquill (1959). These are, in effect, high-pass filters with integration of the filter output. The filter characteristics are not sharp, since the cutoffs come simply from two cascaded R. C. Filters. By taking differences between the energies shown by the different sigma meters, some information is obtained on the turbulence spectra, and the scale of turbulence. Measurements with the sigma meters quickly verified that the major energy in the vertical turbulence was at wavelengths completely covered by the sigma meters.

The other spectrum measurement technique was to speed up the time scale of the records by re-recordings, and then analyze for the turbulence spectrum with a conventional frequency analyzer. Several methods were examined and tested, and the feasibility of the technique was demonstrated. However, the sigma meter analyses proved to be sufficient for the purposes of the project, so this more refined method was not further developed.

The various concepts relating to the turbulence are summarized as follows. Most of these items are treated in detail, with figures and computations, later in this appendix.

- 1) The sigma meters are used after the data are speeded up by a factor of 16 by being recorded in the field at 15/16 inches/second and reproduced in the laboratory at 15 inches/second.
- 2) The sigma meter characteristics are plotted (Fig. B-2 in terms of real time and in terms of the speeded-up scale. In this report,  $\sigma_5$  refers to the RMS of angle fluctuations as observed after a high-pass filter which transmits 50% of the input power at a frequency of .088 cycles per second (11.4 second wavelength). In terms of energy,  $(\sigma_5 \bar{u})^2$  is a measure of the total turbulent energy at frequencies greater than .088 cps where  $\bar{u}$  is the mean wind.  $\sigma_{30}$  corresponds to frequencies over about 0.0147 cps, and  $\sigma_{180}$  to frequencies over about 0.0025 cps. The resolution of the instrumentation system gives significance to sigma values down to 0.10. The sigma meter characteristics depend on distance of wind flow (frequency in cycles per foot of flow). Thus the combined effect should be computed separately for each wind speed.
- 3) Wind tunnel tests show the bivane has a rise distance of 2.3 feet and a damping ratio of 0.31. The bivane characteristics only alter the measured sigma meter energies by at most a few per cent, and so can be ignored for this study. The bivane amplifies the apparent ~~energy at wavelengths around 8 to 15 feet, but cuts out the energy at wavelengths under about 7 feet,~~ and the two effects tend to cancel when measuring the sum of the two energy bands.
- 4) An energy spectrum ( $E(f)$  vs.  $f$  on a log-log plot) is presented (Fig. B-4), representing a likely spectrum for the vertical turbulence at the 150 foot level for Trial 11. It has an energy peak around 1500 foot wavelengths ( $\sim 0.02$  cps for the 20 mph wind), and approximately follows the theoretical  $-5/3$  spectrum law for wavelengths below about 190 feet.
- 5) The same spectrum is plotted (Fig. B-5) in the form  $E(f)$  vs.  $\log f$  for a linear scale, and the effects of sigma meter response and bivane response are depicted. This type of presentation is convenient because the area under the curve shows the true relative amount of energy involved. The observed sigma meter readings:

$$\sigma_5 = 3.22^\circ$$

$$\sigma_{30} = 3.83^\circ$$

$$\sigma_{180} = 3.75^\circ$$

are shown to be reasonably consistent with the assumed energy

spectrum and the sigma meter characteristics. The small effects due to the bivane characteristics are shown graphically.

- 6) By extrapolating the reasoning in the above item, a rough relationship between the observed  $\sigma_5/\sigma_{180}$  values and the frequency of maximum energy is derived (Fig. B-6). Converting from frequency to wavelengths, it is then possible to examine the 'dominant' wavelength  $\lambda_m$  vs. height. At low heights  $\lambda_m \sim 5z$ ; at 1000 feet,  $\lambda_m \sim 1z$ , all with some systematic stability dependence of the relationship. These are the wavelength ranges contributing most to the observed sigma values. The wavelengths of most importance for the diffusion depend on the scale of the project.

## B. Bivane Characteristics

The MRI Model 1040 Bivane was tested in a wind tunnel to ascertain its exact performance characteristics. The bivane was held about  $10^\circ$  off from the line of flow, released, and the damped oscillatory response recorded on a high-speed oscillograph. The results showed the damping ratio to be about 0.31, the natural period distance to be about 10.7 feet, and the rise distance (the distance to go from 90 per cent to 10 per cent of the total change) to be about 2.3 feet. It was verified that the response distances are the same over a wide range of velocities (hence the response times are inversely proportional to mean velocity). The amplitude response characteristics for the bivane are shown in Fig. B-1. The curve is correct for all wind speeds when the abscissa is read as distance; for convenience, frequency coordinates are also given for a wind speed of about 20 mph ( $\sim 30$  fps).

For energy spectrum computations, the dynamic gain or relative amplitude factor shown as the left hand ordinate on Fig. B-1 must be squared. The right hand ordinate has the squared scale.

Obviously, from Fig. B-1, the sensor will appreciably amplify the apparent turbulent energies over the range of about 8-15 feet, and attenuate the energy at shorter wavelengths. In the practical case, when dealing with atmospheric turbulence which has an energy spectrum proportional to the minus five-thirds power of wavelength at these eddy sizes, the total energy subtracted approximately counteracts the total energy added. This will be shown graphically for several wind speeds on Fig. B-5 in the next section. Thus the energy measured by the sigma meters will be the true turbulent energy, within a few per cent. For a vane sensor having a certain response distance, there will be an optimum damping ratio to make the energies balance more exactly (for a vane with the 2.3 foot rise time, a damping ratio of about 0.4 might be more appropriate). The balancing accuracy is of even less importance if the response distance of the sensor is decreased. MRI, during proprietary equipment development and also for a turbulence tower

development for the Army at White Sands, has devised structures and aerodynamic optimization techniques to give operational vanes virtually any desired damping up to critical damping, and rise distances as short as 13 inches, showing these energy corrections can be virtually eliminated. For the purposes of the Dallas Tower project, the important point is that the sensor characteristics do not affect the sigma meter readings within the accuracy needed.

### C. Sigma Meter Characteristics

The sigma meters employed were identical in function to those shown by Jones and Pasquill (1959). The averaging and sampling times were essentially identical to theirs.

$\sigma_5$  refers to a 5-second sampling time with a running mean value over a 100-second time period;

$\sigma_{30}$  refers to a 30-second sampling time, with a running mean value over a 230-second time period;

$\sigma_{180}$  refers to a 180-second sampling time with a running mean value over a 500-second time period.

Actually, the frequency characteristics were all speeded up by a factor of 16, because the meters were only used on the tape playback at 15 inches/second although the original record was obtained at a tape speed of 15/16 inches/second.

Fig. B-2 shows the sigma meter characteristics, both in analyzer time and real time. The left hand ordinate is relative amplitude or dynamic gain; the right hand ordinate shows the squared characteristics, because the square is involved in the energy computations. The curves were obtained by generating a sine wave at the appropriate frequency by means of a rotating potentiometer or a low-frequency electronic generator. The sigma meters were designed so that a high frequency sine wave of 1/2 volt peak to peak gave a full scale meter reading. The gain of the combined sensor bridge and tape record -- playback cycle was such that a  $\sigma$  value of  $12^\circ$  for Gaussian-distributed turbulence gave full scale on the meter.

A low-pass meter was also built which showed the original record smoothed by 180 second averaging. It was not used routinely because so little energy was obtained at such low frequencies.

### D. Energies and Spectra from the Sigma Meters

The sigma meters serve as broad filters and therefore can give some information on the shapes of the turbulence spectra. Fig. B-3 shows the

"band pass" effects of taking the differences between two sigma meters. Since the energies relate to sigma squared, these curves come from the "relative amplitude squared" values shown on Fig. B-2. The exact interpretation of the different sigma values depends on assumptions concerning the spectra shapes, but still Fig. B-3 demonstrates important items. If  $\sigma_{180}^2 - \sigma_{30}^2$  is large, this is almost equivalent to noting that  $\sigma_{30}/\sigma_{180}$  is considerably less than unity. In this case, there must be large atmospheric turbulence energy at frequencies below about 0.03 cps. The measurements show that  $\sigma_{30}/\sigma_{180}$  is usually not far from unity, so for reasonable spectra shapes there is not much energy at frequencies below 0.03 cps. This further implies that  $\sigma_{180}$  includes virtually all the energy, so  $\sigma_{180}$  can be used for the diffusion calculations which are based on the total energy.

It turns out that sometimes  $\sigma_{30}$  exceeds  $\sigma_{180}$ , which would seem impossible from their definitions. However, it should be noted that the  $\sigma_{30}$  meter and the  $\sigma_{180}$  meter have different sampling times (essentially a different sample lag) and so are giving data for slightly different times. In 'steady' turbulence this effect is negligible. It appears most strongly in the non-steady cases of high Richardson's Number where the turbulence is being damped out.

To help relate sigma meter readings to real turbulence spectra, Fig. B-4 has been constructed. It is a suggested spectrum for the vertical turbulence at the 150 foot level for Trial 11 (mean wind was about 20 mph). Following MacCready (1962), a slope of  $-5/3$  is used as a first approximation for wavelengths under about 190 feet (above 0.16 cps). The lower frequency part of the spectrum is a smooth curve which gives appropriate sigma meter value; it does have a logical shape which agrees roughly with the spectrum which would be anticipated in stable conditions.

For quantitative computations, this same spectrum is plotted on a  $f E(f)$  vs.  $\log f$  basis in Fig. B-5. In such a plot, the area under the curve is proportional to the energy involved, and so the effects of filters can be seen graphically. This derives from:

$$\text{Total Energy} = \int_a^b E(f) df = \int_a^b f E(f) d(\ln f).$$

The effects of vane overshoot and vane frequency cutoff can be easily studied on Fig. B-5. The shaded areas somewhat balance each other and so leave the sigma meter readings fairly accurate.

Note that  $\sigma_{180}$  gives virtually the entire energy in the turbulence. If the total energy under the curve is normalized to unity, then one finds  $\sigma_{180}^2 = 1.0$ ,  $\sigma_{30}^2 = 0.94$ ,  $\sigma_5^2 = 0.65$ , giving  $\sigma_{180} = 1.0$ ,  $\sigma_{30} = 0.97$ , and  $\sigma_5 = 0.81$ . The observed values were  $\sigma_{180} = 3.75^\circ$ ,  $\sigma_{30} = 3.83^\circ$ , and  $\sigma_5 = 3.22^\circ$ . This is

one of the cases where  $\sigma_{180} < \sigma_{30}$ , presumably due, as suggested, to the sigma meter lags causing the meters to be sampling slightly different turbulent situations. To obtain logical consistency, assume a value of  $\sigma_{180}$  to be 3 per cent higher than the measured one, then normalize to  $\sigma_{180} = 1$ ,  $\sigma_{30} = 0.99$ ,  $\sigma_5 = 0.83$ , in rough agreement with the values coming from Fig. B-5.

Using the same sort of graphical reasoning, a subjective estimate was made of the dominant frequency in the spectrum as related to the ratio  $\sigma_5/\sigma_{180}$ . See Fig. B-6. The dominant frequency means the peak of the curve on Fig. B-5; the frequency which contributes most to the sigma meter reading,  $\sigma_{180}$ . The dominant frequency certainly depends on other parameters than just  $\sigma_5/\sigma_{180}$ , but the simple relationship suggested in Fig. B-6 is a reasonable first approximation which should show the order of magnitudes of the wavelengths involved. With the mean velocity given, one can convert the dominant frequency to a wavelength distance - 300 feet, for Fig. B-5.

Figs. B-7, B-8, and B-9 show the wavelengths vs. height for the three test series. Only those tests for which the Richardson's Number at release height was less than 1.0 are included in these figures. The omitted tests are generally for more transient cases and have far more scatter. To summarize all the curves together, a reasonable approximation is that at 30 feet  $\lambda_m \sim 5z$ , while at 1000 feet  $\lambda_m \sim z$ . This empirical relationship can be given as

$$\lambda_m = 24z^{0.54} \text{ for } \lambda_m \text{ and } z \text{ in feet.}$$

This relationship is plotted on Fig. B-7.

The main point here is to search for common principles between the various tests, and to provide an estimate of the scale of the turbulence. The turbulence scale relative to the size scale involved in the test is of importance in determining the theoretical approach to diffusion calculation.

#### E. Complete Spectrum Measurements

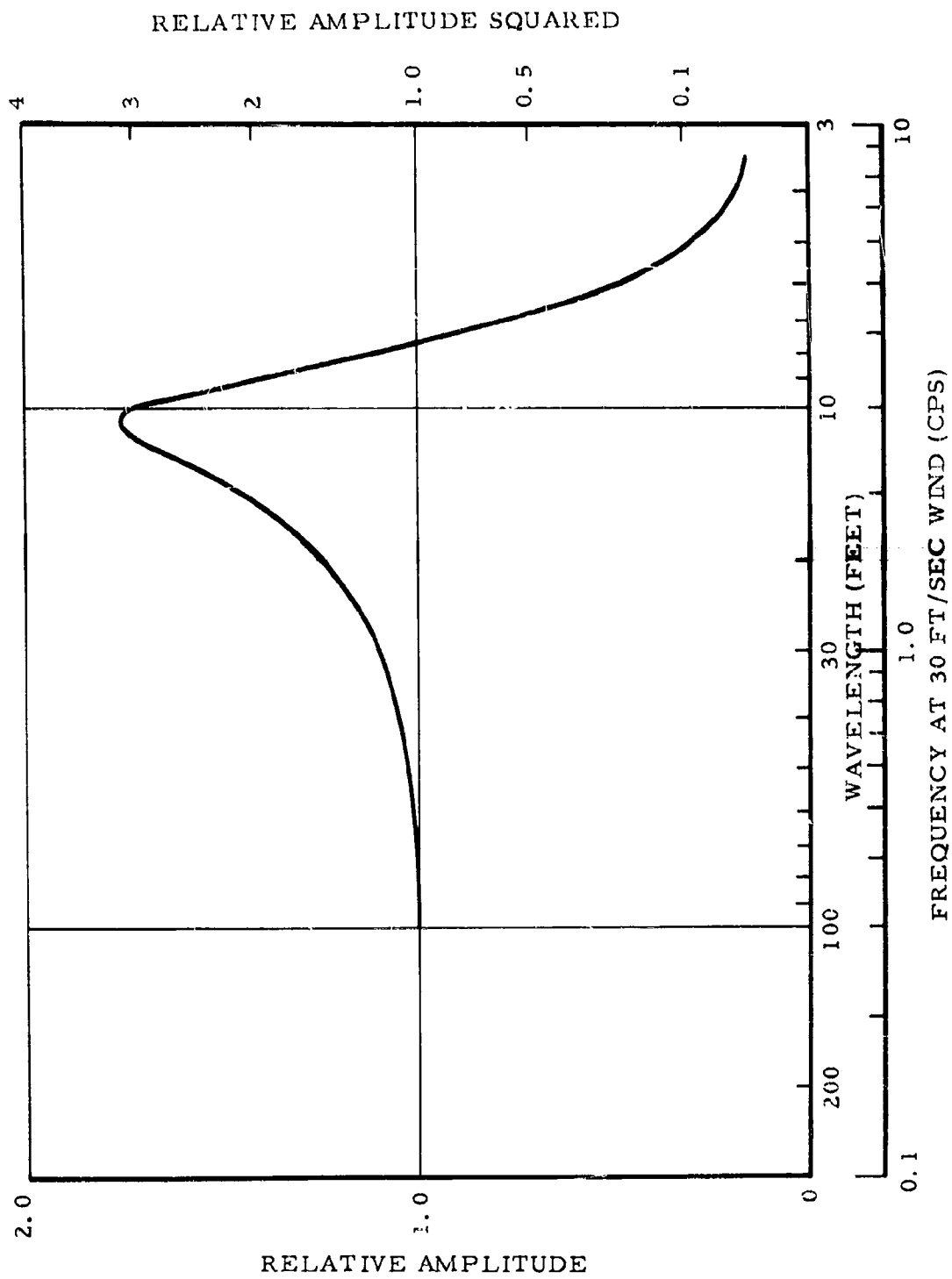
It was intended that the complete energy spectrum be measured by 1) speeding up the turbulence record through one or two recordings, and 2) then putting this signal through a standard frequency analyzer -- a narrow band-pass filter which is slowly varied across the frequency range as the record on a tape loop is replayed continuously. Several variations of this method were successfully demonstrated, but it was not developed to real operational utility because by then it had become apparent that the simple sigma meter records would adequately serve the purposes of this project.

The frequency range of interest, in real time, was assumed to be about 0.004 cps to 4 cps. Lower frequencies would involve too few cycles per run to permit any statistical significance to the results. Since conventional frequency

analyzers cannot be assumed reliable below about 10 cps, this means that the record must be speeded up by a factor of 2500 or more. By recording in the field at 15/16 inches/second and playing back at 15 inches/second, a speedup of 16 was achieved. Using this output, then another tape was made on an Ampex unit at 1-7/8 inches/second at the California Institute of Technology, Jet Propulsion Laboratory. A loop of this tape was used in the frequency analyzer at 60 inches/second, effecting another factor of 32 speedup for a total speedup of 512. The frequency analyzer could then cover all real time frequencies above about .02 cps. It is apparent from the preceding section that this coverage would be adequate for the typical conditions of this project.

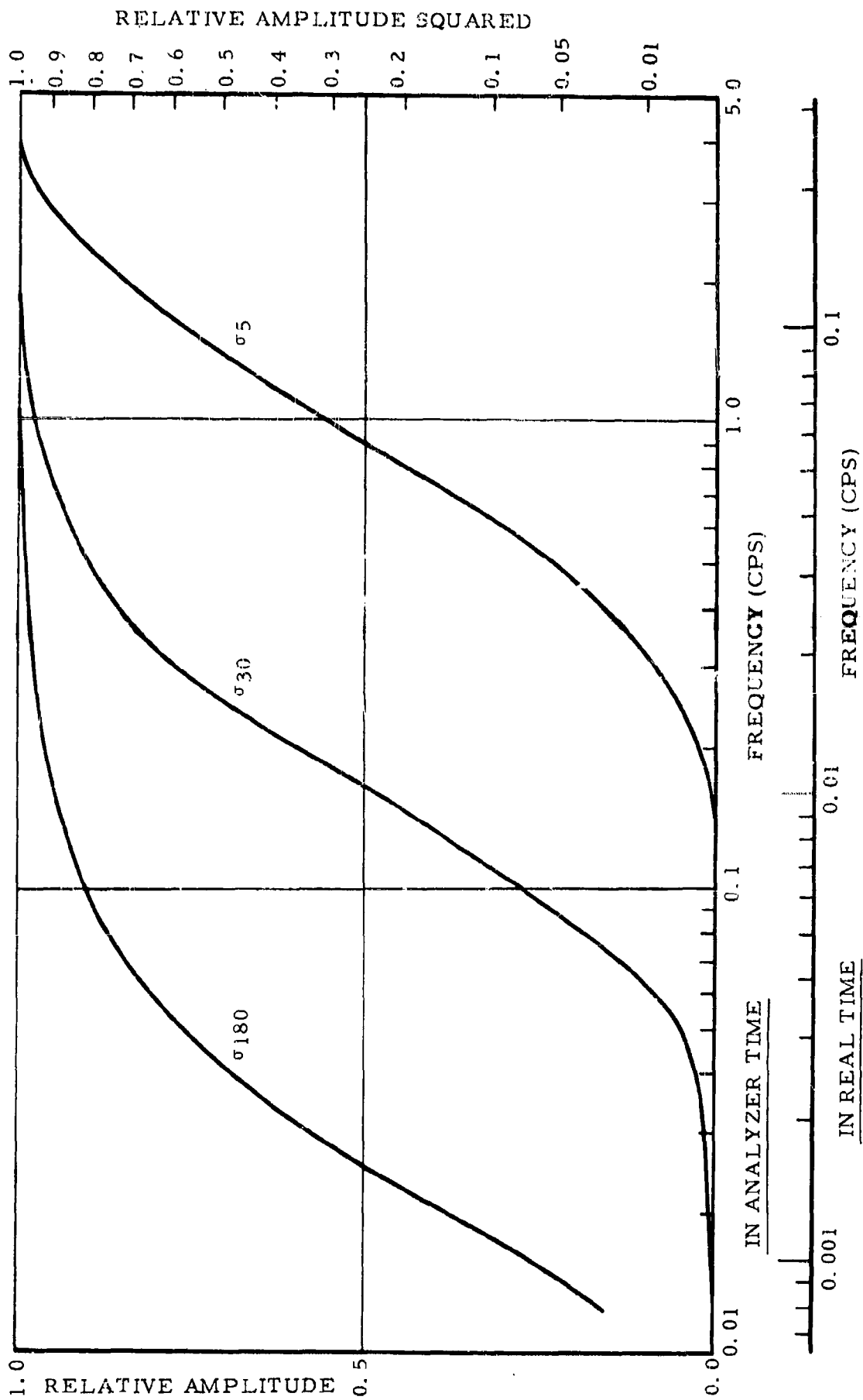
For the lower frequencies, a different speedup technique was employed -- a factor of 10,000 speedup in one step by using a newly developed digital time-shifter at the Jet Propulsion Laboratory. This total speedup of real time of 16,000 was more than adequate for all frequencies involved, but introduced some noise into the record. The alternative scheme of two standard speedups, say 32 and then 16 for a total factor of 8292 from real time, could not be tried because two Ampex recorders would have been required and only one was available at JPL with the needed amplifiers.

In review, it would appear that a single extra speedup of 32 (total from real time, 512) would suffice to permit using a standard spectrum analyzer for **studying the turbulence in the stable conditions encountered in the present** project. This would provide a quick way of ascertaining total turbulent energies but a single sigma meter would be quicker. When detailed spectrum information is desired, the tape speedup-analyzer method is indicated.



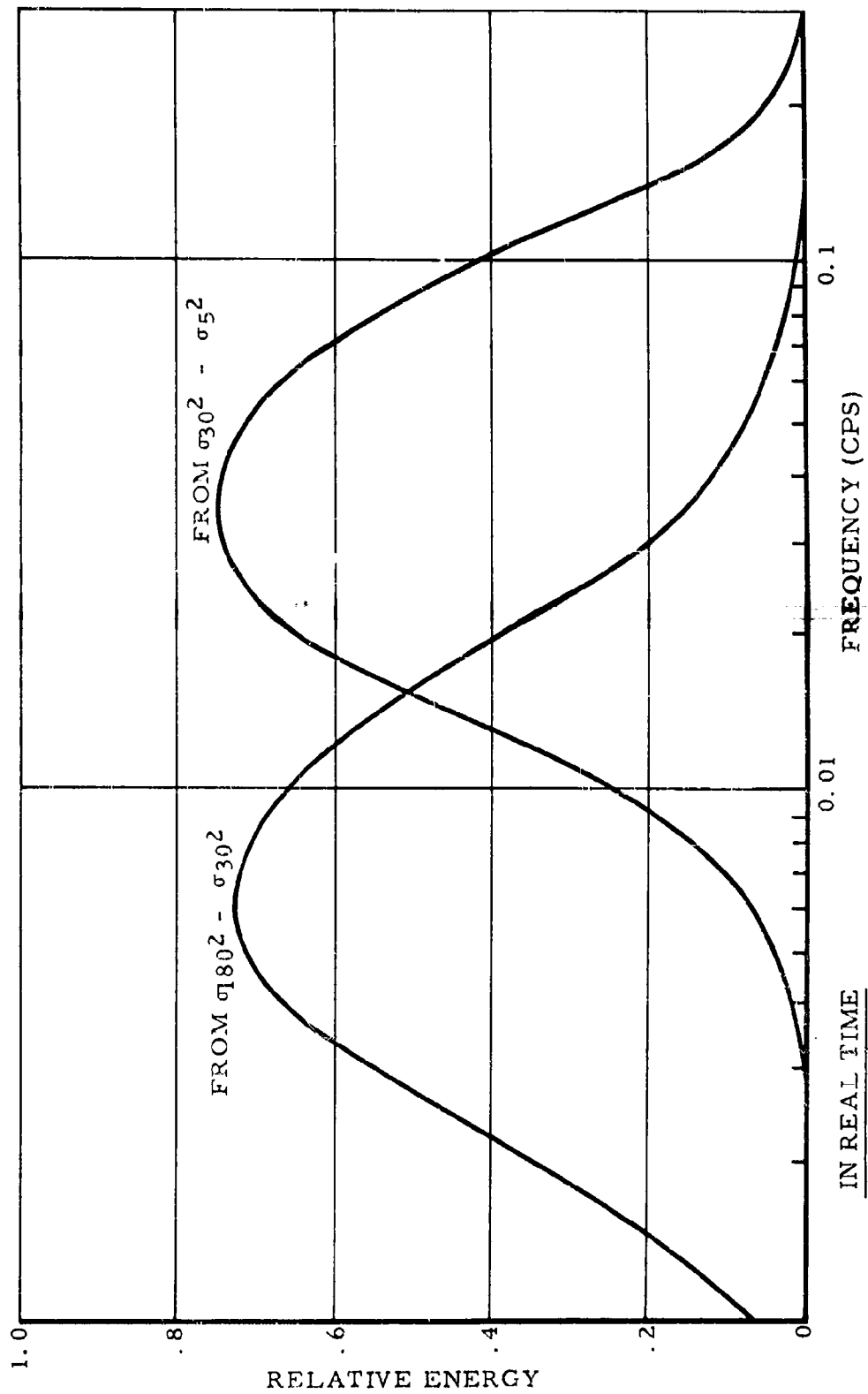
BIVANE RESPONSE CHARACTERISTICS

Fig. B-1



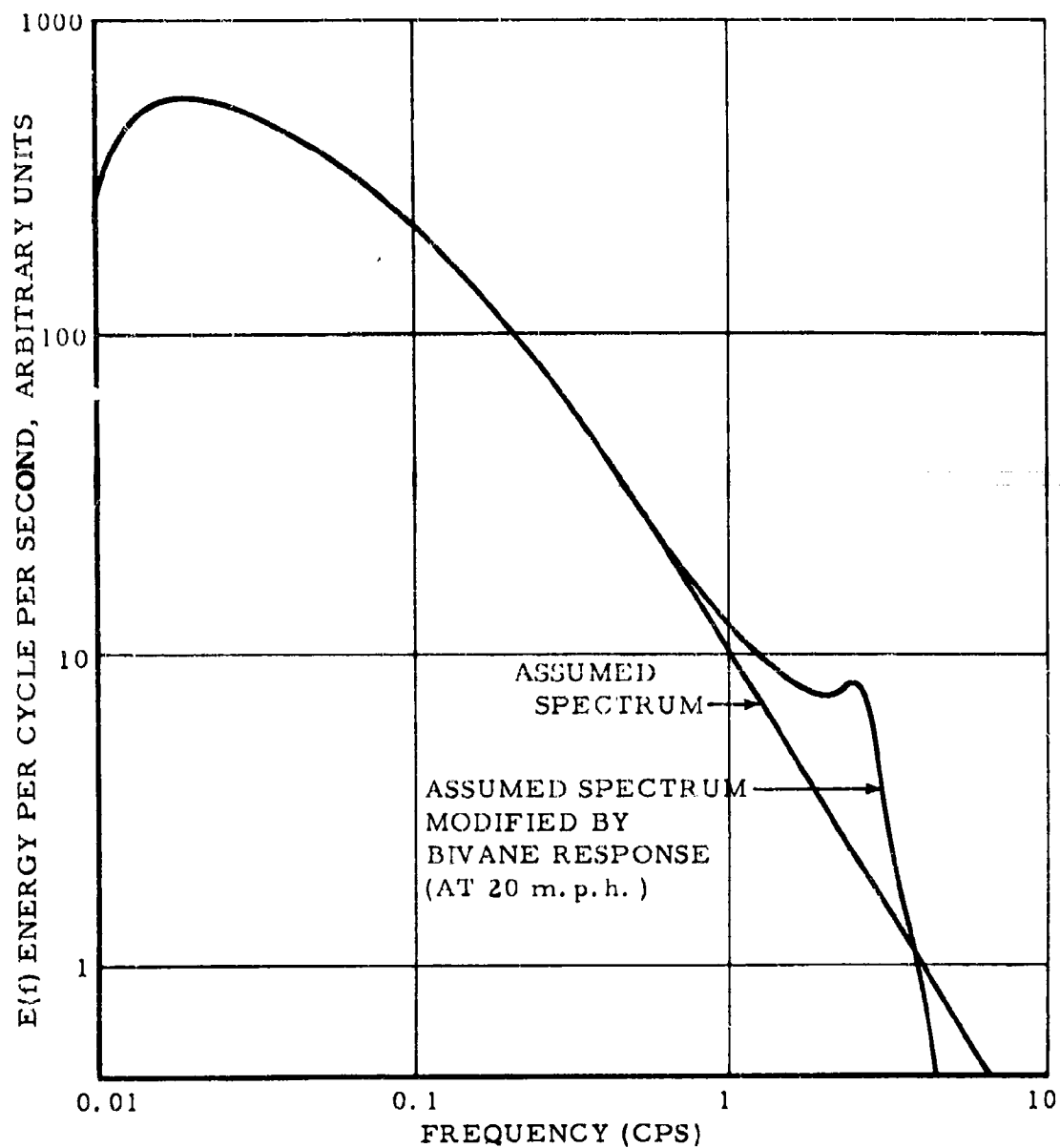
SIGMA METER CHARACTERISTICS

Fig. B-2



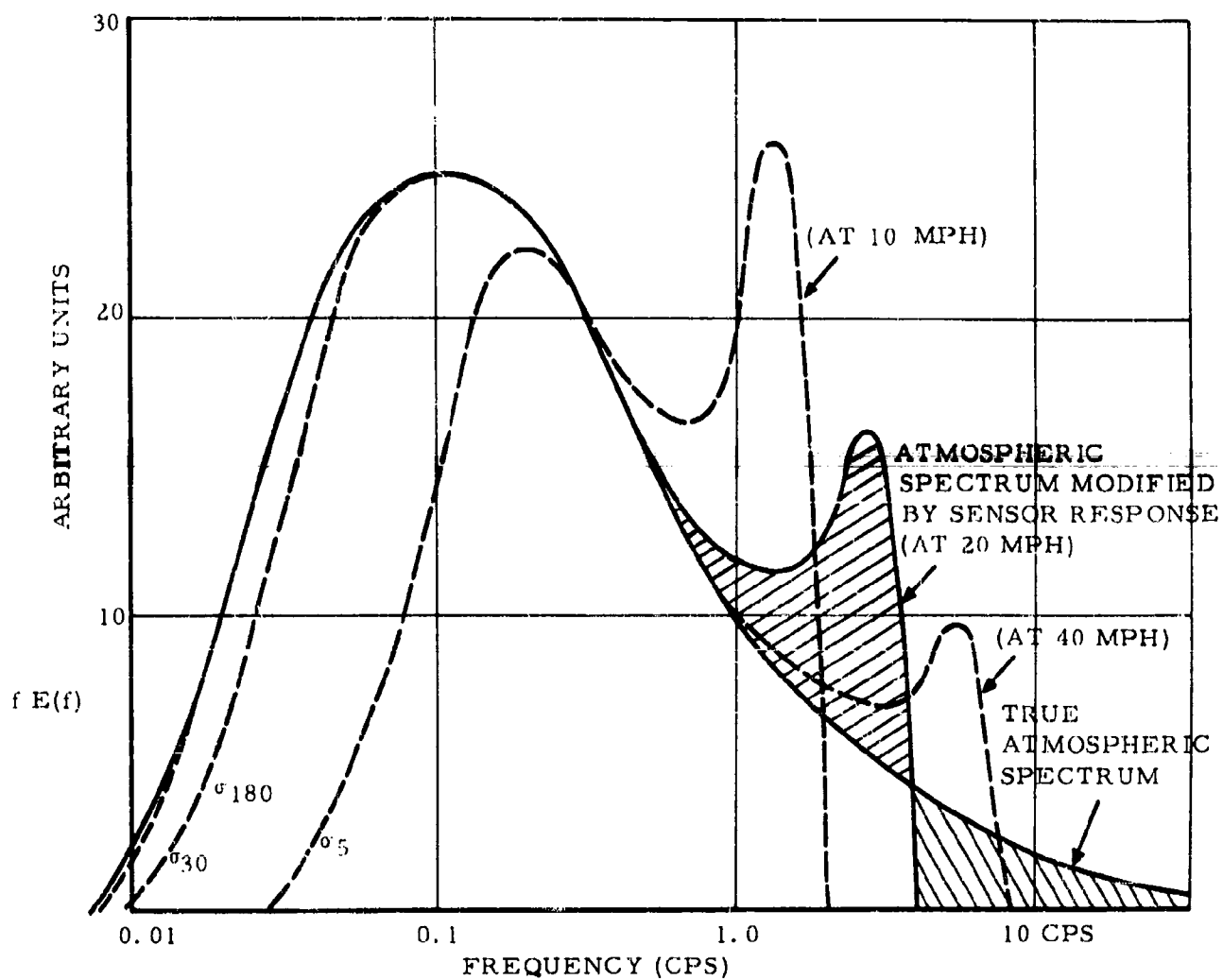
BAND-PASS FILTER EFFECTS OF SIGMA METER DIFFERENCES

Fig. B-3



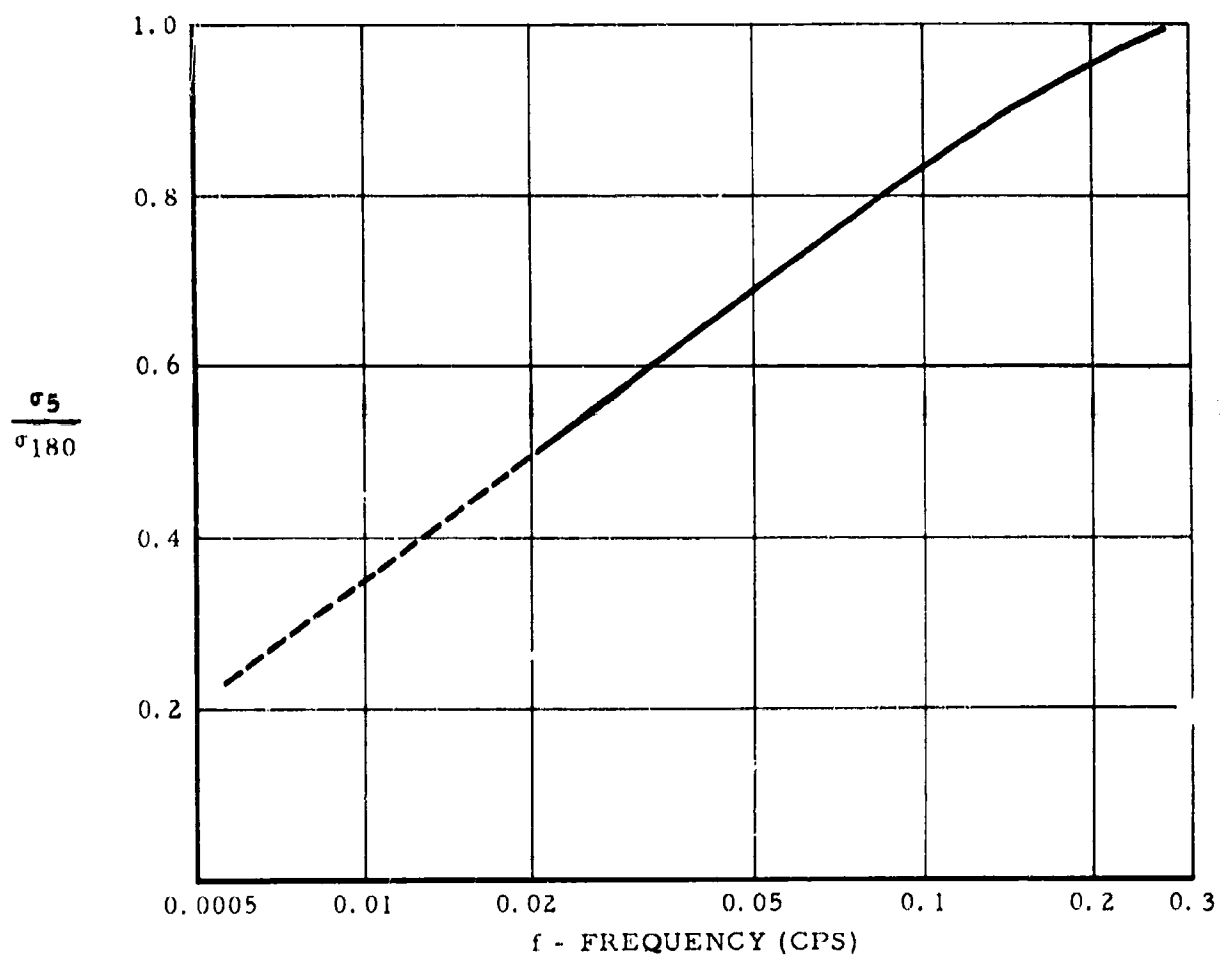
ASSUMED POWER SPECTRUM OF  
VERTICAL TURBULENCE AT 150 FT. LEVEL, TRIAL NO. 11

Fig. B-4



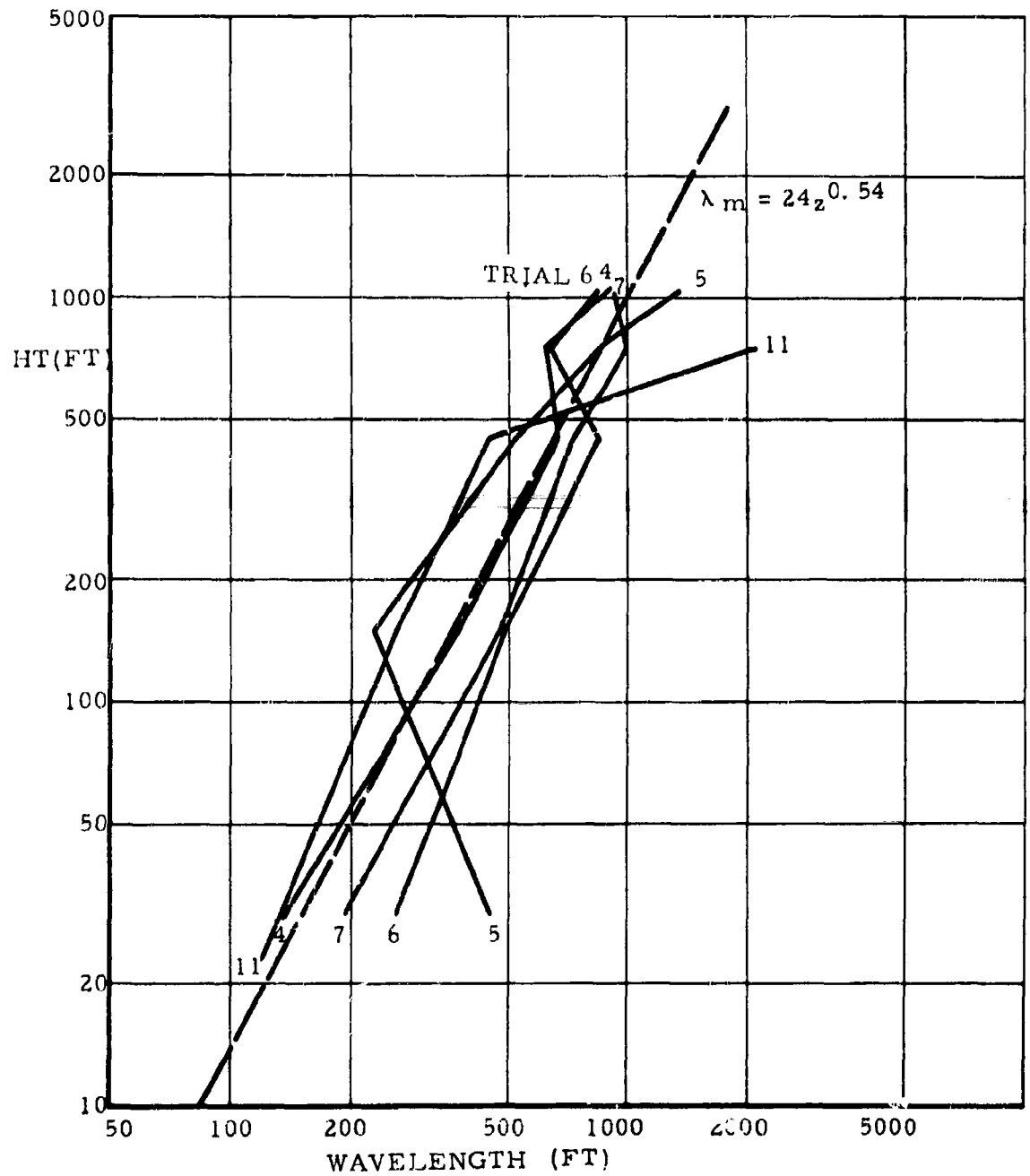
ASSUMED POWER SPECTRUM AND SIGMA METER EFFECTS

Fig. B-5



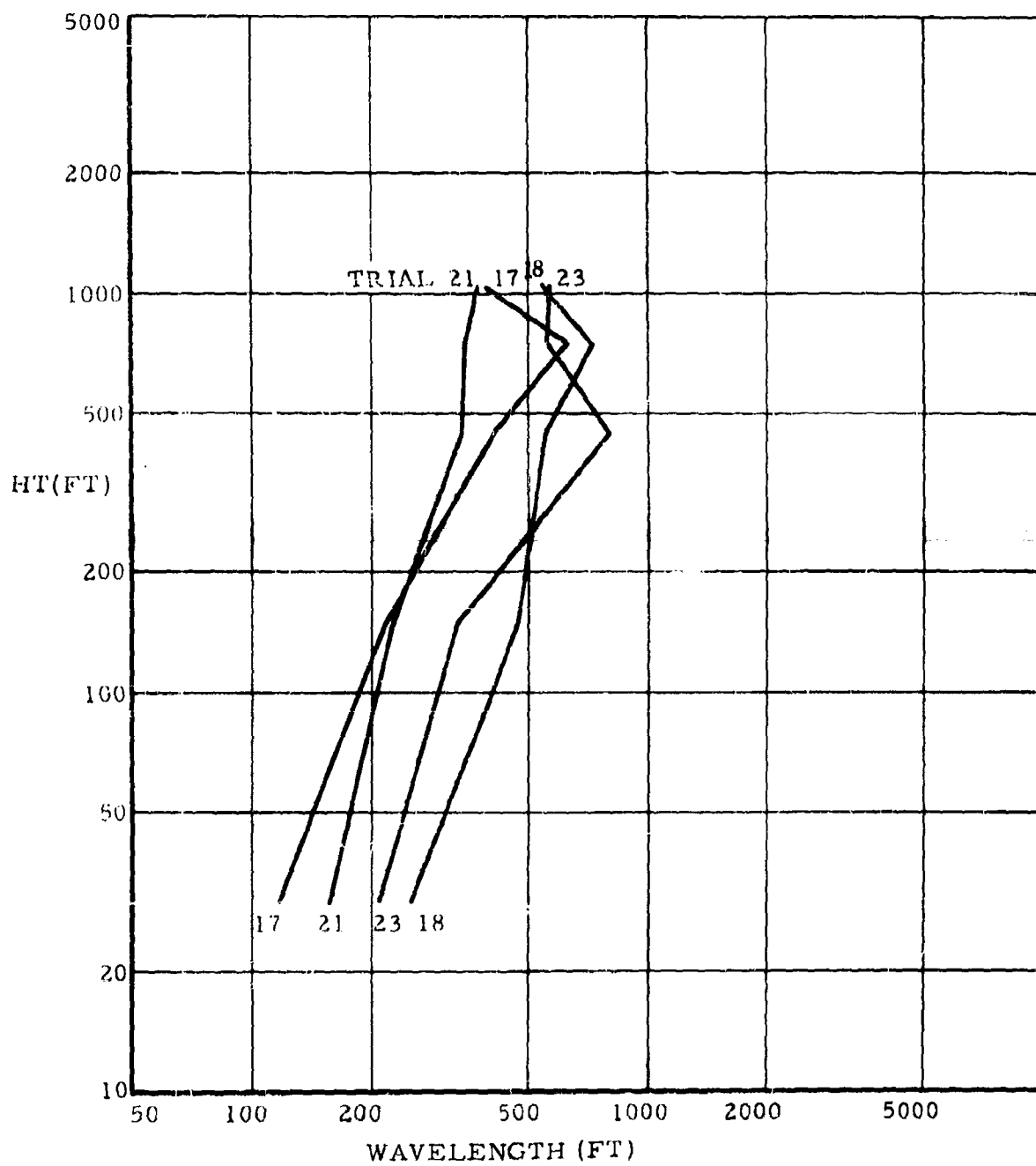
DOMINANT FREQUENCY VS. SIGMA METERS

Fig. B-6



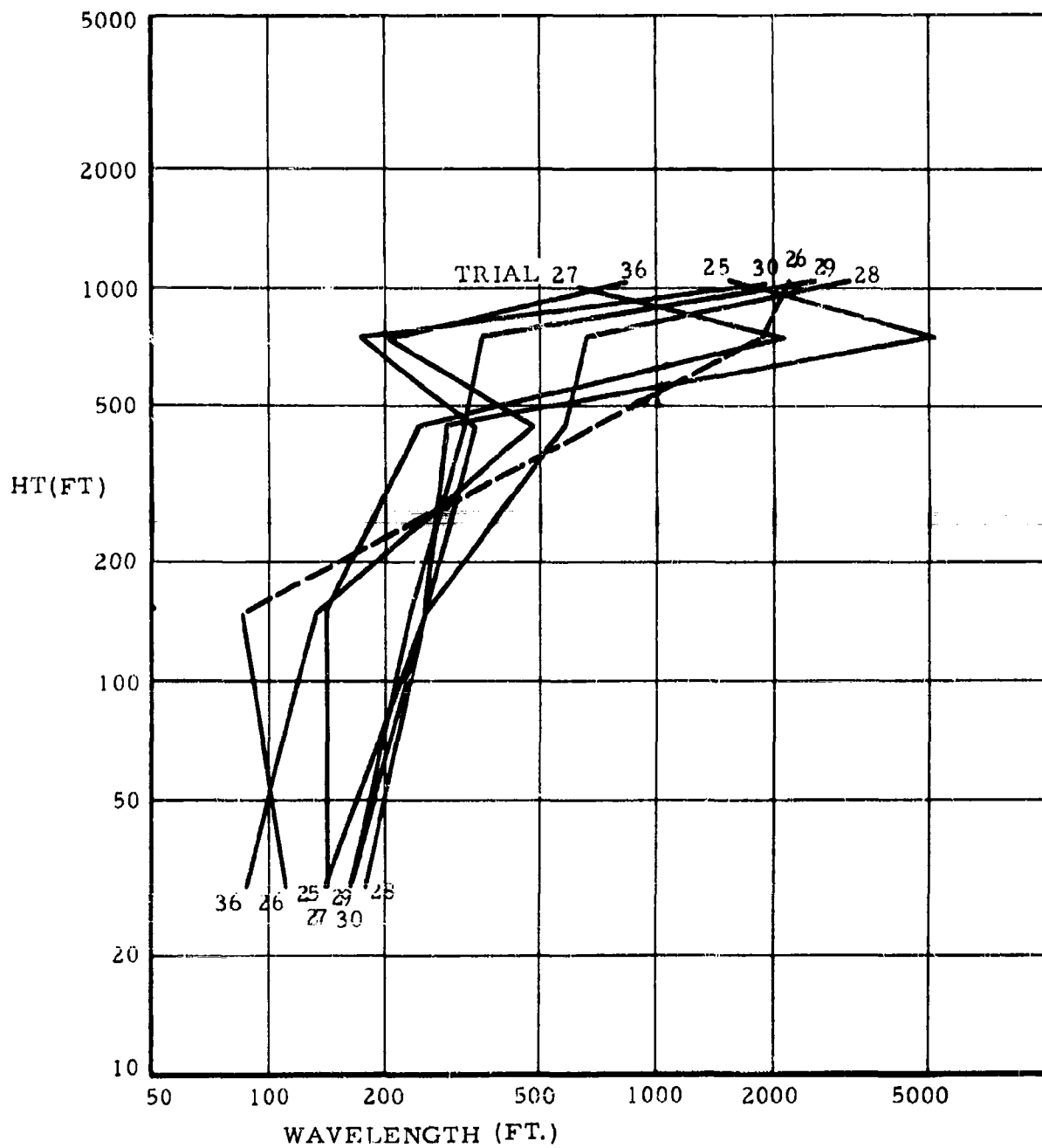
TEST SERIES I  
WAVELENGTH OF PEAK ENERGY AS A FUNCTION OF HEIGHT

Fig. B-7



TEST SERIES II  
WAVELENGTH OF PEAK ENERGY AS A FUNCTION OF HEIGHT

Fig. B-8



TEST SERIES III

WAVELENGTH OF PEAK ENERGY AS A FUNCTION OF HEIGHT

Fig. B-9

## APPENDIX C

### DISSIPATION FACTORS AND AIRCRAFT WAKE EFFECTS

#### A. General

The rate  $\epsilon$ , at which turbulent energy is converted into heat through the action of viscosity, turns out to be a fundamental variable in describing a turbulence field. There are several ways of measuring or estimating it; it has considerable practical significance; and it determines all the statistical properties of small eddies. Thus, for the 1961 Dallas Tower diffusion studies and for forthcoming investigations, consideration of  $\epsilon$  proves helpful in certain instances.

#### B. Review of the Concepts

Kolmogoroff's Similarity Hypothesis presents a picture of turbulence in which a) the energy is put into the system at large wavelengths (large eddies) and removed as heat through viscous effects at small eddy sizes, and b) the turbulence is isotropic for all eddies materially smaller than those by which energy entered the system. The inertial subrange covers those eddies where the turbulence is isotropic, excluding the small viscous eddies. In a steady state case, all the statistical properties of turbulence in the inertial subrange can only depend on  $\epsilon$ , the equilibrium dissipation rate -- and so, for these inertial subrange eddies, simple dimensional analysis provides formulas for power spectra, correlation coefficients, and diffusion. The whole subject is reviewed by MacCready (1962), who concludes that the concept does have adequate experimental justification, and that the formulas work surprisingly well over even broader ranges and in more non-stationary and non-homogeneous turbulence than the restrictions of the theory would imply.

For the Dallas Tower project, the turbulence spectrum is of importance. In the inertial subrange, the one-dimensional energy spectrum is:

$$E(k) = C_2 \epsilon^{2/3} k^{-5/3}$$

where  $k$  is the wave number ( $\text{cm}^{-1}$ ) (wavelengths per unit distance,  $= 1/\lambda = f/U$  where  $\lambda$  is the wavelength,  $f$  is the frequency, and  $U$  is the mean velocity):

$E(k)$  is twice the one-dimensional energy per unit mass per unit wave number ( $\text{cm}^2\text{sec}^{-1}$ ),

$\epsilon$  is the dissipation factor ( $\text{cm}^2\text{sec}^{-3}$ ), and

$C_2$  is a dimensionless coefficient of order unity (found to be near 0.44 for

transverse turbulence, and 0.33 for longitudinal turbulence).

The total one-dimensional 'energy' is  $1/2 \int_0^{\infty} E(k) dk$ .

This spectrum formula should have reasonable validity for wavelengths shorter than the height  $z$  for the stable nighttime cases of the Dallas Tower project. Perhaps a better estimate of the maximum wavelength for which the formula is valid would be to take half of the wavelength,  $\lambda_m$ , at which the energy contribution is maximum, as found in Appendix B. At 30 feet height the wavelength would be about 75 feet, and at 1000 feet height the wavelength would be about 500 feet.

### C. Decay of a Turbulence Field

For simplicity, assume the complete power spectrum consists of two parts,  $E(k) = C_2 \epsilon^{2/3} k^{-5/3}$  for  $k > k_1$ , and  $E(k) = C_2 \epsilon^{2/3} k_1^{-5/3} = \text{constant}$ , for  $k < k_1$ . Setting  $C_2 = 1/3$ , and putting the total turbulent energy  $H$  at three times the one-dimensional energy, one finds approximately that

$$H = \frac{5}{4} k_1^{-2/3} \epsilon^{2/3}.$$

If a mass of air has this turbulence spectrum, and then receives no more energy, its energy will decay slowly at a rate  $dH/dt = -\epsilon$ . Note that this picture differs from the requirements of the inertial subrange concept, but these calculations should provide a reasonable first approximation to the happenings in a real case.

Set  $5/4 k_1^{-2/3} = N$  for convenience, and let  $H = H_0$  at  $t = 0$ . Then  $\epsilon = (H/N)^{3/2}$  and  $\epsilon = -dH/dt$ , from which

$$\int_0^t \frac{dt}{N^{3/2}} = - \int_{H_0}^H \frac{dH}{H^{3/2}}.$$

then

$$H = \left[ \frac{t}{2N^{3/2}} + \frac{1}{H_0} \right]^{-2}$$

To obtain actual numbers from this decay equation, assume  $k_1$  corresponds to a wavelength of 200 meters (this spectrum would be a reasonable one to represent conditions at, say, about 500 feet altitude). Then  $N = 922 \text{ cm}^{2/3}$ . Also assume  $\epsilon = 1000 \text{ cm}^2 \text{ sec}^{-3}$  at  $t = 0$ , and so  $H_0 = 9.22 \cdot 10^4 \text{ cm}^2 \text{ sec}^{-2}$ .

The curve of Fig. C-1 results, wherein H is plotted against t.  $\epsilon$  is given as an alternate ordinate.

With  $1/3 H$  representing the turbulent energy in the vertical direction, then one can calculate the one-dimensional sigma value for a particular wind speed.

$\sigma$  (velocity) =  $\sigma$  (direction) times wind speed for  $\sigma$  (direction) in radians, or  $\sigma$  (velocity) =  $\sigma$  (direction)/57.3 times wind speed for  $\sigma$  (direction) in degrees

$$\frac{1}{3} H = \frac{1}{2} \int_0^{\infty} E(k) dk = \frac{1}{2} \sigma(\text{dir})^2 U^2, \text{ and so, for } \sigma \text{ in degrees, } \sigma = \frac{46.8}{U} H$$

where  $\sigma$  is the RMS vane fluctuation in degrees as used in this study, U is in  $\text{cm sec}^{-1}$ , and H is in  $\text{cm}^2 \text{ sec}^{-2}$ .

For a wind of 10 meters/second (approximately 20 mph), the values of  $\sigma$  are also given as another ordinate on Fig. C-1.

Two important implications are evident in Fig. C-1: 1) the turbulent energy decay is rapid at large values of  $\epsilon$  or  $\sigma$  ( $\epsilon$  can decay by order of magnitude in a minute, and  $\sigma$  diminish by a factor of two); 2) the turbulent energy decay is slow at small values of  $\epsilon$  or  $\sigma$  (it takes an hour to decay from  $\sigma = 3^\circ$  to  $\sigma = 0.5^\circ$ ). The second implication may be of importance to the Dallas Tower project, and even more to previous Windsoc studies, because light turbulence generated over one rough area may then persist for a long time and many miles.

The calculations have been based on the assumption of a contained volume of turbulent air with neutral stability. In an actual case at night at Dallas, there will be some stability, which will serve to damp out the turbulence; turbulent kinetic energy will be drained away both by viscous heating and by conversion to potential energy. The stability effect seems difficult to treat quantitatively. For our assumed isolated air volume, it seems likely that a slight stability will not materially alter the implications of Fig. C-1 because any turbulence tends to reduce the stability. Stability might be expected to operate most strongly on the larger eddies.

In effect, here we are dealing with a Richardson's Number concept with dissipation added. Richardson's Number concerns the conversion of mean kinetic energy and potential energy to turbulent kinetic energy and vice versa. It shows the direction of conversion, and, for steady conditions, implies a little information in the relative rate of energy conversion. In slightly stable situations with small wind gradients, the mean kinetic energy and potential energy are small; then strong viscous dissipation can be a significant kinetic energy sink and can actually dominate the decay of turbulence.

#### D. Effect of the Aircraft Wake

The dispensing aircraft leaves a turbulent wake behind it. When the atmosphere is relatively non-turbulent, this airplane-induced turbulence may provide the dominant diffusion energy. The airplane also gives a downwash to its wake, which can provide a net vertical transport to the released material; the stability of the atmosphere and the mixing of the wake will affect the magnitude of this vertical transport.

There are many interacting factors in determining the evolution of an aircraft wake -- too many to permit a coherent theory before appropriate field measurements are made to investigate this specific problem. This problem is receiving more study in a succeeding project.

The airplane puts energy into its wake through direct heating, through increased water vapor which adds buoyancy and facilitates radiation effects, through the organized kinetic energy of the trailing vortex pattern, and through the turbulent energy associated with the aircraft drag and the propulsion mechanism. The lift introduces a momentum change in the air, resulting in downwash. Two parallel line vortices are formed which interact with each other, and are affected by turbulence and downwash. The wake mixes somewhat with its environment, and a stable atmosphere provides buoyancy for the wake.

A few generalizations are worth mentioning.

- 1) The final position of the wake is not far below the airplane release height. The Dallas Tower data showed the plume to be sometimes above and sometimes below the release height, the variations presumably being due to atmospheric waves and topography differences as well as the stability and wake characteristics. Everything considered, the data might be viewed as implying that the downwash effect is not greater than 100 feet.
- 2) The wake cross-section dimensions are initially slightly larger than the span of the aircraft, and the released material would be well mixed through this volume. Therefore, a diffusion equation should start with the cloud already at this dimension, rather than being a line. The effect on cloud growth computations could be large in very light turbulence.

Information on the initial size of the cloud comes from dispenser calibration trials performed at Dugway. During these trials aircraft (L-23 or C-119) were flown at a distance of about 100 yards upwind from the sampler tower. After about 100 yards of travel the smallest

measured cloud sizes on the tower (standard deviation  $\sigma$ ) are given in the following table:

Initial Cloud Sigmas

<u>L-23</u>	<u>C-119</u>
8.5 ft.	28 ft.
17	29
17	32
18	38
18	45

These sigma values imply that the entire cloud was contained in a vertical depth of about 65 ft. for the L-23 and 130 ft. for the C-119. Theoretical calculations of the depth of the vortex field immediately behind the aircraft indicate that these depths should be about 60 ft. and 145 ft. respectively for the L-23 and C-119.

- 3) The turbulent energy of the wake may not be in the same volume of air as the released material. As the wake moves downward as a discrete entity, some of the material mixes with the environmental air and will be left behind (above). This effect can be noticed in photographs of contrails from the side.

The work done by the aircraft in creating lift can be computed as:

$$\text{Vortex wake energy/unit mass of air} = \frac{2W^2}{\pi \rho v^2 b^2 A} \quad (8)$$

where  $W$  is the weight of the aircraft,  $\rho$  is the air density,  $v$  is the aircraft velocity,  $b$  is the aircraft span, and  $A$  is the cross-sectional area of the vortex field left in the wake (approximately  $1.69 b^2$ ). This energy is left as organized vortex motion in the wake and, after about 45 seconds, becomes turbulent energy as the vortex system breaks up. The energy from skin friction and propeller thrust is put into the wake as turbulent energy and is not easily computed. It may be several times larger in magnitude than the vortex energy but it probably tends to reside in smaller eddy sizes and so decays relatively more quickly than the vortex energy. Using Equation (8) it is possible to estimate the effect of this energy on the growth of the cloud; the remainder of the wake energy will add to the cloud growth to some extent.

The vortex wake energy (8) is included initially in an oval volume of air whose vertical depth for the L-23 case is given by a  $\sigma$  of 15 feet. After the vortex system breaks up the energy is released as turbulence, causing the cloud volume to expand, regardless of outside turbulence. As the volume expands the turbulent density (due to the vortex wake energy) decreases due to

dilution with outside air and the rate of growth due to the turbulent wake energy decreases. Eventually the cloud volume becomes large enough for the vortex wake energy density to become negligible compared to the turbulent energy in the outside air. This process is speeded up to some extent by the continual dissipation of wake energy into heat by viscous effects as discussed earlier in Appendix C. Somewhat balancing the effect of dissipation is the fact that skin friction and propeller sources of turbulent wake energy have been omitted as being difficult to compute.

The effect of the vortex turbulent wake energy can be shown quantitatively with various simplifying conditions by visualizing a bivane being subjected to the passage of the turbulent wake in a wind velocity  $u$ . For the L-23 aircraft with the following characteristics:

$$\begin{aligned} W &= 7000 \text{ lbs.} & A &= 1.69b^2 = 3500 \text{ ft.}^2 \\ v &= 253 \text{ ft./sec.} & \rho &= 2.34 \times 10^{-3} \frac{\text{lbs. sec.}^2}{\text{ft.}^4} \\ b &= 45.5 \text{ ft.} \end{aligned}$$

the turbulent wake energy (8) is given by  $12.3 \text{ ft.}^2/\text{sec.}^2$ . As this energy density drifts by the bivane, the turbulent energy read by the bivane would be  $1/2 u^2 i_W^2$  and

$$\frac{1}{2} u^2 i_W^2 = 12.3.$$

In a 25 mph wind, for example, a turbulence  $i_W$  value of  $4.47^\circ$  (or .078 radians) would be read by the bivane during the passage of the cloud. From the expression

$$\frac{d\sigma}{dx} = 3i_W^2$$

the effect of this turbulent energy on the growth of the cloud can be computed. If natural atmospheric turbulence is present:

$$\frac{d\sigma}{dx} = 3i_W^2 + 3i_N^2 \text{ where } i_N \text{ is the level of natural turbulence.}$$

This value of  $i_W$  holds only during the initial growth stages. After the turbulent wake has grown in size, the turbulent wake energy density decreases and  $i_W$  would decrease until, eventually, it becomes negligible compared to  $i_N$ .

As  $\sigma$  (cloud size) increases, the turbulent wake energy should decrease according to the change in cross-sectional area or according to  $1/\sigma^2$ . By using this functional dependence and the initial turbulent energy levels described above, the effects of vortex wake energy shown in Figs. 9 and 10 have been computed.

A direct observation of the aircraft wake was seen in Trial 36; the release was at 6 miles upwind of the tower at 450 feet, and  $\sigma_{180}$  at release altitude was very low, about  $0.3^\circ$ . The apparent effect of the wake could be seen on the bivariate trace as the wake blew past the tower one-half hour later. This patch of turbulence, the only appreciable turbulence to appear on that trace for hours, passed 31.3 minutes after release; considering the aircraft position and the tower winds, the timing would have been 29.5 minutes, well within the accuracy permitted when considering the inaccuracy in plane position and wind information. This turbulence patch was about 1500 feet wide in the upwind-downwind direction. It had a sigma value of about  $0.7^\circ$ , as estimated visually from the chart record. These values are not materially inconsistent with the decay rates noted on Fig. B-1, as applied to this case.

It seems likely that this turbulence may be strongly limited as to vertical extent because of the stability of the air, say, 50 feet or so. In the shallow layer which is thoroughly mixed, viscous dissipation can be the dominant decay mechanism. Diffusion sideways is easier, and is aided by a small amount of wind shear acting through this depth. The turbulence would of course be contained within the particle plume, but it might be in only a portion of the plume.

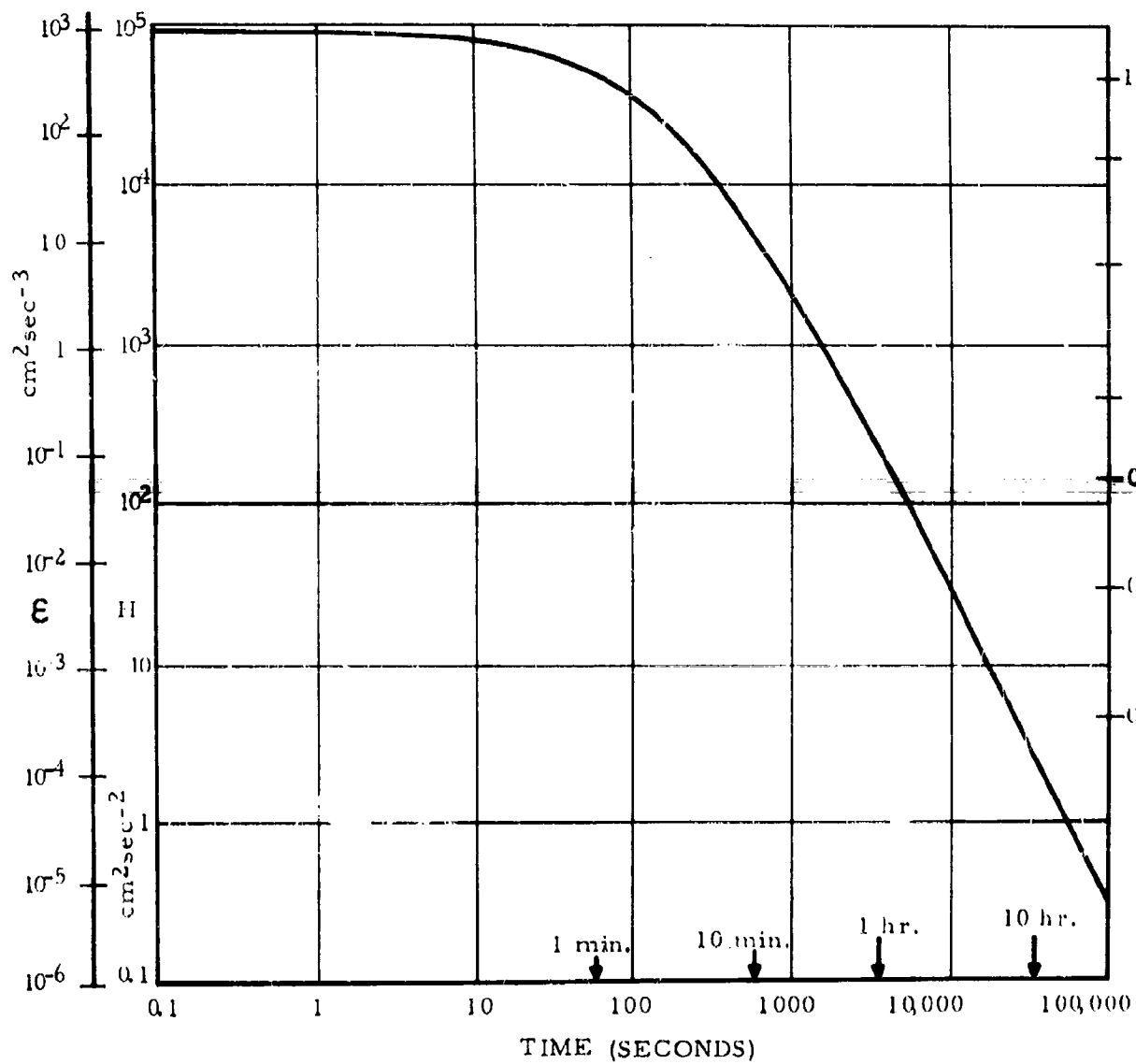
The turbulence in Trial 36 appeared rather dramatically on the trace at 450 feet (which was also approximately the fluorescent particle peak), but was not apparent at the adjacent measuring heights of 150 or 750 feet. Trial 36 was the only one showing this effect. In Trials 16, 23, 32, and 33, the plume was centered at a bivariate location, but only in Trial 32 is there even a slight suspicion of an effect of the wake turbulence appearing over the natural turbulence. This might constitute evidence that the turbulent wake is very shallow, and thus the chances of it crossing a bivariate are slim.

#### E. Estimates of $\epsilon$ and Spectra

A simple relation between  $\epsilon$  and  $\sigma$  has already been noted in the subsection "Decay of a Turbulent Field". There, by assuming a specific constant spectrum ( $-5/3$  law for  $k > k_1$ , constant for  $k < k_1$ ),  $\sigma = 46.8 H = 46.8 \frac{5}{4} k_1^{-1/3} \epsilon^{1/3} = \sigma(\epsilon)$ . The relationship is indicated on Fig. C-1, for  $1/k_1 = \lambda_1 = 200$  meters. This approximate method of determining  $\epsilon$  is probably adequate for the dissipation and scale computations of this present project. If  $\lambda_1$  were assumed to depend on  $z$ , say, setting  $\lambda_1 = \lambda_m$  for Fig. C-1, then a more realistic relationship  $\sigma = \sigma(z, \epsilon)$  would be obtained.

Further refinements in the assumed spectrum shape would give an even more accurate  $\sigma = \sigma(z, \epsilon)$  relationship, and empirical studies with the data could also derive formulas for  $\sigma$  or  $\epsilon$  as functions of height, wind speed, roughness, and stability. All these refinements are beyond the scope of the present project, but may be involved in future studies.

It is apparent from the foregoing that, given  $\epsilon$  and  $z$ , and some empirical knowledge of the effects of roughness and stability, it will be possible to compute  $\sigma$  to the accuracy needed for typical operational diffusion projects.  $\epsilon$  can be measured continuously in flight. MRI personnel have already used an  $\epsilon$  meter in a light plane in cloud physics studies, and have now developed an improved unit which measures  $\epsilon$  without being affected by the characteristics of the measuring airplane. Thus, realistic simple in-flight diffusion computations are feasible.



# TURBULENT DISSIPATION

Fig. C-1